USGS
science for a changing world

Prepared in Cooperation with Pacific Gas and Electric Company

Framework Geologic Map and Structure Sections along the Bartlett Springs Fault Zone and Adjacent Area from Round Valley to Wilbur Springs, Northern Coast Ranges, California

By Robert J. McLaughlin, Barry C. Moring, Christopher S. Hitchcock, and Zenon C. Valin

Pamphlet to accompany
Scientific Investigations Map 3395
Version 1.1, September 2018

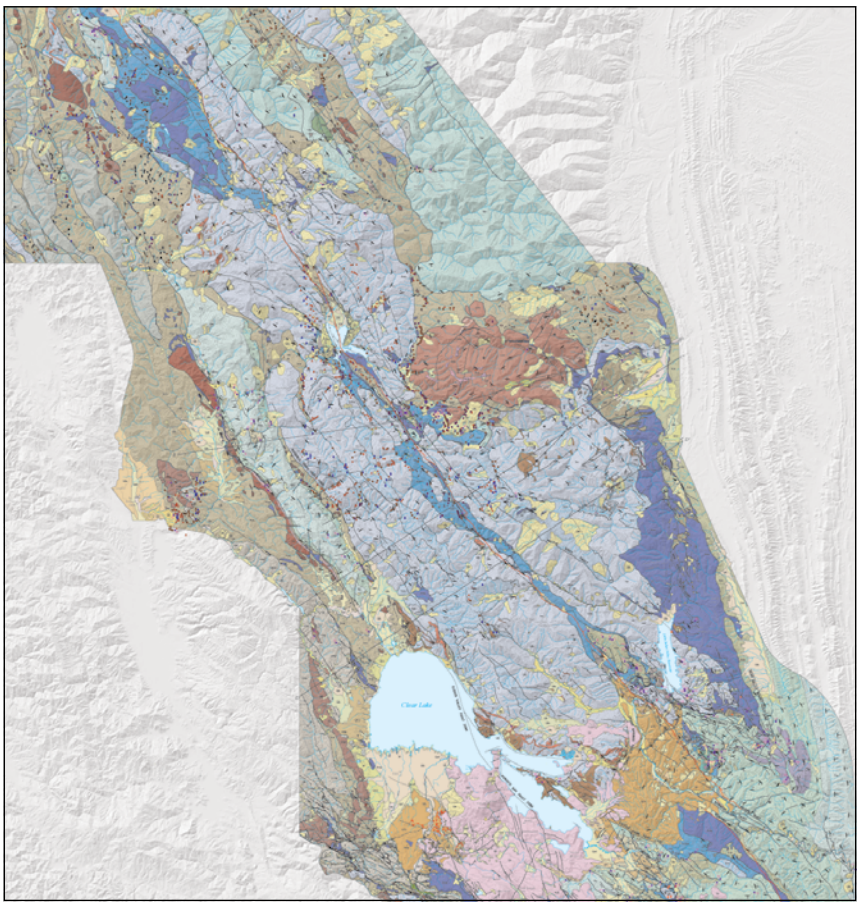

2018

U.S. Department of the Interior
U.S. Geological Survey

U.S. Department of the Interior
RYAN K. ZINKE, Secretary

U.S. Geological Survey
James F. Reilly II, Director

U.S. Geological Survey, Reston, Virginia: 2018
First release: 2018
Revised: September 2018 (ver. 1.1)

Suggested citation:
McLaughlin, R.J., Moring, B.C., Hitchcock, C.S., and Valin, Z.C., 2018, Framework geologic map and structure sections along the Bartlett Springs Fault Zone and adjacent area from Round Valley to Wilbur Springs, northern Coast Ranges, California (ver. 1.1, September 2018): U.S. Geological Survey Scientific Investigations Map 3395, 60 p., https://doi.org/10.3133/sim3395.

ISSN 2329-132X (online)

Contents

Figures

Table

Introduction

This geologic mapping investigation was undertaken by the U.S. Geological Survey (USGS) in cooperation with Pacific Gas and Electric Company (PG&E) under a joint USGS-PG&E CRADA agreement to determine the extent, complexity, architecture, and evolution of the Bartlett Springs Fault Zone between Clear Lake and Round Valley, California. The Bartlett Springs Fault Zone is the eastern-most known active member of the San Andreas transform margin in northern California (fig. 1, sheet 1) and is of particular interest for its apparent long-lived history as a Miocene and older subduction-margin fault that, more recently, was reactivated as an active, creeping member of the San Andreas Fault system. The northern part of the Bartlett Springs Fault Zone is apparently still influenced by subduction of the Gorda Plate beneath North America, but it is also accommodating strike-slip displacement associated with Pacific Plate interaction with North America (fig. 1, sheet 1). South of the map area, the Bartlett Springs Fault Zone has been shown to step into and merge with active faults of the eastern San Francisco Bay region; to the north of the map area and Round Valley, the fault zone steps into several other fault zones, such as the Lake Mountain Fault (Herd, 1978), that connect with offshore thrust faults of the Cascadia subduction margin (Carver, 1987; Clarke, 1990; Clarke and Carver, 1992; Lienkaemper, 2010; McLaughlin and others, 2000). PG&E owns or operates hydro-electric facilities and infrastructure in northern California that are directly or indirectly impacted by the Bartlett Springs Fault Zone, so the geologic framework of the region along and adjacent to the fault zone as depicted in this study are of interest to PG&E for planning and upgrading purposes.

Present and Previous Studies

Previous geologic mapping in the area of this investigation has occurred sporadically for more than six decades, with focus on different aspects of the framework geology at different times, and most of the mapping has not been formally published (see fig. 2, sheet 2). These studies include investigations in the 1960s to 1970s, mostly at 1:62,500 scale, by the California Department of Water Resources (CDWR) for construction of tunnels to divert and transport water from the Eel River drainage system; quadrangle mapping in the 1950s and 1970s by Ph.D. students at the University of Texas, Austin, and Stanford University; mapping by John Suppe and students at Princeton University in the 1960s to 1980s; and some M.S. thesis mapping of a few small areas in the 1970s and 1980s by students at California State University, Hayward, and at San Jose State University.

A large part of this geologic mapping investigation has involved the compilation of previously unpublished mapping and its merging with published mapping by the USGS in the Covelo 30′ × 60′ quadrangle to the north (Jayko and others, 1989), with 1:30,000-scale (Ohlin and others, 2010) and 1:62,500-scale (Etter, 1979) mapping in the Lake Pillsbury region, and with 1:24,000-scale mapping in the Clear Lake region to the south (for example, Hearn and others, 1995; McLaughlin and others, 1990; McLaughlin, 1978).

In 2012–14, new geologic reconnaissance mapping was conducted across the Bartlett Springs Fault Zone corridor in Mendocino National Forest and adjacent areas north of Clear Lake. For this new field work, we traversed the region on Forest Service and county roads (fig. 3, sheet 1), collecting structural, stratigraphic, and lithologic data and sampling for petrographic work. We used Google Earth and high-altitude air-photo imagery to delineate approximate boundaries, distribution, and continuity of mélange terrains, intact rock units, and ultramafic rocks composing the Mesozoic and Tertiary basement of the map area. We also delineated major landslides and linear features associated with faulting (fig. 4, sheet 1; sheets 1, 2). For some traverses, a computer operated from our field vehicle enabled us to enter field data into a digital database in the field. For other traverses, field data was not entered until return to the office.

Christopher Hitchcock conducted mapping of the Quaternary geology in northern Clear Lake basin, Potter Valley, and associated subsidiary basins and drainages in 2012–14. This mapping, delineating the stratigraphy of Quaternary fluvial, stream, and terrace deposits, was integrated with the mapping of McLaughlin and Moring during the compilation process. Major landslide deposits mapped by McLaughlin and Moring and separately by Hitchcock were combined in the map database. Only large, major landslide deposits are shown on this geologic map. The reader is herein referred to detailed landslide and slope stability maps by the California Geological Survey (http://www.conservation.ca.gov/cgs/geologic_hazards/landslides) and the USGS (https://www2.usgs.gov/natural_hazards/) to determine more accurately the hazard posed by landsliding in this region. Faults interpreted as geomorphically youthful, active parts of the Bartlett Springs Fault Zone, shown by red fault lines on the geologic map, are incorporated from Lienkaemper (2010).

In this report, geologic ages and designations of Mesozoic periods and epochs are taken from the Geologic Time Scale of the Geological Society of America (Walker and others, 2012; Geologic Time Scale, v. 4.0, Geological Society of America, https://doi.org/10.1130/2012.CTS004R3C). Cenozoic and Quaternary epochs are based on their assignments by the U.S. Geological Survey Geologic Names Committee, 2010.

Acknowledgments

The mapping investigation was funded from a Cooperative Research and Development Agreement (CRADA) between the Earthquake Hazards Program of the U.S. Geological Survey (USGS) and Pacific Gas and Electric Company (PG&E) as a follow-up to an earlier USGS-PG&E CRADA-funded geologic mapping investigation of the Bartlett Springs Fault Zone in the Lake Pillsbury area (Ohlin and others, 2010). The authors have appreciated the continued interest and encouragement from Scott Steinberg (PG&E Geosciences Department) in this investigation. Steinberg also provided access to several unpublished reports prepared by PG&E geotechnical consultants, as well as photographs taken from a helicopter reconnaissance of the region by Steinberg and Hitchcock in 2012 that were helpful in our map compilation.

Diane Moore (USGS Earthquake Science Center) provided the senior author with expert consultation and corroboration on mineralogy and petrography of serpentinitic fault rocks along the Bartlett Springs Fault Zone at several localities in the map area, as well as help with numerous petrographic issues with the Franciscan Complex.

Large wildfires that prompted extended road closures in Mendocino National Forest during the course of our mapping

study made it critical to establish good communications with the U.S. Forest Service. We are grateful to them for their cooperation, particularly personnel in the Upper Lake (A. Downhour and D. Mackintosh), Willows (R.P. Mikulovsky), and Red Bluff (D.R. Elder and J.A. Delafuente) offices, for providing us with updated Forest Service road maps, road conditions, gate access, and contact information for private landowners within Mendocino National Forest. We thank several landowners in the map area for providing access to their land in the course of mapping, as well as information on the drivability of access roads. Northeast of Willits, we thank the Adams family, owners of Emandel Resort for access to their land and for providing information on access along other parts of the Eel River. In Rice Valley and the McCloud Creek area, the Kompf family and Dave Rinker were helpful in allowing access to their land in Rice Valley and sharing a long-term knowledge of this area.

This mapping investigation has cooperated with the Geology, Minerals, Energy, and Geophysics Science Center (GMEG) Delta project (R. Graymer, USGS project lead), a 3–D framework geologic mapping investigation that includes the area between Wilbur Springs to the north and Lake Berryessa to the south, as well as the subsurface of southwestern Sacramento Valley and the San Francisco Bay part of the Sacramento-San Joaquin Delta.

The report was peer reviewed for scientific content by P.A. Stone and B. Melosh (both at GMEG Science Center, USGS).

Geologic Setting

The area of this geologic mapping investigation is in the northern coast ranges of California. Complexly deformed Mesozoic and lower Cenozoic rocks of the Franciscan Complex, an accumulation of sedimentary, metamorphic, and igneous rocks that were assembled in a subduction zone and accreted to the western continental margin between the Late Jurassic and Miocene, underlie the region. Oceanic rocks of the Coast Range ophiolite that form the basement of coeval fore-arc strata of the Great Valley complex structurally overlie the Franciscan Complex. Subduction continues at present in the modern Cascadia subduction margin northwest of the map area but has been largely replaced by dextral strike-slip faulting associated with northward propagation of the San Andreas transform system in the map area.

A consequence of the very long history of deposition of strata in the Franciscan Complex is that these rocks were intensely deformed during several episodes of subduction-accretion that formed three broad, westward-younging structural belts. These belts, the Eastern, Central, and Coastal Belts, are younger, but overlap in age westward, and pressure/temperature (P/T) conditions from metamorphic mineral assemblages in the rocks in each belt imply that the depth to which the rocks were subducted increases eastward. Due in part to oblique subduction-accretion, some of the Franciscan rocks, particularly oceanic basaltic rocks and their overlying pelagic sedimentary covers in the Central Belt, have undergone relatively large northward translation along the eastern Pacific Ocean margin since the Jurassic. This complex structural framework was followed in the Early to middle Cretaceous (Hauterivian–Albian), and even later in the Late Cretaceous (Maastrichtian) to early Tertiary (early Eocene), by uplift of the subduction complex, extensive detachment faulting in the overlying ophiolitic and lower sedimentary section of the fore arc, and unroofing of the deeply subducted Eastern and Central Belts of the Franciscan Complex. This unroofing of the Coast Ranges and exposure of deeply subducted Franciscan rocks to erosion has been linked to shallowing of Farallon Plate subduction during the Laramide orogeny (Saleeby, 2003; Dickinson and others 1979). In northern and central California, this was accompanied at depth by east-directed emplacement of Franciscan rocks as tectonic wedges into the western Great Valley fore arc and the mafic igneous and metamorphic rocks of the Sierra Nevada batholith (Ernst and McLaughlin, 2012; Wentworth and others, 1984; Wentworth and Zoback, 1990).

The Franciscan Complex is structurally overlain in the map area by the Jurassic Coast Range ophiolite, which is highly disrupted as the result of (1) extensional shearing and serpentinization of the structurally low ultramafic section of the ophiolite during its upward migration from mantle to midcrustal levels in the Jurassic and (2) later contraction and extension that corresponded with unroofing of the Franciscan Complex in the Late Cretaceous and Tertiary. Although still debated, the ophiolitic rocks are widely considered to have formed in a fore-arc, supra-subduction setting east of the paleotrench in which the Franciscan Complex was assembled (Shervais and others, 2005a, b; Ernst and McLaughlin, 2012). Serpentinite matrix mélange that forms a large part of the ultramafic section of the Coast Range ophiolite and is attributed to low-angle extension (Jayko and others, 1987) may result both from the Jurassic and the Late Cretaceous–early Tertiary deformation.

Unmetamorphosed sedimentary rocks of the Upper Jurassic Great Valley fore arc were initially deposited unconformably on extrusive and high-level intrusive rocks of the ophiolitic basement of the map area. The Upper Jurassic to Lower Cretaceous (Hauterivian and younger) part of this sedimentary section, however, was subsequently deformed by folding and attenuated with the underlying ophiolite.

This deformation resulted in incorporation of the lower Great Valley sedimentary section into a regionally extensive thick zone of mélange (here mapped as ophiolitic mélange; earlier mapped as Grizzly Creek mélange terrane near Wilbur Springs by McLaughlin and Ohlin, 1984) consisting of rocks of the Coast Range ophiolite tectonically mixed with Upper Jurassic and Lower Cretaceous strata of the Great Valley sedimentary section (McLaughlin and others, 1990; also see photos of "Grizzly Creek mélange terrane" in McLaughlin and Ohlin, 1984). Significant penetrative shearing in the serpentinized ultramafic rocks of the map area may reflect upward migration of these rocks to the ocean floor from mantle depths in the Jurassic. Continued unroofing of ophiolitic basement is reflected in the Late Jurassic (Oxfordian–early Tithonian) deposition of coarse megabreccia derived from the Coast Range ophiolite at the base of the Great Valley complex sedimentary section. Exposure of serpentinite on the seafloor during early Great Valley complex evolution further led to deposition of sedimentary serpentinite (unit Kssp) in Valanginian–Hauterivian time.

Detachment faulting rooted along the serpentinized base of the Coast Range ophiolite (Jayko and others, 1987), which involved both the ophiolite and the lower Great Valley complex (McLaughlin and others, 1990), produced ophiolitic mélange (unit KJom). The timing of extension associated with formation of the ophiolitic mélange was Early Cretaceous (Valanginian) or younger, based on the youngest fossils present in sedimentary slabs and blocks in the mélange (McLaughlin and others, 1990). The somewhat younger (Valanginian–Hauterivian) sedimentary serpentinites and associated complex folding in the overlying

lower Great Valley section could reflect extensional deformation in the stratigraphically lower part of the section. Erosion of the unroofed Coast Range ophiolite apparently resulted in deposition of ophiolite-derived sediment in the fore-arc basin as olistostromal deposits of serpentinitic breccias and sandstones ("sedimentary serpentinites" of this report). Early Cretaceous (Hauterivian) cold-seep-related fossil faunas are associated with some of the sedimentary serpentinites, but fossils this young are not known as part of the ophiolitic mélange (McLaughlin and others, 1990; Campbell and others, 1993; Campbell and others, 2002, 2008; Kiel and others, 2008).

Others (for example, Macpherson and Phipps, 1988) have interpreted both the serpentinized ultramafic rocks and ophiolitic mélange units of this report to be olistostromal and explain their penetrative fabrics as formed by large-scale gravitational collapse. This implies that penetrative deformation of the serpentinized ultramafic rocks (unit Josp) and ophiolitic mélange (unit KJom) was a process that occurred in the shallow lithosphere. Although near-surface sedimentary processes are clearly associated with deposition of Lower Cretaceous (Hauterivian) sedimentary serpentinites (unit Kssp) in the lower Great Valley complex, tectonic shearing and boudinage in the serpentinized ultramafic rocks (unit Josp) and ophiolitic mélange (unit KJom) lack clear evidence of a sedimentary origin and, as pointed out, some of the penetrative deformation in the serpentinized ultramafic rocks was likely imposed during upward migration of the serpentinite from the mantle to the ocean floor in the Jurassic and later. Detachment and attenuation faulting in the serpentinized ultramafic rocks and ophiolitic mélange units is here viewed as too deep-seated to be easily relatable to near-surface processes. The mélange process may be linked to progressive shallowing of subduction and unroofing of the Coast Ranges that continued into the Late Cretaceous and early Tertiary during the Laramide orogeny.

Both the ophiolitic mélange and the sedimentary serpentinite in the Lower Cretaceous section of the Great Valley complex resulted from deep unroofing of the Coast Range ophiolite and (or) buried mafic basement beneath the northern Sacramento Valley (Jayko and others, 1987; Wentworth and others, 1984; Macpherson and Phipps, 1988). In contrast to sedimentary processes involved with deposition of the sedimentary serpentinite, the ophiolitic mélange, instead, may have formed as a series of low-angle detachments associated with extension at depth. Extension that triggered unroofing of ophiolitic basement must have followed Valanginian basinal deposition of Great Valley strata incorporated into the ophiolitic mélange. In the Hauterivian, deposition of unroofed and recycled ophiolitic debris occurred in the fore arc, including olistostromal deposits and sedimentary serpentinite. Fluids associated with cold-seep-related fossil faunas in the sedimentary serpentinites may well have been channeled along detachment structures.

Another major pulse of uplift and unroofing of Franciscan Complex basement in the region occurred between the latest Cretaceous (Maastrichtian) and late Paleocene, as indicated by local remnants of Paleocene to Eocene fore-arc-basin strata preserved near Covelo and Rice Valley and in the Lower Lake area that are unconformable on underlying Great Valley strata. In Rice Valley, a local conglomerate unit at the base of upper Paleocene strata that is unconformable on the Upper Cretaceous section contains clasts of lawsonitic metagraywacke derived from the Franciscan Complex. This relation suggests (for example, Berkland, 1973) that the Franciscan source of the lawsonitic metasandstone was exhumed from subducted depths greater than 25 km between the latest Cretaceous (~66 Ma) and late Paleocene (~56 Ma).

In the late Miocene (~8–5 Ma), following this major tectonism over the subduction margin, faulting in the northern Coast Ranges between Covelo and Clear Lake began to link southward to the northwardly propagating transform system. Faults of the transform system to the south extended into the accretionary margin inboard of the present San Andreas Fault and Mendocino Triple Junction. The Bartlett Springs Fault Zone appears to be a fault zone present in the Miocene and older subduction margin that provided a pre-existing zone of crustal weakness that accommodated the transition from dominant subduction convergence to dominant strike slip, with northward propagation of the main San Andreas transform and its more inboard segments (the Hayward-Calaveras-Rodgers Creek-West Napa-Maacama and the Concord-Green Valley-Bartlett Springs Fault Zones).

Starting about 4 Ma, a 70-km-wide band of the northern California margin began its northwest-directed transition from a margin dominated by head-on to oblique subduction-driven convergence to one dominated by transpression and transtension associated with steep faults of the northwardly propagating San Andreas Fault system. The modern Bartlett Springs Fault Zone appears to have developed largely during this period of transition from subduction to strike-slip tectonics. Favorably oriented faults of the Bartlett Springs Fault Zone that initially were active as part of the subduction margin in the Miocene were re-occupied by steeper dipping, discontinuous, stepping strike-slip faults of the transform margin.

The geologic map and accompanying structure sections delineate the course of the active Bartlett Springs Fault Zone over a distance of ~110 km, from the vicinity of Clear Lake northwestward to Covelo. The fault zone is divided into northern and southern segments, separated by a prominent right step, across which the two fault zone segments overlap. The northern Bartlett Springs Fault Zone appears to follow a complex northwest-oriented path of crustal weaknesses that were established in the subduction margin realm, prior to initiation of strike-slip faulting. The southern Bartlett Springs Fault Zone (fig. 5, sheet 2), which includes the southwest side of a 2.5-km-wide right step southeast of State Highway 20 near Grizzly Spring, departs from the prominent zone of pre-transform deformation and follows a less maturely developed path that cuts across the structural grain of the older pre-transform margin. The southeasternmost mapped extent of the northern Bartlett Springs Fault Zone segment east of the right step, separating it from the southern segment, overlaps the southern segment for ~5 km. The overlapping part of the northern segment, however, does not exhibit geomorphically youthful fault features (see later description of northern and southern Bartlett Springs Fault Zone). Farther southeastward, this overlapping segment of the northern Bartlett Spring Fault Zone may die out as a bedding plane-parallel fault within strata of the Mesozoic Great Valley complex, though its full extent is unknown and the focus of more detailed ongoing investigations by the USGS.

Lithologic and Structural Features of the Metamorphic Basement Terranes

Franciscan Complex

The Franciscan Complex is considered to represent the "type" subduction-zone rock assemblage of the eastern Pacific basin rim (for example, Ernst and McLaughlin, 2012). Subdivisions of the Franciscan Complex are based on their field and aerial map expression, integration of numerous informal local unit names applied to various parts of the Franciscan at different times, and regional geologic mapping and geophysical investigations (Jayko and others, 1989; McLaughlin and others, 2000; Blake and others, 1992, 2000; Lanphere and others, 2007, 2011). The Correlation of Map Units (sheet 2) summarizes the tectonostratigraphic framework of these rocks as used in this report. Regionally, the Franciscan Complex is divided into three thick, eastwardly inclined and folded, sheet-like belts, containing rocks that generally become younger but overlap in age westward. These belts, referred to from northeast to southwest as the Eastern, Central, and Coastal Belts (Irwin, I960; Bailey and others, 1964), include rocks that were metamorphosed at high P/T conditions (for example, blueschist facies, deeply subducted to tens of kilometers) in the Eastern Belt, at intermediate P/T conditions (for example, low greenschist facies burial conditions) in the Central Belt, and at much lower P/T conditions in the Coastal Belt (for example, zeolite to prehnite-pumpellyite facies), where maximum structural burial was only to a few kilometers (Ernst and McLaughlin, 2012). Rocks assigned to the Eastern and Central Belts of the Franciscan Complex are present in the map area, but the Coastal Belt is at the surface only to the west of the map. If conceptual views of crustal structure are valid, however, it may underlie rocks of the Central Belt at some depth in the western part of the map area.

Several subsidiary map units are recognized in the Eastern and Central Belts, which we consider to be fault-bounded and which we refer to as tectonostratigraphic terranes of the Eastern or Central Belts. We also recognize subunits of mélange in both the Eastern and Central Belts that may be of different age and which are mapped as different units. Mélanges in both belts, however, contain similar high-grade blueschist blocks (for example, glaucophane schist, eclogite, and amphibolite) that may be derived from the same or similar protoliths. The matrix material of these mélange terranes in the Eastern and Central Belts differ in metamorphic grade, consistent with metamorphism of the belts in which they occur.

Central Belt

The Central Belt is the westernmost belt of the Franciscan Complex exposed in the map area. West of Ukiah valley and U.S. Highway 101, it is underlain structurally by the Coastal Belt beneath a regionally warped low-angle fault referred to as the Coastal Belt Thrust. In the map area, the Central Belt comprises at least 30 to 40 percent of the surface exposures of Franciscan Complex rocks, but it is inferred to structurally underlie the entire area west of Sacramento Valley. The Central Belt is predominantly a large-scale mélange that, along with meter- to tens-of-meter-scale sheared blocks of blueschist, eclogite, amphibolite, metasandstone, metachert, metaigneous, and ultramafic rocks, also encloses numerous kilometer- to tens-of-kilometers-scale slabs of broken metasandstone and argillite ± pelagic chert or limestone ± basaltic volcanic rocks ± other mafic to ultramafic parts of the Mesozoic ocean floor. Many slabs enclosed by mélange are composed solely of metasandstone and argillite. These various metasedimentary slabs have metamorphic signatures that vary from strongly to moderately foliated blueschist grade to unfoliated low- to medium-greenschist grade (for example, pumpellyite and prehnite-pumpellyite-bearing) and minor zeolite-grade (laumontite-bearing) rocks. The surrounding mélange matrix is no higher than low-greenschist grade (pumpellyite-bearing) to perhaps incipient blueschist grade (traces of lawsonite) locally.

In the map area, we divide the Central Belt into (1) an undivided mélange matrix unit (Central Belt Mélange terrane) and (2) numerous large slab-like bodies of rock enclosed by the undivided mélange matrix. These slabs are mapped either as generic lithotectonic terrane units or, locally, as named terranes (Pomo terrane, Marin Headlands-Geysers terrane, and Snow Mountain volcanic terrane), where a distinctive tectonostratigraphy is evident.

Pomo Terrane (Upper Cretaceous to Upper Jurassic)

This unit is recognized only east of Potter Valley, in the eastern part of the Central Belt, along the contact with serpentinite and structurally overlying Cretaceous strata of the Great Valley complex of Middle Mountain. The rocks of the Pomo terrane appear to represent slabs of a dismembered seamount (Berkland, 1972, 1978). The lower part of this section consists of alkalic basaltic pillow flows, flow breccias, and intrusive diabase, overlain locally by, or intercalated locally with, radiolarian chert. Radiolarians in the chert are Jurassic, equivalent in age to a part of the nearby Geysers chert section. However, the basaltic rocks are overlain unconformably by a thin carbonate-cemented bioclastic basalt-clast breccia, sandstone, and shale containing a latest Cretaceous (Maastrichtian) mollusk fauna that, in turn, is faulted against serpentinite and overlying Upper Cretaceous Great Valley complex strata of the Middle Mountain block or enclosed by undivided mélange of the Central Belt.

Marin Headlands-Geysers Terrane (Upper Cretaceous–Upper Jurassic)

The Marin Headlands-Geysers terrane is named for the two areas south of the area of this map where these rocks have been studied in great detail (McLaughlin and Pessagno, 1978; Pessagno, 1977; Murchey, 1984; Murchey and Jones, 1984; Hagstrum and Murchey, 1993). In the Marin Headlands area and at The Geysers, east of Healdsburg, the terrane consists of a sequence of oceanic basaltic flows and breccia overlain by a section ~67 m (The Geysers) to 80 m (Marin Headlands) thick of pelagic radiolarian chert that, in turn, is depositionally overlain by metasandstone turbidites derived from the Cretaceous continental margin. The radiolaria in the chert sections of the Marin Headlands-Geysers terrane have been studied in great detail and shown to represent a condensed pelagic section deposited on basaltic ocean floor at equatorial latitudes, far

from the continental margin, between the Middle Jurassic (Pliensbachian, ~190 Ma) and the early Late Cretaceous (early Cenomanian or late Albian, ~100 Ma). The terrane is widely considered to represent the remnants of an extensive large oceanic igneous province such as an oceanic plateau, similar to the large plateaus preserved on the west side of the Pacific Ocean basin. The overlying metasandstone, of low-greenschist (pumpellyite) grade in these areas, preserves the initial encounter of the oceanic rocks with the North American Plate subduction margin. The metasandstone turbidites were deposited on the oceanic basalt and chert no earlier than Cenomanian time in the Marin Headlands, based on an ammonite (Murchey and Jones, 1984) and recent dating of detrital zircons in the metasandstone (maximum depositional age of ~100 Ma; McPeak and others, 2015). At The Geysers, the chert section is virtually identical in age to the Marin Headlands based on the radiolarian zonation (Murchey and Jones, 1984; Hagstrum and Murchey, 1993). The overlying metasandstone at The Geysers is petrographically similar to the Marin Headlands based on point-count data (McLaughlin and Ohlin, 1984), but an analysis of detrital zircons in the metasandstone showed that the youngest zircon population is 114 Ma (data of G. Gehrels, cited in Dumitru and others, 2015), considerably older than the youngest radiolaria in the underlying Geysers area chert section. This is explained by recognizing that the detrital zircon data from The Geysers provides only a maximum depositional age for the metasandstone overlying the chert and only coincidentally will date actual deposition of sediment transport systems. However, the similarity of framework grain compositions in metasandstones from the Marin Headlands and The Geysers (McLaughlin and Ohlin, 1984) is taken to indicate that the clastic rocks in both areas were derived from a similar set of source regions but may have interacted at somewhat different times with the oceanic rocks due to the large original aerial extent of the chert-basalt terrane (suggested by distribution of similar rocks from Baja California to southern Oregon) or possibly the oceanic rocks had an orientation that was oblique to the margin during accretion.

We have identified several semi-intact, large slabs of broken, complexly intercalated basalt, radiolarian chert, and metasandstone that extend into the map area from The Geysers region to the south and are surrounded by other rocks of the Central Belt. We have assigned these rocks to the Marin Headlands-Geysers terrane, where we have radiolarian ages (table 1; sheet 1) from the cherts, and the basalt-chert-metasandstone relations seem consistent with their correlation to the Marin Headlands-Geysers terrane. Many other large to small blocks of basalt, undated chert, and metasandstone that are enclosed by mélange and adjacent to or near the rocks we assign to the Marin Headlands-Geysers terrane may also be pieces of this terrane. However, they are instead designated only as blocks of chert, basalt, or metasandstone where there is no data to confidently correlate the rocks with the Marin Headlands-Geysers terrane.

Snow Mountain Volcanic Terrane (Lower Cretaceous–Valanginian or younger)

The Snow Mountain volcanic terrane is an unusual sequence of metamorphosed rhyolitic to basaltic volcanic and volcaniclastic rocks interpreted to have formed in a seamount setting (Macpherson, 1983). These rocks were earlier mapped and assumed to be a structural outlier of a part the Stonyford section of the Coast Range ophiolite (Brown, 1964). Subsequent mapping and petrologic and geochemical study of these rocks by Macpherson (1983), however, showed that the Snow Mountain rocks have undergone low-blueschist-grade metamorphism and thus were subducted with rocks of the Franciscan Complex. Map relations and modeling of the geometry of a thin sheet of ultramafic rocks beneath the Snow Mountain rocks (Griscom, *in* Brown and others, 1981), suggest that they structurally overlie or are enclosed by mélange of the Central Belt that bounds these rocks to the north, west, and south. Rocks of the Yolla Bolly and Pickett Peak terranes of the Eastern Belt also structurally overlie the Central Belt regionally. However, metavolcanic rocks like those described from the Snow Mountain volcanic terrane have not been recognized in the Yolla Bolly terrane, and metavolcanic rocks of the Pickett Peak terrane are of higher blueschist grade than the Snow Mountain volcanic terrane. We therefore assign the Snow Mountain volcanic terrane to the Central Belt, although we acknowledge that the Snow Mountain rocks could actually represent a seamount accreted with the Yolla Bolly terrane rather than part of the Central Belt. Early work (for example, Brown, 1964) also assumed a Jurassic age for the Snow Mountain volcanic terrane based on an erroneous correlation of metacherts associated with the Snow Mountain volcanic terrane with the radiolarian fauna of cherts in the Coast Range ophiolite at Stonyford. Efforts to separate radiolarians from metachert in the Snow Mountain volcanic section have been unsuccessful (B. Murchey, oral commun., 2015). Consequently, at the time of this writing, reliable age data for the Snow Mountain volcanic terrane do not exist.

Eastern Belt

The Eastern Belt represents the structurally highest belt of the Franciscan Complex and was the earliest assembled of the three belts. It apparently was subducted to deeper levels, with accompanying higher blueschist-grade metamorphism than in the Central and Coastal Belts (Ernst and McLaughlin, 2012; Dumitru and others, 2010, 2015; Blake and others, 1988). In northern California, development of the higher blueschist-grade metamorphic mineral assemblages was commonly accompanied by textural reconstitution of the metasedimentary rocks to textural zones 2–3 (Blake and others, 1967) and conversion of the metasedimentary rocks to slate, phyllite, and schist, with increasing textural grade. In general, the increase in textural reconstitution and in P/T relations based on metamorphic mineral assemblages has been shown to increase structurally upward in parts of the Eastern Belt that are thrust beneath the Klamath Mountains (Blake and others, 1967). This structurally upward increase in metamorphic grade ("inverted-metamorphic zonation") is interrupted in places by low-angle faults that may repeat or truncate the gradual upward progression from low- to high-metamorphic mineral assemblage and textural grade (Blake and others, 1967; Worrall, 1981). In parts of the Diablo Range south of San Francisco Bay, this relation is not so clear; here, high P/T neoblastic blueschist minerals, including jadeitic pyroxene, are present in metasandstones that are not highly reconstituted (Raymond, 2014; Ernst, 1971; Wentworth and others, 1999). This suggests that kinematic relations between

metamorphic mineral facies and development of metamorphic fabric do not correspond everywhere to equivalent burial depths.

In the map area, we divide the Eastern Belt into the three tectonostratigraphic terranes described below.

Yolla Bolly Terrane (Upper and Lower Cretaceous to Upper Jurassic, Tithonian)

The Yolla Bolly terrane is named for rocks north of the map area in the Yolla Bolly Mountains Wilderness area of the northern Coast Ranges (Blake and Jayko, 1983; Jayko, 1984; Blake and others, 1985; Worrall, 1981). These rocks represent the structurally lower part of the Eastern Belt. Previous workers have used various local names (such as the Taliaferro Complex of Suppe, 1973; the Pacific Ridge Complex of Suppe and Foland, 1978; and the East Clear Lake and Little Indian Valley terranes of McLaughlin and Ohlin, 1984) to describe the character of these rocks in different areas. We include all of these locally named rock units in the Yolla Bolly terrane of this report. Inclusion of rocks in the Little Indian Valley terrane (McLaughlin and Ohlin, 1984) in the Yolla Bolly terrane, however, raises some unresolved issues with the depositional age assignment of the Yolla Bolly terrane.

The Yolla Bolly terrane is divided into two major units in the map area: a structurally low mélange (unit fym) and a higher unit (unit fys) of more or less coherent rocks (broken formation). The mélange unit comprises slaty, sheared, and foliated metasandstone and argillite containing blocks and slabs of metagreenstone, metachert, and metaconglomerate, rare blocks of high-grade blueschist and amphibolite locally containing garnet, and rare lenses of metaserpentinite found along shear planes associated with the mélange fabric. The mélange is interpreted as a continuous, thick, fault-bounded, folded layer (see structure sections, sheet 2) that overlies structurally lower mélange of the Central Belt. Given this relation, some blocks in this mélange of largely Eastern Belt sedimentary rocks may contain some high-grade blueschist blocks incorporated (possibly plucked from) the underlying mélange of the Central Belt during emplacement of the Yolla Bolly terrane (and east-directed wedging of the Central Belt beneath the Eastern Belt). In particular, high-grade blueschist and amphibolite blocks and slabs in the area of Goat Mountain along the crest of the Pacific Ridge antiform (see map, sheet 1**)** are here viewed as a part of the Yolla Bolly terrane mélange unit. This interpretation differs from the suggestion of others (Suppe and Foland, 1978; Ernst and others, 1970; Coleman and Lanphere, 1971) that the Goat Mountain rocks represent structurally overlying thrust remnants of a higher-grade-blueschist metamorphic terrane, perhaps part of a schuppen complex (Suppe and Foland, 1978).

The structurally higher part of the Yolla Bolly terrane consists primarily of metasandstone and argillite complexly intercalated locally with a unit of thin metabasalt flows and breccias overlain by tuffaceous metachert. The sequence of metabasalt-metachert-metasandstone is further characterized by development of a slaty cleavage that is in many places axial planar to isoclinal folding of the rocks. These rocks, together with the mélange, are further characterized as having a planar metamorphic fabric and have undergone textural reconstitution varying from high textural zone 1 to high textural zone 2 (Blake and others, 1967) during subduction. Textural reconstitution was accompanied by development of neoblastic pumpellyite in textural zone 1 to low textural zone 2 metaclastic rocks and pumpellyite + lawsonite ± jadeite ± sodic amphibole in rocks of low to high textural zone 2 (Ernst and McLaughlin, 2012; McLaughlin and Ohlin, 1984; Ohlin and others, 2010; Blake and others, 1967; McLaughlin and others, 1990). The metamorphic fabric appears to have developed prior to development of the mélange, and for this reason we believe the mélange is related to post-depositional tectonic processes such as uplift and unroofing of the Franciscan Complex and (or) to tectonic wedging.

Locally, some unusual alkalic and mafic intrusive rocks are present in the map area and elsewhere in the Yolla Bolly terrane that have been studied petrologically and dated by $^{40}Ar/^{39}Ar$ and U-Pb methods (Layman, 1977; Echeverria, 1980; Mattinson and Echeverria, 1980; Mertz and others, 2001). In the Monkey Rock area, these intrusive rocks intrude slaty metasandstone and argillite and metachert and display chilled margins (Layman, 1977; Ohlin and others, 2010). North of the map area, similar field relations are also present in a slab of Yolla Bolly terrane rocks enclosed in Central Belt mélange at Island Mountain (McLaughlin and others, 2000, table 1; Koski and others, 1993; Stinson, 1957). An intrusion at Leech Lake Mountain north of the map area yielded an ~119 Ma $^{40}Ar/^{39}Ar$ age (Mertz and others, 2001); whereas, a U-Pb age of 95 Ma on zircon was determined for gabbroic intrusive rocks near Ortigalita Peak in the Diablo Range south of the map area (Mattinson and Echeverria, 1980). A single blueschist metamorphic event that followed folding of wall-rock greywacke and post-folding intrusion of the gabbro was dated at 92 Ma (Turonian) in the Ortigalita Peak area. Although the timing of these intrusions into widely separated rocks correlated with the Yolla Bolly terrane extends over 24 m.y., these rocks have similar alkalic geochemistry (Ohlin and others, 2010).

Fossils and detrital zircons from metasedimentary rocks, including metachert and metasandstone of the Yolla Bolly terrane, imply a long depositional history (from ~155 to 94 Ma) beginning in the Late Jurassic (Kimmeridgian–Tithonian), based on radiolarians in the metacherts and several localities of *Buchia* in the Little Indian Valley area northwest of Wilbur Springs. Deposition continued through the Early and middle Cretaceous (Albian) and into earliest Late Cretaceous (Cenomanian) based on radiolarians in the metacherts, on megafossils (an *Inoceramus*, see Ohlin and others, 2010), on detrital zircon data in the map area and to the north and south (Dumitru and others, 2010, 2015), and on the ages of mafic intrusive rocks described above. Several localities in the Yolla Bolly terrane that have previously yielded *Buchias* of Late Jurassic to Early Cretaceous age (Tithonian–Valanginian), have been shown to be enclosed by metasandstone that yielded much younger (111–104 Ma) detrital zircons (Dumitru and others, 2015), prompting the proposal that all of the Jurassic and Early Cretaceous fossils from the Yolla Bolly terrane clastic section are redeposited and not accurate indicators of maximum depositional age. The *Buchias* from the Little Indian Valley area, however, were found to be in strata that yield detrital zircons consistent with a Tithonian–Valanginian (~152–134 Ma) maximum depositional age (T. Dumitru, written commun., 2015). The proportion of age-equivalent older sedimentary rocks that are present elsewhere in the Yolla Bolly terrane is poorly constrained at present. A better understanding of structural complexity (particularly fold history) will be necessary to place emerging

detrital zircon age data into proper context with paleontologic ages in the map area and more regionally.

Pickett Peak Terrane (Lower Cretaceous, Aptian–Barremian)

The Pickett Peak terrane is the structurally highest unit of the Franciscan Complex in the map area; the rocks were subdivided into the metamorphic rocks of Black Butte and Bald Mountain and the metamorphic rocks of Lake Pillsbury by Ohlin and others (2010). Here we collectively describe all of these rocks under the Pickett Peak terrane. These rocks structurally overlie mélange of the Central Belt, as well as metasedimentary rocks of the Mendocino Pass terrane (described below) along low-angle faults inferred to be thrusts. The low-angle fault separating metamorphic rocks of the Pickett Peak terrane from the Mendocino Pass terrane might also have a later extensional history associated with uplift and unroofing of the Coast Ranges (for example, see Jayko and others, 1987).

Metamorphic rocks of the Pickett Peak terrane are present in the map area as an isolated slab at Bald Mountain, but to the northeast, metamorphosed metasedimentary and metavolcanic rocks also underlie Black Butte. Southeast of Black Butte, the unit is contiguous with rocks previously mapped as the South Fork Mountain Schist (Ghent, 1965; Blake and others, 1967; Lehman, 1974; Bishop, 1977; Brown and Ghent, 1983). These rocks are also considered to be a part of the Pickett Peak terrane of the Eastern Belt (Irwin and others, 1974; Blake and others, 1982), which is in fault contact with rocks of the Coast Range ophiolite to the east. Pickett Peak terrane rocks of Black Butte and Bald Mountain are dominantly metasandstone and phyllite and, from regional map relations and drill-hole data (CDWR, 1966), have a structural thickness of as much as 3 km. A 500- to 1,000-m-thick lens of pillowed, upright metavolcanic rocks occurs in the high Coast Ranges at Black Butte in an abandoned cirque formed during Pleistocene glaciation (Bishop, 1977; Irwin, 1960). These rocks are reconstituted to textural zone 2 of Blake and others (1967), but reconstitution increases to textural zone 3 northward, with increasing topographic elevation. The textural zone 2 metasandstone contains only small amounts of pumpellyite and lawsonite. At Bald Mountain, the metasandstone is largely medium to coarse grained with lenses of stretched-pebble conglomerate that structurally overlies finer grained, laminated metasandstone and argillite containing blocks and lenses of foliated mafic volcanic rocks and gabbro. Finer grained, lower Pickett Peak terrane rocks are well exposed in the headwaters of the Eel River and the Cushman Lake-Hells Half Acre area (see map, sheet 1). The coarser-grained metasandstone at Bald Mountain is exposed along the Hull Mountain Road and north of Devils Rock Garden. A large mass of fine-grained to pegmatitic, foliated metadiabase, possibly intrusive into the Bald Mountain rocks, is present just north of Bald Mountain peak at Coyote Rock in the Plaskett Ridge 7.5′ quadrangle (fig. 3, sheet 1). The thickness of the structural outlier of Pickett Peak rocks at Bald Mountain is approximately 700–1,000 m, significantly less than at Black Butte. Crosscutting foliations and associated fold trends indicate the Pickett Peak terrane to have undergone multiple periods of deformation, although only one high P/T metamorphic event is evident petrographically (Ohlin and others, 2010). Petrographic evidence suggests that the fold trends and planar fabrics in Pickett Peak rocks at Bald Mountain are younger than the high P/T metamorphic event in these rocks (Ohlin and others, 2010).

Numerous Early Cretaceous (~Aptian–Valanginian), whole rock K-Ar dates, generally interpreted as maximum metamorphic ages because of incomplete recrystallization of grains in these rocks to new metamorphic minerals, have been reported for metasandstone from the Black Butte and Bald Mountain rocks. Suppe and Armstrong (1972) dated three samples of metagraywacke in the vicinity of Black Butte that yielded ages of 127, 125, and 123 Ma. Lehman (1974) reported ten whole-rock dates from south of Black Butte ranging from 129 to 119 Ma and three dates from the Bald Mountain area of 138, 133, and 127 Ma. Both Lehman (1974) and Lanphere and others (1978) indicate that their ages cluster around 120 Ma, suggesting a regional metamorphic event in the Early Cretaceous (~Aptian). This agrees with recent U/Pb detrital zircon ages from metachert and with $^{40}Ar/^{39}Ar$ metamorphic ages—both from the South Fork Mountain Schist of the Pickett Peak terrane (Dumitru and others, 2009). This metamorphic age is considerably older than the Cenomanian depositional age (about 99–94 Ma) of lawsonitic metasandstones in the Yolla Bolly terrane, implying that the Yolla Bolly terrane was subjected to later high P/T metamorphism, as well as younger metamorphic textural reconstitution than seen in the Pickett Peak terrane. The later blueschist metamorphism in the Yolla Bolly terrane may have overprinted earlier blueschist metamorphism in the Pickett Peak rocks, which is consistent with field and petrographic observations (Ohlin and others, 2010).

Mendocino Pass Terrane (Lower Cretaceous, Valanginian)

This unit is present only in the northeastern part of the map area, in two fault-bounded wedges between mélange of the Central Belt and structurally overlying schistose rocks of the Pickett Peak terrane. Ohlin and others (2010) tentatively assigned these rocks to the Pickett Peak terrane as possibly correlative with the Valentine Spring Formation of Worrall (1981) and Blake and others (1992), but here, we describe the rocks separately as the Mendocino Pass terrane of the Eastern Belt. Regionally, the Mendocino Pass terrane occurs as a structural wedge composed of slightly sheared, moderately foliated metasandstone and interbedded argillite, with rare structurally interleaved lenses of metachert and greenstone. The unit is distinguished by its uniform, coherent nature, in contrast with the underlying mélange of the Central Belt, and by a moderate foliation, differing from the pronounced foliation and recrystallized metamorphic character of structurally overlying schist in the Pickett Peak terrane. *Buchias* that occur in a small, structurally isolated slab of the metasedimentary rocks of Mendocino Pass terrane along the road between Hells Half Acre and Bean Rock, about 0.4 mi (0.6 km) south of Calamese Rock, are Early Cretaceous (Valanginian) in age (see fossil localities, table 1; also see Ohlin and others, 2010, and locality 29 of Blake and Jones, 1974). The fossils occur with clasts of volcanic breccia, as much as 12 cm in diameter, dispersed in sheared metasandstone. Given the recent demonstration that some *Buchia* localities in Eastern Belt Franciscan rocks are redeposited (Dumitru and others, 2010, 2015), the fossils in this breccia unit may be problematic for dating deposition, which could actually be considerably younger than the fossils. Correlation of this isolated structural slab to the Mendocino Pass terrane is based on the uniform and characteristic metamorphic grade and composition of the metasandstone, its structural position beneath the metasandstone and metavolcanic rocks of the Pickett Peak terrane, and its position above mélange of the Central Belt. The thrust-fault contact between the Mendocino Pass terrane and overlying Pickett Peak terrane

rocks is marked by shearing and (or) serpentinite. Relations found in similar rocks to the northeast (Bishop, 1977; Blake and others, 1967), however, suggest that the Mendocino Pass terrane rocks may have once increased in metamorphic grade gradually structurally upward toward the base of the Pickett Peak terrane, in the sense of Blake and others (1967). In the map area, significant parts of this intervening metamorphosed section are apparently missing and possibly were structurally removed by later low-angle faulting that post-dated metamorphism and accompanied unroofing and exhumation of the Franciscan Complex. If so, then metamorphism of the Mendocino Pass and Pickett Peak terranes must have post-dated the Early Cretaceous (Valanginian, 140–136 Ma) or younger depositional age of the metasedimentary rocks of Mendocino Pass and predated the later structural erosion occurring during unroofing and exhumation of the Franciscan Complex.

Coast Range Ophiolite (Upper and Middle Jurassic)

The Coast Range ophiolite consists of layered and unlayered ultramafic and gabbroic rocks, mafic sills and dikes, pillowed basaltic flows and flow breccias, pelagic chert, and local mafic aquagene tuff that are broadly interpreted as the oceanic basement of the Great Valley complex. These ophiolitic rocks locally underlie the Elder Creek terrane of the Great Valley complex depositionally. We interpret the Coast Range ophiolite here to have formed in a mantle wedge within a supra-subduction setting, rather than at a mid-ocean-ridge spreading center (for example, Ernst and McLaughlin, 2012). Much of the original section of the Coast Range ophiolite is missing in the map area and the ophiolite is highly modified by Cretaceous and younger tectonism, uplift, and erosion that gave rise to sedimentary serpentinite (unit Kssp), ophiolitic mélange (unit KJom), and megabreccia (unit Jgb) at the base of the Great Valley (Elder Creek terrane) sedimentary section. Some serpentinized ultramafic rocks may have been remobilized as diapirs and locally extruded onto the seafloor in the Cretaceous and even later along younger faults during Tertiary and Quaternary deformation events. One such diapir is present along the Bartlett Springs Fault Zone at Coyote Rocks just north of Lake Pillsbury, where the serpentinite has been mobilized and intrudes Pleistocene terrace and fan deposits along the Bartlett Springs Fault Zone (Ohlin and others, 2010; Moore and others, 2015).

Great Valley Complex

Elder Creek Terrane of the Great Valley Complex (Lower Cretaceous and Upper to Middle Jurassic)

As defined on the geologic map of the Red Bluff 30′ × 60′ quadrangle (Blake and others, 2000), the Elder Creek terrane consists of the Middle to Upper Jurassic oceanic basement of the Great Valley complex (the Coast Range ophiolite plus serpentinite matrix mélange), overlain unconformably by Upper Jurassic to Lower Cretaceous strata of the Great Valley complex, locally exhibiting a basal, coarse megabreccia derived from the Coast Range ophiolite at the base. These rocks are collectively folded, sheared, and complexly faulted. Overlapping younger Cretaceous strata of the Great Valley complex are less severely deformed. In the map area, Upper Jurassic to Lower Cretaceous sedimentary serpentinite locally makes up a significant component of the Elder Creek terrane.

To the south of the map area, between Lake Berryessa and San Francisco Bay, Elder Creek terrane rocks appear to be divisible into three fault-bounded structural domains (Graymer and others, 2002a): (1) a domain of disharmonically folded and broken, thin- to medium-bedded mudstone, sandstone, and conglomeratic turbidites, underlain by (2) a discontinuous domain of sheared and broken serpentinized peridotite with sheared screens of microgabbro or amphibolitic dike rocks overlain in places by cumulate gabbro ± microgabbro ± basaltic intrusives ± pillowed basalt flows and flow breccia, in turn, underlain by or grading laterally into (3) a domain of ophiolitic mélange, including blocks of basaltic rocks, gabbro, intact slabs of less-sheared serpentinite and gabbro, and also slabs of intact but complexly folded or sheared Elder Creek terrane sedimentary rocks, all of which are enclosed in a penetratively sheared and gouged serpentinitic or argillitic matrix. In the map area, we have not separately mapped a domain of disharmonic folding but recognize its presence. It is not clear on our map if there is a distinct separation between the folded and mélanged domains everywhere that can be mapped regionally at the same structural levels or whether there is structural repetition vertically or lateral transitioning between domains 1–3 defined above. On our map, disharmonically folded, broken ophiolitic and mélanged ophiolitic domains are incorporated into a single unit of ophiolitic mélange.

Structural Relations

Major Faults

Coast Range Fault

Throughout the California Coast Ranges, the fundamental fault boundary between subducted Mesozoic rocks of the Franciscan Complex and overlying exhumed basement of the Great Valley complex (the Coast Range ophiolite) is referred to as the Coast Range Fault. The Coast Range Fault was originally characterized (Bailey and others, 1970) as the hanging-wall-thrust boundary between the subducted rocks of the Franciscan Complex and Mesozoic strata deposited in the overlying Great Valley fore arc, with the Coast Range ophiolite representing the Jurassic oceanic basement on which the Great Valley complex was deposited. Later work, however, has shown that this fault boundary has a more complex history that involved major low-angle normal faulting associated with unroofing of the subduction complex (Jayko and others, 1987), followed by east-vergent, tectonic wedging initiated during the Late Cretaceous and early Tertiary Laramide orogeny (Ernst and McLaughlin, 2012), followed by an even later period of transpression. Characterization of the Coast Range Fault as a Mesozoic thrust, therefore, is a misleading oversimplification. Here and on other recent maps and reports by others (Platt, 1986; Jayko and others, 1987; Blake and others, 2000), this boundary is referred to as the Coast Range Fault, recognizing that the fault has a complex history involving subduction overprinted by major later extensional and compressional deformation.

Much disruption of the Coast Range Fault was imposed in the Tertiary, beginning before and continuing during the development of the San Andreas transform system. The origin(s) and evolution of the

later disruption of the Coast Range Fault is very poorly understood, but it has played a key role in the development and evolution of the Northern Bartlett Springs Fault Zone, which has evolved from the Coast Range Fault. The later development of the Bartlett Springs Fault system substantially obliterated initial kinematic relations along major parts of the Coast Range Fault southwest of Wilbur Springs. For this reason, we label the Coast Range Fault along the west side of the Coast Range ophiolite only north of the Wilbur Springs antiform, although we acknowledge that segments of the Coast Range Fault are likely incorporated into, but overprinted by, Tertiary transpression along the Bartlett Springs Fault Zone.

Bartlett Springs Fault Zone

The Bartlett Springs Fault Zone, a major active and creeping fault, is the easternmost major fault of the San Andreas transform system in this part of northern California. Though it was recognized as seismically active in the 1980s (Depolo and Ohlin, 1984; Bolt and Oakeshott, 1982; Eberhart-Phillips, 1988), its role as a significant, active, creeping member of the San Andreas Fault system linking the active Cascadia subduction margin north of Cape Mendocino with the inboard part of the transform margin has been recognized only in recent years (Lienkaemper, 2010; Murray and others, 2014; Lozos and others, 2015). Details of how the Bartlett Springs Fault Zone evolved from an active member of the former subduction margin south of the Mendocino Triple Junction to its present role as a right-lateral strike-slip fault is poorly understood, partly because the fault-zone history has evolved over a long time span beginning as early as the Miocene, and it appears to have reactivated parts of Paleogene and older fault boundaries associated with subduction.

Detailed descriptions of numerous segments of the Bartlett Springs Fault Zone have been presented by Ohlin and others (2010) in the Lake Pillsbury region. For the more regional map of this report, however, we divide the Bartlett Springs Fault Zone into the Northern and Southern Bartlett Springs Fault Zone segments (fig. 5, sheet 2) that differ in their long-term history and expression as crustal features. We contrast the character of these segments of the fault zone and discuss how the two segments may have evolved structurally. The Southern Bartlett Springs Fault Zone is also referred to as the Berryessa Fault, which is described mainly on the basis of its late Quaternary expression and history (Lienkaemper, 2010). The Southern Bartlett Springs Fault Zone also includes several previously named local faults, including the Wilson Valley and Hunting Creek Faults (Lawton, 1956).

The Bartlett Springs Fault Zone continues southeastward and is now linked to faults of the eastern San Francisco Bay dextral fault system, having a Miocene and younger cumulative displacement of 170 km (McLaughlin and others, 1996; Graymer and others, 2002b). The fault zone apparently represents the northeastern boundary of the Humboldt Plate of Herd (1978), although Herd did not recognize the significance of strike-slip faulting along the Bartlett Springs Fault Zone and, instead, assigned the northeast boundary of his Humboldt Plate to the Maacama Fault south of Round Valley. Of further significance to the long-term evolution of the Bartlett Springs Fault is that it appears to follow and to have reactivated segments of the broad, highly sheared east fault boundary of the Central Belt of the Franciscan Complex, particularly in the eastern Coast Ranges north of Round Valley (fig. 4, sheet 1).

Northern Bartlett Springs Fault Zone

The Northern Bartlett Springs Fault Zone extends across nearly the entire length of this map area, from its northern boundary in Round Valley to Cache Creek, south of Highway 20 and southwest of Wilbur Springs. North of Highway 20, the Northern Bartlett Springs Fault Zone consists of numerous straight to somewhat curvilinear northwest-trending, right- and left-stepping fault segments and splays that we interpret to follow the dextrally sheared and translated axial area of the Bartlett Springs Synform (figs. 5, 6, 7, sheet 2). The fault zone is also partly aligned along the southwest limb of a major antiform (the Wilbur Springs Antiform) northeast of the fault and is subparallel to a relict part of the Bartlett Springs Synform and the en echelon Pacific Ridge Antiform farther to the northeast (figs. 5, 6, 7, sheet 2). The original synformal and antiformal geometry of bedrock in the southern part of the map area becomes increasingly obscured northwestward between Wilbur Springs and Lake Pillsbury due to dextral dismemberment of the Bartlett Springs Synform along the Northern Bartlett Springs Fault Zone (McLaughlin and Moring, 2013).

The Northern Bartlett Springs Fault Zone cuts upper Pleistocene–Holocene deposits in Lake Pillsbury basin, which appears to have formed as a right-stepped or releasing bend structure along the creeping section of the fault. Just north of the map area in Round Valley near Covelo, the fault zone again takes a right step that has resulted in the Round Valley pull-apart structure, filled with Holocene and Pleistocene sediment (Jayko and others, 1989). Southeast of Lake Pillsbury, the Northern Bartlett Springs Fault Zone structurally entrains or isolates thin accumulations of Pleistocene or younger alluvial deposits, stream terraces, alluvial fans, and abandoned meanders as indicated by geomorphic features in Rice and Twin Valleys, Soap Creek, Bartlett Creek, Wolf Creek, and North Fork Cache Creek. Northeast of State Highway 20 and High Valley, the fault zone is aligned along and truncates the east side of fluvial and lacustrine sediments of the Pliocene–Pleistocene Cache Formation, which forms a prominent structural basin southwest of the Northern Bartlett Springs Fault (McLaughlin and others, 1990; Hearn and others, 1995; Rymer, 1981). Southeast of Highway 20 and Grizzly Spring, youthful fault morphology steps ~2.5 km to the southwest across North Fork Cache Creek to the Southern Bartlett Springs Fault, which is aligned mostly with various bedrock contacts between ultramafic rocks of the Coast Range ophiolite and sedimentary units of the lower Great Valley complex. The Cache Formation is also involved in the faulting in the right-stepped area between the Northern and Southern Bartlett Springs Faults (Gaines, 2008). Southeast of the step to the Southern Bartlett Springs Fault, the Northern Bartlett Springs Fault continues southeastward into the Lower Cretaceous section of the Great Valley complex. No data are presently available to evaluate the possibility that some Quaternary faulting may be partitioned farther to the southeast along the Northern Bartlett Springs Fault. Previous mapping of Quaternary fault features by Lienkaemper (2010) does not recognize young faulting on the Northern Bartlett Springs Fault southeast of the step-over to the Southern Bartlett Springs zone.

Displacement on the Northern Bartlett Springs Fault

Although clearly definitive field criteria are lacking, geologic relations along the Northern Bartlett Springs Fault Zone suggest large, long-term dextral displacement estimated at ≥37–50 km at

~3–4 mm/yr since the Miocene (McLaughlin and others, 2010; McLaughlin and Moring, 2013). Estimate of the approximate amount and timing of displacement on the Northern Bartlett Springs Fault Zone is based on a fragmentary knowledge of Late Cretaceous to Neogene paleogeography and on the structural evolution of the northern California margin. This area has transitioned from a largely convergent, east-dipping, thrust-fault-dominated subduction margin in the latest Cretaceous to early Cenozoic to one of west-stepped subduction and east-vergent crustal wedging in the Paleogene. This was accompanied by major Paleogene uplift, unroofing, and erosion of previously subducted rocks of the Franciscan Complex and the western Great Valley fore arc. The distribution and configuration of Coast Range ophiolite, Great Valley complex, and Franciscan Central Belt rocks west of Sacramento Valley, at Wilbur Springs and in the Geysers-Clear Lake region, suggest that convergence and crustal wedging was oblique to the margin at this time, resulting in dextral displacement and folding along the Great Valley fore-arc and subduction margin (Franciscan Complex) interface (McLaughlin and others, 1988). Between the Eocene and middle Miocene, this was followed by development of a west-stepped fore-arc basin deformed by Miocene and younger northwest-southeast-oriented transpressional folds (figs. 6, 7, sheet 2). Regionally, the transpressional folding appears to have developed ahead, or north, of the northwardly propagating Mendocino Triple Junction and San Andreas Fault system (fig. 6). The Northern Bartlett Springs Fault traverses and right-laterally dismembers the Bartlett Springs Synform that is subparallel to, and probably formed with, folding that developed between the Eocene and middle Miocene. The reconstructed former Bartlett Springs Synform forms the southwest flank of a southeast-plunging antiformal warp (the Wilbur Springs Antiform) along the current southwest margin of the Great Valley. The dismembered, former Bartlett Springs Synform and southwest flank of the Wilbur Springs Antiform, together with several subparallel warps in the core of the antiform (fig. 6; fold axes 1–3 in fig. 7), collectively define a composite structure that is here referred to as the "Wilbur Springs Dextral Hook" (figs. 6, 7, 8, sheet 2). These structures will be discussed further in the section on folding.

Approximate paleogeographic reconstruction of the former Mesozoic to Eocene Great Valley and later Neogene fore-arc basins, coupled with interpreting the sequence of subsequent transpressional folding and dextral dismemberment of the Bartlett Springs Synform, provides a crude basis for estimating long-term displacement along the Northern Bartlett Springs Fault (figs. 6, 7; see also later discussions of the Bartlett Springs Synform and Wilbur Springs Dextral Hook). In restoring the pre-Northern Bartlett Springs Fault configuration of the Bartlett Springs Synform, we relate similarities in the stratigraphies of several remnants of Great Valley complex, dismembered along the Northern Bartlett Springs Fault, that formerly were associated with the westernmost edge of the Great Valley fore-arc basin. Important relations in these stratigraphic remnants include correlative fossil assemblages of Lower Cretaceous (Hauterivian) cold-seep deposits, the presence of Paleocene and Eocene strata deposited unconformably on Cretaceous and older Great Valley complex rocks, and Miocene marine strata deposited in the former Neogene fore-arc basin (Nilsen and Clarke, 1989). We consider the slip restoration along the Bartlett Springs Fault in figure 7 to provide the minimum estimate of fault displacement (~38–45 km) needed to restore the original geometry of the former Bartlett Springs Synform, although larger displacement >50 km is also possible. Although not present in Rice Valley or farther south, Miocene estuarine strata in Round Valley, associated with the uplifted and eroded southeastward extension of the Eel River fore-arc basin (Nilsen and Clarke, 1989), are interpreted to provide a maximum post-folding (~middle Miocene, 15–12 Ma) age for initiation of Northern Bartlett Springs faulting and a minimum long-term displacement rate of 2.5–3.9 mm/yr. A permissive larger minimum displacement of 50 km since 15–12 Ma yields a slip rate of 3.3–4.2 mm/yr. This admittedly crude estimate in the range of long-term slip (~2.5–4.1 mm/yr or ~3.35±0.85 mm/yr) is low in comparison to the rate of Holocene slip of 6±2 mm/yr (Lienkaemper, 2010; Lienkaemper and others, 2014) but similar to repeated Global Positioning System (GPS) measurements across the fault that yielded a rate of 3.1±0.2 mm/yr along the creeping segment of the Northern Bartlett Springs Fault at Lake Pillsbury (Murray and others, 2014).

Lake Pillsbury Releasing Bend

The releasing bend or pull-apart that forms Lake Pillsbury basin has been considered to be a possible barrier to through-going fault rupture (DePolo and Ohlin, 1984; Geomatrix Consultants, 1986; Lienkaemper, 2010; Sibson, 1985). The structural geometry of the Gravelly Valley (Lake Pillsbury) basin is well constrained from geologic mapping by Ohlin and others (2010). Gravity and aeromagnetic data (Langenheim and others, 2007, 2011) further indicate that the basin is about 2.5 km wide and 5 km long and underlain by a roughly 400-m-thick section of sediments (Langenheim and others, 2007). Magnetic data shows the fault trace below Lake Pillsbury as continuous, with a 30° right bend (Langenheim and others, 2007). Faulted, basinward-tilted, and uplifted Pleistocene gravels are exposed in road cuts at Logan Spring, along the Northern Bartlett Springs Fault southwest of Scott Dam.

Several prominent flights of old terraces that border the east and southwest sides of Gravelly Valley (Ohlin and others, 2010) are recognized as "strath terraces" (planar terraces eroded into bedrock). These strath terraces are interpreted to record a period during which ongoing subsidence of the Gravelly Valley alluvial basin was punctuated by temporally stable times, allowing the Eel River to erode bedrock along the east and west sides of the basin. Based on the degree of weathering observed along these strath surfaces the terraces are estimated to be upper and middle Pleistocene (tens to hundreds of thousands of years old; Ohlin and others, 2010).

Lidar-derived elevation data collected along the Northern Bartlett Springs Fault Zone (Metro Engineering, 2011) were used to evaluate Quaternary deposits in the Lake Pillsbury basin as part of this mapping effort. Some previously mapped Quaternary deposits (Ohlin and others, 2010) in the vicinity of Scott Dam were remapped by Hitchcock in this study using lidar data and field checked during field reconnaissance work in December 2014.

Tectonic geomorphology along the Northern Bartlett Springs Fault Zone suggests a dominantly right-lateral sense of displacement, including a mix of east- and west-facing scarps and dextral stream deflections. Evidence of secondary displacement on normal faults is present locally at Gravelly Valley (Lake Pillsbury basin), which is bounded by right-stepping normal faults. Secondary normal faults are also present at a right step in the fault at Round Valley and at Twin Valleys near Bartlett Springs, where fault-bounded sediments are ponded on the down-thrown side of the fault trace. Evidence for reverse faulting is indicated just north of Lake Pillsbury at the location

of a fault-creep-monitoring array, where left-stepping cracks in the asphalt road crossing the main fault zone and creep array clearly indicate active transpressional surface deformation.

A 2- to 3-m-wide shear zone, composed largely of diapiric serpentinite, forms a natural exposure of the western strand of the Northern Bartlett Springs Fault (fig. 9) and offsets the uppermost Pleistocene terrace gravels of Salmon Creek, north of Lake Pillsbury, and the creep array (Moore and others, 2015; Ohlin and others, 2010; Lienkaemper, 2010). The prominent, 183-m-long, 6.1-m-high stream-bank exposure of the fault is located about 250 m north of Coyote Rocks (figs. 9, 10). The exposure is evident in terrestrial lidar scanning (TLS) imagery and at least three lithologic units are exposed in the stream bank (fig. 10). The oldest unit (fig. 10*C*, unit 1) is serpentinitic bedrock located within the several-meter-wide fault zone. Moore and others (2011, 2015) interpreted this unit as tectonically entrained from considerable depth and to have risen to the ground surface along an active strand of the Northern Bartlett Springs Fault Zone (the Coyote Rocks strand). The next youngest unit (fig. 10*C*, unit 2) is a moderately well stratified sequence of sand and gravel with lenses of sand and imbricated gravels recording deposition in a bar-and-swale setting similar to the morphology of the adjacent streambed. Stratification of unit 2 defines an apparent dip of about 30° S. Soil profiles are absent within unit 2, indicating rapid deposition. Unit 2 is overlain by unit 3 (gravel and sand similar lithologically to unit 2) along a prominent, wavy, angular unconformity that truncates stratification. A soil profile is developed in unit 3, but it does not obscure the sandy texture and common gravel strings in the unit. Units 2 and 3 are present on both sides of the fault zone (figs. 9, 10).

Near-surface fault orientation was documented at Lake Pillsbury by Geomatrix Consultants (1986) in a trench near the above-described exposures across the Coyote Rocks Fault strand. The trenching exposed a fault plane dipping 65° NE. with slickensides plunging at 15° SE. Assuming that slip was dextral, this suggests east-side-down, oblique-normal displacement. This relation, together with the active transpression exhibited at the creep array site a short distance to the southeast and the overall releasing bend geometry of Lake Pillsbury basin, points to a high degree of along-strike fault-zone complexity.

Seismicity of the Northern Bartlett Springs Fault Zone

Microseismic data predating 2012 indicate that the Northern Bartlett Springs Fault Zone dips steeply east (at about 70–85°) between Lake Pillsbury and Bartlett Springs (figs. 11, 12; also see fig. 5, sheet 2), and some focal mechanisms from the microseismicity suggest normal (transtensional) strike slip, consistent with east-side-down displacement. An east-side-down sense of displacement, however, is inconsistent with the apparent long-term, west-down sense of displacement suggested by higher elevations and erosional relief on the east side of the Northern Bartlett Springs Fault Zone, as well as mapped structural relations across the fault zone southeast of Lake Pillsbury. The modern topographic relief might be interpreted as merely reflecting a previous compressional tectonic setting now overprinted by normal faulting. As outlined below, however, it is likely that focal mechanisms that indicate steeply dipping fault planes for many of the small earthquakes (generally ≤M 3.0) along the Northern Bartlett Springs Fault have large uncertainties in the dip and dip direction, inherent in fault plane solutions. We, therefore, view

Figure 9. View southeast at serpentinite diapir in Bartlett Springs Fault Zone north of Coyote Rocks and Lake Pillsbury. Diapir and faulting cuts tilted and flat-lying Pleistocene deposits. See discussion of diapir.

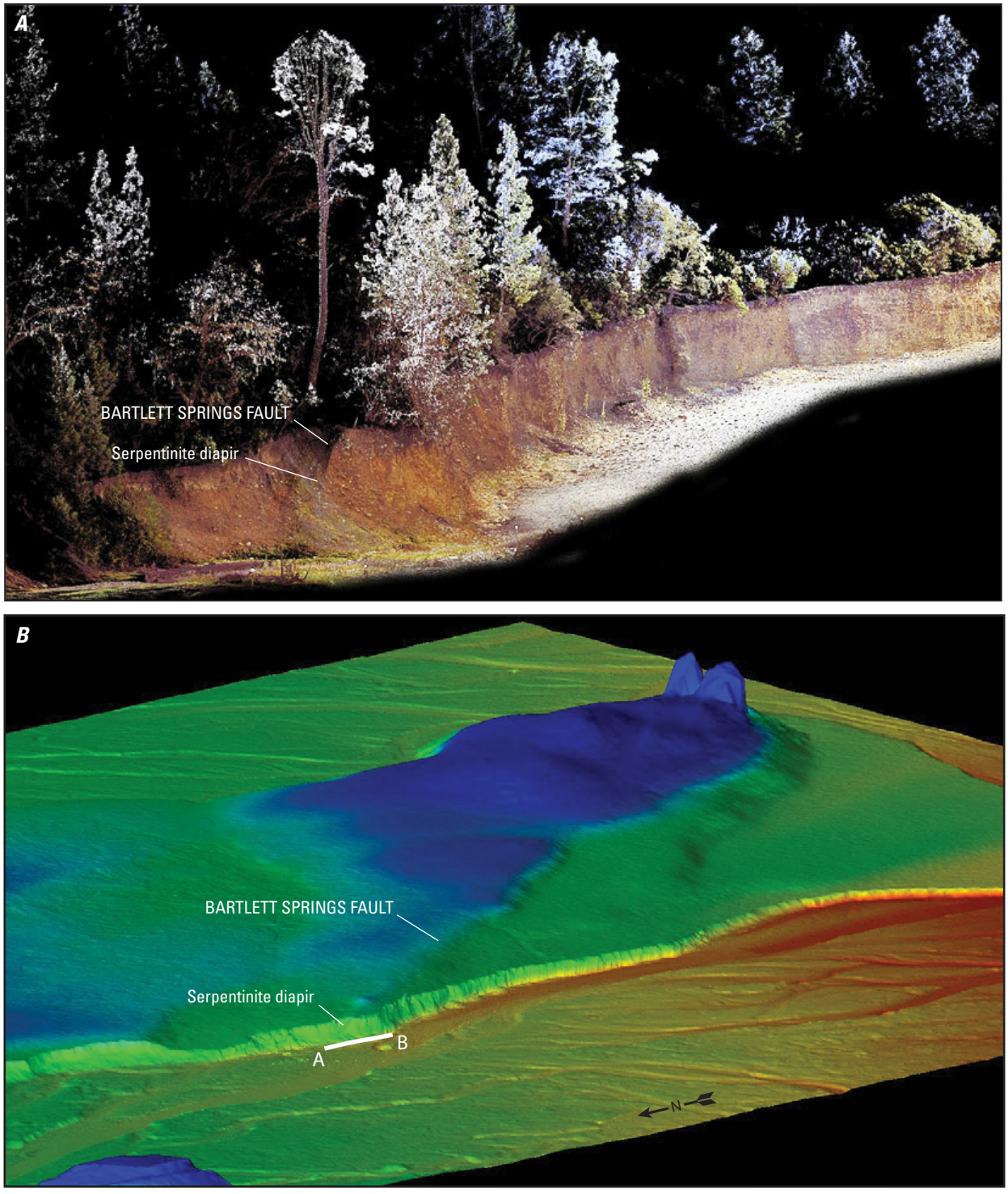

Figure 10. Views southeast across Bartlett Springs Fault Zone north of Coyote Rocks, distinguished by serpentinite diapir within stream-cut exposure along Salmon Creek. Fault cuts Quaternary fluvial gravels, an overlying paleosol, and younger flat-lying stream terrace deposits. *A*. Terrestrial lidar point cloud image, looking southeast across Salmon Creek, from a survey across the Bartlett Springs Fault Zone. *B*. A color-relief map from merged terrestrial and aerial lidar datasets, showing location of serpentinite diapir exposure along Salmon Creek and expression of surface fault scarp in the Bartlett Springs Fault Zone. Heavy white line indicates approximate northwest (A) and southeast (B) ends of stream-cut view in figure 10*C*. *C*. Orthorectified photomosaic of stream-cut exposure of three Quaternary units cut by serpentinite diapir and Bartlett Springs Fault. See text for discussion of stratigraphy (numbered units).

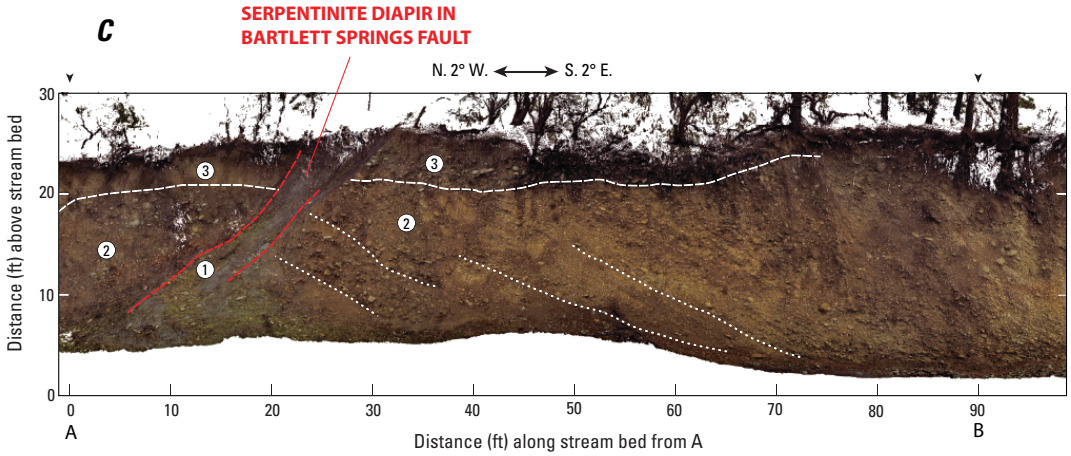

Figure 10.—Continued

the dip directions based only on the focal mechanisms as suspect, especially when compared to mapped structural relations across the Northern Bartlett Springs Fault.

Earthquakes along the Northern Bartlett Springs Fault commonly range in magnitude from <M 1.0 to >M 4.0, with hypocenters that reach ≥12 km (fig. 11; figs. 1, 4, sheet 1)—significantly deeper than earthquakes on active faults to the west, such as the Maacama Fault. Focal mechanisms of Northern Bartlett Springs Fault earthquakes (mostly ≤M 3.0) favor dominant dextral strike slip, but as indicated above, include focal mechanisms having normal slip components. Although earthquakes large enough to have multiple aftershocks have not previously been recorded, a M 5.1 event followed by numerous aftershocks (figs. 11, 12, sheet 2) within the area of most frequent previous microseismicity occurred on August 10, 2016. The focus of this earthquake was 14.3 km (moderately deep for a strike-slip event). Based on the orientations of faults mapped at the surface, the first motion data for this earthquake favor a right-lateral fault plane oriented parallel to the surface trace of the Northern Bartlett Springs Fault, dipping steeply to the southwest (80°, with a dip uncertainty of 45°) and up on the northeast side (https://earthquake.usgs.gov/earthquakes/eventpage/nc72672610#focal-mechanism). We plot the location of the double-differenced M 5.1 event together with its aftershocks and associated double-differenced previous microseismicity in figure 11 (Waldhauser and Schaff, 2008; see http://ddrt.ldeo.columbia.edu). Double-differenced relocation of the main shock places the hypocenter at a depth of 11.3 km (fig. 11; fig. 12, sheet 2).

Notably, the hypocenter of the 8/10/16 main shock and aftershocks (see fig. 13) and earlier Northern Bartlett Springs Fault microseismicity are mainly east of the surface traces of the Northern Bartlett Springs Fault Zone. In seismicity cross sections (fig. 12, sheet 2), these earthquakes are seen to define a distinct ~70–85° northeast-dipping zone of seismicity south of Lake Pillsbury that extends to within a few kilometers of the surface beneath the Northern Bartlett Springs Fault. We interpret this to indicate that the fault zone is predominantly a steeply northeast-dipping right-lateral reverse structure that is up to the northeast, in spite of the steep southwest dip implied by the 8/10/16 earthquake focal mechanism. The 45° uncertainty in dip from the 8/10/16 event first-motion data, with a focal mechanism dip direction opposite to that indicated by aftershock and other microseismicity distribution, suggests that the focal mechanism dip direction is incorrect. A moment tensor data plot further suggests a steep northeast dip for the favored northwest-striking fault plane (https://earthquake.usgs.gov/earthquakes/eventpage/nc72672610#moment-tensor). We therefore consider the fault geometry defined by depth location of the main shock and associated microseismicity as a more reliable indicator of the geometry of the Northern Bartlett Springs Fault Zone than the dip suggested by first-motion data. The fault-zone geometry implied by the depth distribution of the double-differenced earthquakes (figs. 11, 12), moreover, is consistent with the structural framework indicated by our geologic mapping along the fault. The distribution of microseismicity associated with the northeast and southwest sides of the Northern Bartlett Springs Fault north of Lake Pillsbury, however, indicates that the fault-zone geometry is more complex in that area. The local releasing-bend geometry of the Northern Bartlett Springs Fault and associated fault splays, such as the Logan Springs Fault, that offset Pleistocene deposits at Lake Pillsbury (fig. 5, sheet 2; Ohlin and others, 2010), as well as local restraining bends along the length of the Northern Bartlett Springs Fault Zone, further point to fault-zone complexity. These surface features indicate local extensional and compressional patches that possibly are, in part, related to vertical and lateral irregularities in fault orientation and fault rock textural and compositional variations and fluid distribution at depth. The observed variations in slip character along the length of the Northern Bartlett Springs Fault Zone might be characteristic of dipping fault zones that have experienced long-lived structural histories in which the forces driving fault slip have changed over time. In the case of the Northern Bartlett Springs Fault, this change was likely associated with the transition from dominant subduction to right-lateral strike slip.

Fault Creep along the Northern Bartlett Springs Fault

Recent geodetic work (McFarland and others, 2016; Murray and others, 2014) has documented fault creep (fig. 5, sheet 2; fig. 7)

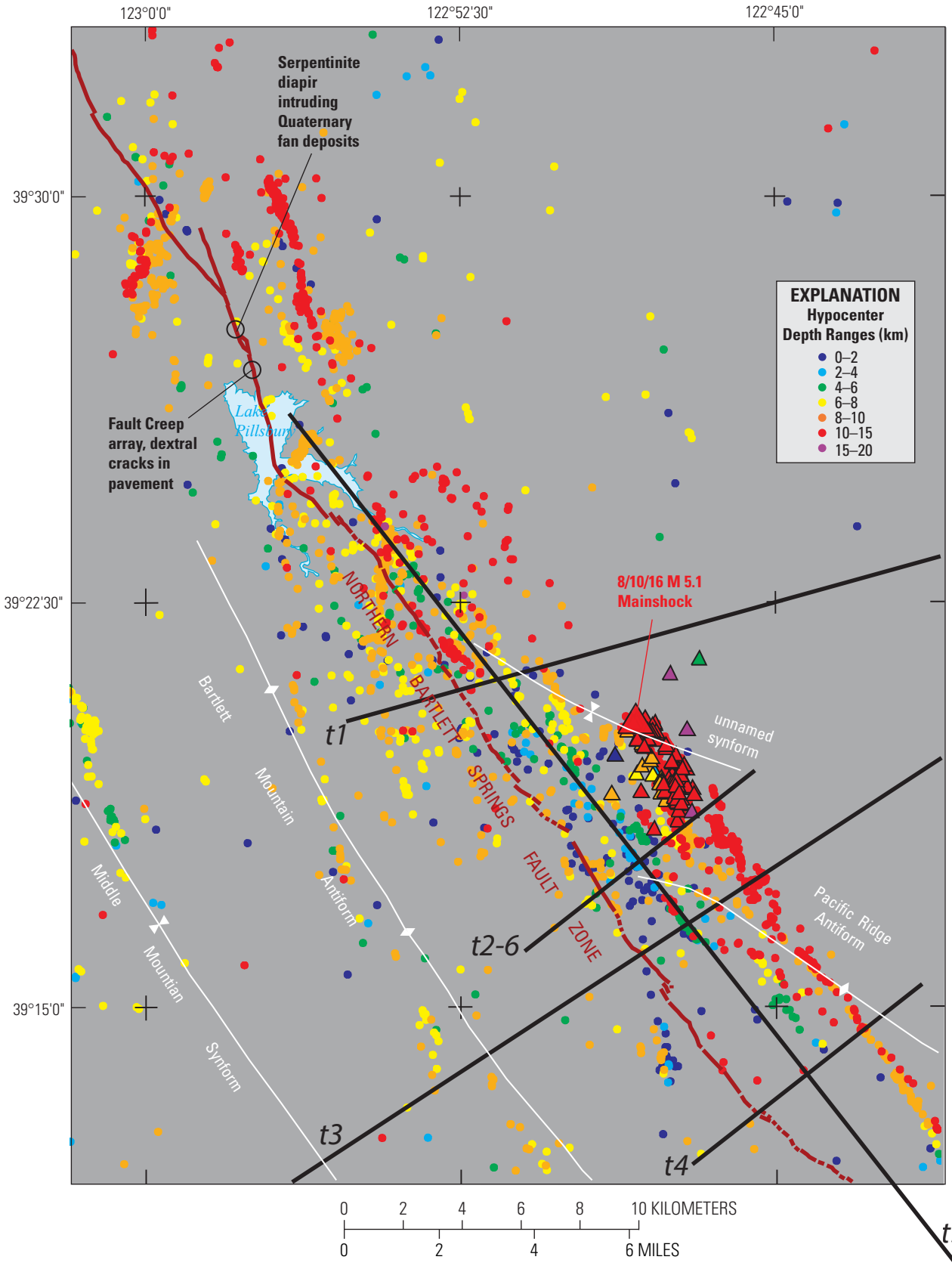

Figure 11. Map of double-differenced locations for epicenters of the main shock (large triangle) and aftershocks (smaller triangles) of the August 10, 2016, M 5.1 earthquake on the Northern Bartlett Springs Fault. In addition, we plot the double-differenced distribution of post-1984 microseismicity (small dots); epicenters are color indexed according to their hypocentral depth in kilometers. Earthquake locations are from the Real-Time Double-Difference Earthquake Locations for Northern California (Waldhauser and Engebreth, 2016). Fold axes and surface traces of the Northern Bartlett Springs Fault are from map (sheet 1) and figure 5 (sheet 2). Seismicity cross-section lines show earthquake hypocenters explained in figure 12 (sheet 2): cross section t1 corresponds to a part of structure cross section *B*–*B*′–*B*″; cross section t3, to a part of structure cross section *C*–*C*′; and cross section t5 to a part of structure cross section *E*–*E*′.

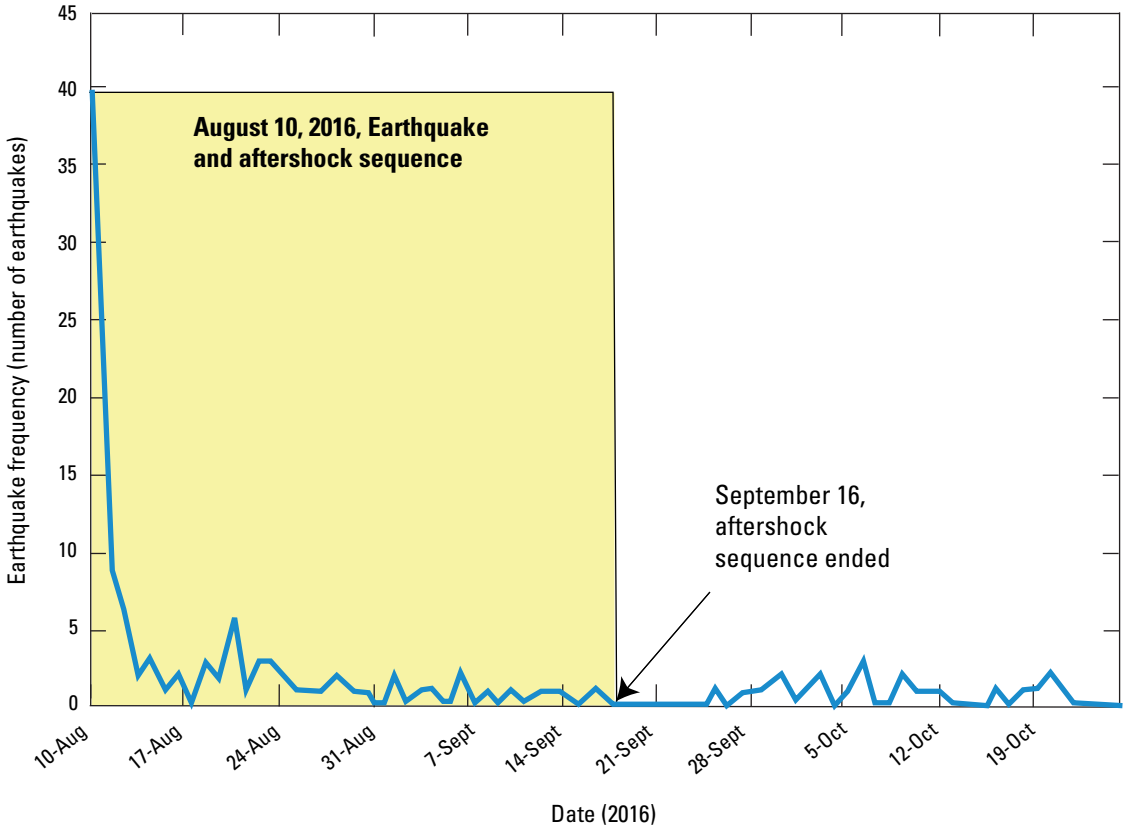

Figure 13. Histogram showing main shock and aftershocks defining the August 10, 2016, earthquake sequence on the Northern Bartlett Springs Fault Zone. Aftershocks continued in the area of the August 10 main shock at a low level until September 16, after which microseismicity lapsed for about 10 days before resuming in the area. For our purposes, the distinct lapse in microseismicity following September 16 approximately defines the end of the August 10 earthquake sequence.

along a segment of the Northern Bartlett Springs Fault at the north side of Lake Pillsbury basin just north of the lake and south of the serpentinite diapir described above (figs. 9, 11, 12). Here, the creeping fault segment has produced a 1.5-m-wide zone of left-stepped (transpressional) en echelon cracks where the fault zone crosses the asphalt road around the lake (Moore and others, 2015; Ohlin and others, 2010). Repeated measurements of the alignment array and GPS measurements across the zone of creep indicate an average shallow creep rate of 3.2±0.1 mm/yr (McFarland and others, 2016, ver. 1.8, table 1b; McFarland and others, 2009, ver 1.0, was cited in Murray and others, 2014), about half of the estimated Holocene slip rate of 6±2 mm/yr (Moore and others, 2015; Lienkaemper, 2010; Lienkaemper and others, 2014) for the northern plus the southern segments of the Bartlett Springs Fault. Below the locking depth of the fault, at ~5–13 km, the creep rate is estimated at 7.7±2.4 mm/yr (Murray and others, 2014).

Southern Bartlett Springs Fault Zone

Southeast of State Highway 20 near Grizzly Spring, a 2.5-km right step separates the northern and southern Bartlett Springs Faults (see southeastern corner of fig. 4 [sheet 1]and fig. 5 [sheet 2]). Here, youthful fault morphology steps to the southwest across North Fork Cache Creek to the Southern Bartlett Springs Fault (Lienkaemper and others, 2014) from where the Cache Formation is bounded on the northeast by the Northern Bartlett Springs Fault. Faulting along the Northern Bartlett Springs Fault continues to the map boundary along the northeast side of the step as en echelon bedrock faults, but evidence of youthful geomorphic expression of the fault zone dies off southeast of the step to the Southern Bartlett Springs Fault. The Northern Bartlett Springs bedrock faulting nevertheless continues southeastward beyond the map area along the southwest side of the Bartlett Springs Synform and the Wilson and Kennedy Faults (see fig. 5, sheet 2), subparallel or oblique to bedding and folding in the Jurassic and Lower Cretaceous Great Valley complex and its contacts with the Coast Range ophiolite. This Northern Bartlett Springs bedrock faulting is superposed on, or associated with, long-term transpression and major dextral drag that dismembered the Bartlett Springs Synform in the Wilbur Springs area (fig. 5, sheet 2).

Because the Southern Bartlett Springs Fault Zone is only present in the southernmost part of the map area, an extensive description of the fault is not provided here, but the reader can access detailed descriptions of late Quaternary features and data from paleoseismic investigations of the Southern Bartlett Springs Fault Zone in Lienkaemper (2010) and references therein.

Quaternary faulting in the stepover area between the Northern and Southern Bartlett Springs Faults has recently been documented (Lienkaemper and others, 2014). Cache Creek flows through the central part of a right-stepped pull-apart depression cut by several intermediately spaced faults between the Hunting Creek Fault segment of the Southern Bartlett Springs Fault and the Wilson Valley segment of the Northern Bartlett Springs Fault (map, sheet 1; fig. 5, sheet 2). This pull-apart depression is interpreted to exhibit ~6 km of incremental Quaternary dextral offset of Cache Creek, where it flows through the depression in the stepover (Lienkaemper and others, 2014). A 2- to 3-km-long oblique-dextral fault exhibiting steep dipping scarps as much as 2.5 m high (the Kuikui Fault) within this stepover was trenched in 2011 (Lienkaemper and others, 2014), and one short strand of this fault was found to have vertically displaced the youngest soil layer 7 cm, which is a minimum offset for the broader fault zone of the stepover area (Lienkaemper and others, 2014). Dextral fault creep is documented both on the Hunting Creek Fault segment of the Southern Bartlett Springs Fault Zone and near Highway 20 on the Northern Bartlett Springs Fault Zone north of the stepover, based

on the modeling of repeated measurements across GPS site arrays (Murray and others, 2014; Lienkaemper, 2010).

The Southern Bartlett Springs Fault Zone appears to continue southward to the map boundary subparallel to the Northern Bartlett Springs Fault Zone, but in contrast to the Northern Bartlett Springs Fault Zone, the southern fault zone crosses many Mesozoic bedrock units at a steep angle with little, if any, apparent offset in most places. The faulting within the map area and beyond to the southeast is expressed primarily geomorphically, showing little evidence of significant strike-slip or dip-slip displacement of bedrock unit contacts (compared to probable displacements of as much as tens of kilometers along the Northern Bartlett Springs Fault), especially where the southern fault zone crosses contacts between the Coast Range ophiolite and stratified units of the Great Valley complex. As discussed above in part, Lienkaemper (2010) and Lienkaemper and others (2014) suggested that Cache Creek, parts of the Pliocene-Pleistocene Cache Formation, and Clear Lake Volcanics could be right-laterally offset along the Southern Bartlett Springs Fault Zone as much as 5–6 km and that, farther south, volcanic rocks correlated with the Mesozoic Coast Range ophiolite and modern stream drainages are right-laterally offset 1–2 km by western traces of the Southern Bartlett Springs Fault Zone (Lienkaemper, 2010; Lienkaemper and others, 2014). The suggested bedrock offsets, however, are unsupported by any data confirming age or compositional equivalence for the Quaternary and Mesozoic volcanic rocks correlated across the fault zone. No sedimentologic data is available to establish continuity of paleoflow direction and other sedimentologic affinities in the Pleistocene and Pliocene sedimentary units cut by the Southern Bartlett Springs Fault Zone, with the exception of the thesis work of Gaines (2008). Major long-term displacement associated with the Northern Bartlett Springs Fault must be partitioned southward to other faults, perhaps to the presently inactive Northern Bartlett Springs Fault southeast of the stepover to the Southern Bartlett Springs Fault. Alternatively, some slip could be accommodated by folding above blind transpressional reverse faults. Additional investigations will be needed to establish specific structures involved with slip partitioning and to test and determine the timing of suggested long-term displacements.

Faults of the Middle Mountain and Sanhedrin Mountain Areas

The Middle Mountain area (fig. 4, sheet 1) is a narrow northwest-trending ~45 km long synformal fault block made up of a structurally thinned section of lower Eocene–Paleocene strata overlying Lower and Upper Cretaceous strata of the Great Valley complex, underlain locally by structurally thinned igneous rocks of the Coast Range ophiolite. The block is flanked on the southwest by rock units of the Central Belt of the Franciscan Complex (including the Pomo terrane) and to the northeast by both Central Belt and Yolla Bolly terrane rocks of the Franciscan Eastern Belt (map, sheet 1). The Yolla Bolly terrane rocks to the northeast form a transpressionally warped structural slab, the Sanhedrin Mountain slab, that is more than 85 km long and overlies the Central Belt northeast of Clear Lake. The Sanhedrin Mountain slab is antiformally warped northeast of Clear Lake (Bartlett Mountain Antiform, cross sections and figs. 5, 7, sheet 2), as suggested by the distribution of metachert and metavolcanic rocks in the slab, and it is largely devoid of seismicity (see map, sheet 1; seismicity distribution on fig. 5, sheet 2).

The Middle Mountain synformal block, in contrast, exhibits a significant linear zone of microseismicity largely between 2 and 8 km deep, with epicenters in part aligned with the Bucknell Creek Fault that bounds the east side of the Middle Mountain block (map, sheet 1; fig. 5, sheet 2). Northwest of this alignment with the Bucknell Creek Fault, however, the linear trend of microearthquake epicenters veers southwest, away from the Bucknell Creek Fault and the eastern boundary of the Middle Mountain block, to extend beneath the central Middle Mountain area, where no faults are mapped at the surface (fig. 5, sheet 2). Hayes and others (2006) interpreted the seismicity beneath the northern Middle Mountain block to be associated with active dike intrusion in the lower crust. Thomas and others (2013), however, pointed out that this interpretation is inconsistent with the orientation of the seismicity relative to maximum regional principal stress and argued that dike intrusion in the lower crust should produce compressive stress in the upper crust that inhibits shallow seismicity. Alternatively, Thomas and others (2013) proposed that the seismicity is more likely related to incipient fault development, as also suggested earlier by McLaren and others (2007). The fault zone inferred from distribution of double-differenced hypocenters of the microearthquakes dips vertically to steeply to the northeast at 70–80°, and the earthquakes have focal mechanisms consistent with dextral normal and reverse slip (Thomas and others, 2013). Departure of the earthquakes from the mapped northern extent of the Bucknell Creek Fault presumably is associated with a northwest splay from the Bucknell Creek Fault at depth that has not ruptured to the surface; or if it has, existing surface geologic mapping does not document the fault splay.

Faults of the Clear Lake Area

The southwestern part of the map area includes Clear Lake, the Quaternary Clear Lake Volcanic Field, and extensive coeval and post-volcanic Pliocene, Pleistocene, and Holocene fluvial and lacustrine sediments and underlying bedrock units of the Franciscan Complex (map, sheet 1; fig. 5, sheet 2). Several significant northwest- and west-northwest-trending fault zones, as well as one east-northeast- and one north-northeast-trending fault zone, extend through this area and cut the Quaternary volcanics and clastic sedimentary rocks. The most significant faults include the Scotts Valley, Big Valley, Wight Way, Clover Valley, Collayomi, Konocti Bay, Borax Lake, Sulphur Bank, and Cross Springs Faults (fig. 5, sheet 2). Microseismicity is associated with some of these faults, such as the Collayomi and Konocti Bay Faults (Eberhart-Phillips, 1988; Bufe and others, 1981), and some of this seismicity includes long-period events (near Mount Konocti) linked to magma activity at depth (Pitt and others, 2002).

The Cross Springs Fault is an east-side-down normal fault that splays southwest from the Northern Bartlett Springs Fault and bounds the northwest side of the main depositional basin of the Cache Formation (Rymer, 1981; Hearn and others, 1995). The Wight Way Fault also is a normal fault that cuts Pleistocene lacustrine and fluvial sediments southwest of Lakeport and is considered to be one of the structures controlling subsurface distribution of aquifers southwest of Clear Lake (Rymer, 1981; Hearn and others, 1988, 1995). The curvilinear trend of the Big Valley Fault, which subparallels the southwest margin of Clear Lake and the western side of Big Valley, suggests that it may be associated with subsidence (possibly volcanogenic) along the west margin of the Clear Lake Volcanic Field (map, sheet 1).

The Konocti Bay Fault is mapped mainly within the Clear Lake Volcanics (Hearn and others, 1988, 1995), is intimately associated with the distribution of eruptive units, and displaces volcanic units within the volcanic field (Hearn and others, 1995). The orientation of the fault zone also aligns with faults mapped beneath Clear Lake that vent CO_2 into the lake (Sims and Rymer, 1976) and that align with the Clover Valley and Bucknell Creek Fault Zones farther to the north, which separate the Franciscan Eastern Belt on the northeast from the Middle Mountain block and Franciscan Central Belt to the southwest. The Borax Lake and Sulphur Bank Fault Zones to the northeast of the Konocti Bay faulting control the configuration of the elongated northeast and southwest arms of Clear Lake, and these faults also expose faulted, mineralized, and hydrothermally altered metachert, metasandstone, and metavolcanics of the Franciscan Eastern Belt. This relation strongly suggests that the Konocti Bay Fault Zone is the likely southeastern extension of the Clover Valley-Bucknell Creek Fault Zones that, in places, cut through the suture between Franciscan Central and Eastern Belt basements (as illustrated in structure sections *C–C′* and *D–D′*, sheet 2). The Borax Lake Fault Zone, furthermore, exhibits a prominent youthful pull-apart basin (Borax Lake) that we interpret as indicating that the fault zone has been active since latest Pleistocene time.

The Collayomi Fault that is near the southwest boundary of the map area is well known from previous mapping of the framework geology of the Geysers-Clear Lake geothermal region by McLaughlin (1978) and also from mapping of the Clear Lake Volcanics by Hearn and others (1995). The Collayomi Fault Zone acts as the northeast structural boundary of The Geysers Geothermal Field, where steam is produced from a fracture-controlled reservoir largely in slabs of greywacke in the Franciscan Central Belt. The Collayomi Fault Zone extends along the northeast side of a major slab of Coast Range ophiolite and separates the ophiolite and rocks mainly of the Franciscan Central Belt on the southwest from a thick section of attenuated and folded Coast Range ophiolite and Upper Jurassic to Upper Cretaceous strata of the Great Valley complex to the northeast (McLaughlin, 1978; McLaughlin and Ohlin, 1984). These rocks are covered by Quaternary volcanics in Clear Lake basin to the northeast. It is not understood in detail how the thick section of covered Coast Range ophiolite and Great Valley complex relates to the Middle Mountain area northwest of Clear Lake, except that the synformal Middle Mountain block clearly aligns with these rocks and is broadly equivalent in age. Where exposed east-southeast of the Collayomi Fault Zone outside of the map area, the Great Valley complex rocks have been interpreted as attenuated along imbricate low-angle normal faults (Jayko and others, 1987). This is contrary to earlier interpretations explaining younger-over-older low-angle faulting in the Great Valley rocks by out-of-sequence thrusting (Swe and Dickinson, 1970; Suppe, 1979).

We suggest that the younger-over-older faulting may best be explained by attenuation associated with incremental unroofing of the Coast Ranges (1) partly in the Late Jurassic, producing ophiolitic fault-scarp breccias in the basal Great Valley complex; (2) again in the Early Cretaceous (Hauterivian) when detrital serpentinites were deposited as part of the lower Great Valley complex in the Wilbur Springs-Knoxville areas (McLaughlin and others, 2016); and (3) also in the latest Cretaceous to early Tertiary, when the Franciscan Complex was unroofed during westward stepout and shallowing of slab subduction (Ernst and McLaughlin, 2012). Unroofing of the Franciscan may have been driven by contraction and uplift in the roof-thrust zone of east-vergent tectonic wedges of the structurally low Franciscan Coastal and Central Belts that were thrust beneath the structurally higher Eastern Belt. Tectonic wedge-driven contraction induced warping and uplift in the roof of the wedge complex, followed by exposure, erosion, and sedimentary recycling of the structurally higher rocks of the Eastern and Central Belts, as well as attenuation faulting in the western Great Valley (Jachens and others, 1995; Godfrey, 1997). Ages of the strata involved in younger-over-older faulting in the Clear Lake area suggest that much of it occurred during this latter (Late Cretaceous–early Tertiary) period of low-angle extension.

Faults Northeast of the Bartlett Springs Fault Zone

In the southeastern part of the map area northeast of the Northern Bartlett Springs Fault Zone, several complex north- to northwest-striking zones of bedrock faulting are mapped, some of which exhibit youthful physiographic expression, but they are not well studied (map, sheet 1; fig. 5, sheet 2). These fault zones mainly flank the northeast and southwest sides of the Wilbur Springs Antiform, cutting rocks of the Coast Range ophiolite and overlying Great Valley complex and local Quaternary basin fills of Bear Valley and smaller depressions. One of the faults (Pacific Ridge Fault Zone) transects the Yolla Bolly terrane of the Franciscan Eastern Belt along the southwest flank of the Pacific Ridge Antiform (see structure section *D–D′*) and is subparallel in trend to the Northern Bartlett Springs Fault Zone.

The Bad Ridge Fault Zone is mapped as a wide zone of diffuse short fault segments entirely within the broad sheet of ultramafic rocks of the Coast Range ophiolite northeast of Little Indian Valley (map, sheet 1; fig. 5, sheet 2; McLaughlin and others, 1990). The faults of this zone locally exhibit scarps that bound or flank small basin-like depressions with thin accumulations of locally derived Quaternary sediment. Mineral springs also vent along some of these faults (Slowey and Rytuba, 2008). The crustal geometry of this diffuse fault zone is largely unknown, except that the overall character of the faulting is extensional. No data are available to evaluate whether these faults are associated with active faulting beyond suggestions from geomorphology. The relation of the Bad Ridge faulting to the other faults northeast of the Bartlett Springs Fault Zone is unknown.

The Bear Valley-Resort Fault Zone is mapped as a straight N. 15–20° W. fault that is subparallel to and disrupts bedding in the enclosing Jurassic and Lower Cretaceous section of the Great Valley complex (map, sheet 1; fig. 5, sheet 2; McLaughlin and others, 1990). To the northwest, the fault is mapped along the southwest side of the Quaternary fill of Bear Valley, in part from alignment of fluid seeps and subtle inflections in tributaries to Bear Creek (J. Rytuba, personal commun., 2015; Slowey and Rytuba, 2008). Entrenchment of the sediments in Bear Creek along the linear northeast side of Bear Valley possibly is associated with a buried right-stepped fault along the east side of the valley, which, if present, would suggest that Bear Valley is a dextral pull-apart basin. Further investigations are necessary to determine if displacement along the Bear Valley-Resort Fault Zone is right lateral and, if so, what the timing constraints are for the faulting. To the southeast of Bear Valley, the Bear Valley-Resort Fault Zone extends to the Wilbur Hot Springs area to merge with west-northwest-trending faults of the Little Indian Valley Fault Zone.

The Little Indian Valley Fault Zone aligns with the northeast side of the Bartlett Springs Synform, whose southwest side is highly disrupted and sheared along the Northern Bartlett Springs Fault Zone (map, sheet 1; fig. 5, sheet 2). Both the Bear Valley-Resort and Little Indian Valley Fault Zones are oriented along the northeast and southwest limbs, respectively, of the Wilbur Springs Antiform and together represent integral parts of the Wilbur Springs Dextral Hook (discussed below). Displacement along the Little Indian Valley Fault Zone contributed to dismemberment of the Bartlett Springs Synform along the Northern Bartlett Springs Fault Zone. The Little Indian Valley Fault is mapped as offsetting rocks of the Coast Range ophiolite and lower Great Valley complex, including detrital serpentinite that is folded around the axis of the Wilbur Springs Antiform. The merged Bear Valley and Little Indian Valley Fault Zones, in turn, are the locus of past and present hydrothermal venting and mineralization over the Wilbur Springs Antiform, but these diffuse fault zones do not extend southeast of the main body of detrital serpentinite in the core of the Wilbur Springs Antiform. Instead, a zone of structurally higher, diffuse, east-west-oriented faults traverses across the axis and nose of the antiform (map, sheet 1; fig. 5, sheet 2). We view the distribution of these faults around the nose of the Wilbur Springs antiformal structure as associated with flexural slip and dextral drag of Great Valley complex strata and ophiolitic rocks into the Northern Bartlett Springs Fault Zone. As such, all of these faults may have experienced displacement associated with initiation and continued right-lateral displacement along the Northern Bartlett Springs Fault Zone. The significance of these structures as potentially active in the modern context of seismic hazard is presently unclear but should be considered in the modeling of crustal structure over this area.

Major Folds

Wilbur Springs Dextral Hook

The regional geometry of the contact between the Franciscan Complex and structurally overlying Coast Range ophiolite and Great Valley complex is dominated in the map area by a structure here referred to as the Wilbur Springs Dextral Hook (figs. 7, 8, sheet 2). This major structure comprises a paired southeast-plunging antiform (Wilbur Springs antiform) flanked to the southwest by a synform (Bartlett Springs Synform) that has been highly attenuated and dismembered by dextral strike-slip faulting along the Northern Bartlett Springs Fault and the southwest side of the Great Valley fore-arc basin (figs. 6, 7, 8, sheet 2). The dextral hook in this area is defined by prominent right-lateral shearing of the former Bartlett Springs Synform along the Northern Bartlett Springs Fault, which truncates the southwest limb of the Wilbur Springs Antiform. Combined transpressional folding and extensive right-lateral shearing that accompanied or post-dated folding define the dextral hook.

Figure 7, a reconstruction of the northeastern Coast Ranges, is focused over the Northern Bartlett Springs Fault Zone between Wilbur Springs and Round Valley and emphasizes structural features associated with the Wilbur Springs Dextral Hook. The Wilbur Springs Antiform, Bartlett Springs Synform (figs, 6, 7, 8) and Northern Bartlett Springs Fault Zone represent integral parts of the structural hook. The antiformal character of the northeast side of the Wilbur Springs Dextral Hook is exhibited by the Wilbur Springs Antiform, but instead of being coupled on the southwest with a simple synformal fold, the southwest limb of the antiform is truncated and right-laterally attenuated along the Northern Bartlett Springs Fault Zone, parallel to what is interpreted as the axial trend of a dismembered former synform (the Bartlett Springs Synform; previously discussed in-part in the Northern Bartlett Springs Fault Zone section). The extensive shearing and dismemberment of the synform extends from Wilbur Springs to Round Valley (~55–60 km), forming the "hook" component of the Wilbur Springs Dextral Hook. The structure provides relatively clear evidence of right-lateral displacement along the Northern Bartlett Springs Fault Zone and the regional contact between the Franciscan Complex and western side of the Mesozoic Great Valley fore arc. Because the Northern Bartlett Springs Fault Zone evolved from faulting rooted in the pre-transform subduction margin (see earlier section on Northern Bartlett Springs Fault Zone), the timing of initiation and evolution of the dextral hook is critical to an understanding of how the northern San Andreas system evolved from the subduction margin. The long history of the western side of the Great Valley fore arc as a part of the subduction margin, followed by its reactivation as a folded transpressional boundary and even later by right-lateral strike-slip associated with the Northern Bartlett Springs Fault Zone, however, forms a complex pattern of superposed structures that obscure evidence of the earliest strike-slip faulting and the timing of initiation of the related Wilbur Springs Dextral Hook.

Distinctive fossil cold-seep-related Lower Cretaceous (Hauterivian) and older Great Valley complex strata in Rice Valley correlate with similar strata in the Wilbur Springs area ~50 km to the southeast (Campbell and others, 1993, 2002; Kiel and others, 2008; McLaughlin and others, 2010). These strata, along with overlying Paleocene–Eocene deposits in the Round Valley, Rice Valley, Middle Mountain, and Lower Lake areas, indicate that, prior to the Miocene, the outer Great Valley fore arc and its ophiolitic basement must have extended across much of the area that now exposes the Eastern and Central Belts of the Franciscan Complex (fig. 6*A*, sheet 2).

Units of the Coast Range ophiolite, ophiolitic mélange and Great Valley complex overlain by Paleogene strata in Round Valley, are now separated ~56 kms along the Northern Bartlett Springs Fault from a downwarped synformal sliver in Rice Valley having similar stratigraphy. Estuarine coal-bearing middle Miocene strata present in Round Valley (Clark, 1940), however, are not present in Rice Valley, perhaps indicating that initial dextral displacement of these rocks occurred between the Eocene and middle Miocene, although in our earlier discussion of long-term fault displacement we favored the Miocene for initiation of strike slip. We suggest that right-lateral separation may have begun in the Miocene but somewhat earlier than the middle Miocene estuarine deposition of strata in Round Valley.

Our reconstruction of the pre-Northern Bartlett Springs Fault configuration of the Bartlett Springs Synform (fig. 7, sheet 2) places Round Valley adjacent to and west of Rice Valley between the Eocene and middle to late Miocene along approximately the same outer part of the Great Valley fore arc (fig. 6*A*, *B*, sheet 2). A synclinally folded Paleocene conglomerate unit in the Rice Valley section contains clasts derived from blueschist-facies Franciscan metasandstone

(Berkland, 1973), indicating that Paleocene deposition post-dated or accompanied major latest Cretaceous to Paleocene unroofing of rocks buried >20 km before being folded, deformed, and isolated as part of the Bartlett Springs Synform and the Wilbur Springs Dextral Hook. This crude timing suggests that the Wilbur Springs Dextral Hook formed no earlier than the Late Paleocene.

The Bartlett Springs Fault Zone is also linked southward with the Hayward-Calaveras Fault System of the eastern San Francisco Bay area, which has accommodated ~170 km of ~12 Ma and younger cumulative dextral displacement partitioned to the Calaveras Fault from the San Andreas Fault southeast of Hollister (McLaughlin and others, 1996). If the Bartlett Springs Fault Zone connected to the northern Hayward-Calaveras Fault system 12 Ma, then it is possible that the Northern Bartlett Springs Fault formed in the late middle Miocene. Folding associated with the Wilbur Springs Dextral Hook, thus, would have occurred earlier.

Recent studies in the southern Great Valley and Sierra Nevada batholith have described as much as 90° of vertical-axis clockwise rotation accompanying extensional collapse of the Tehachapi Mountains and southern Sierra Nevada batholith that occurred in the Late Cretaceous (fig. 8, sheet 2). Rotation and extensional collapse of the batholithic rocks was interpreted as driven by shallow subduction of an over-thickened Farallon Plate during the Laramide orogeny (Saleeby, 2003; Chapman and others, 2010, 2012). Shallowed subduction of the Farallon Plate in the Late Cretaceous to Paleocene is proposed to have produced east-directed tectonic wedging, uplift, and unroofing of the Franciscan Complex in the northern Coast Ranges (Ernst and McLaughlin, 2012). Major Late Cretaceous rotation of the batholithic rocks in the southern Sierra Nevada batholith was taken up in the adjacent southern Great Valley complex and its ophiolitic basement, as well as in the underthrust Franciscan Complex of the accretionary margin. Accommodation of the Late Cretaceous (approximately 95–85 Ma, Chapman and others, 2012) clockwise rotation might conceivably have extended into northern California and been accommodated as dextral transpression along the contact between the northern Great Valley complex and the Franciscan Complex. However, as noted earlier, folding and down-warping of the Bartlett Springs Synform ("hook" component of the Wilbur Springs Dextral Hook) into underlying ophiolitic basement of the Great Valley and unroofed Franciscan Complex rocks was no earlier than late Paleocene, much later than the timing of southern Sierra Nevada batholith rotation. The proposed timing of rotation, therefore, is too early to relate to transpressional deformation along the Great Valley-Franciscan interface in northern California. The timing of rotation in southern California also corresponds to the timing of deposition of some pelagic Campanian–Cenomanian rocks of the Coastal and Central Belts of the Franciscan Complex on oceanic basement, far from the continental margin, that did not accrete to northern California and become unroofed until the Paleogene (<60 Ma). It must be concluded that Cretaceous clockwise rotation in the southern Great Valley is not related to initiation of transpressional deformation associated with the Wilbur Springs Dextral Hook. This timing, instead, is more closely related to the timing of tectonic wedging and unroofing of the Franciscan Complex in northern California, which appears to have predated initiation of transpressional deformation and the Wilbur Springs Dextral Hook (fig. 8, sheet 2).

Significantly later, well-documented major ~15 to 5 Ma clockwise rotation of the southwestern Tehachapi Mountains, western Transverse Ranges, and Salinian block were associated with early to middle Miocene displacements of the San Andreas Fault System (Colgan and others, 2012).

We suggest that the Franciscan Complex in northern California was wedged into the western side of the Great Valley complex and its ophiolitic basement north of the Tehachapi Mountains in the Late Cretaceous–Paleogene (~70–56 Ma). Simultaneously, the Franciscan wedge may also have been pushed obliquely northward by the clockwise rotation of the southern Sierra Nevada, accompanied by rapid uplift (Chapman and others, 2012). In northern California, however, significant transpressional deformation along the Great Valley-Franciscan interface mainly followed latest Cretaceous and Paleogene uplift and unroofing of the Franciscan tectonic wedge and its roof-thrust system composed of the Coast Range ophiolite, ophiolitic mélange, and Great Valley complex. The timing of transpressional deformation—resulting in uplift and folding of the northern California Neogene fore arc and the initiation of the Wilbur Springs Antiform, Bartlett Springs Synform, and the resultant Wilbur Springs Dextral Hook (fig. 8, sheet 2)—corresponds approximately with San Andreas Fault system-related early Miocene and younger rotation and northward translation of the southwestern Tehachapi Mountains, western Transverse Ranges, and Salinian block (Colgan and others, 2012).

Antiforms and Synforms

All of the fold structures discussed below are associated with major slab-like fault blocks in the Franciscan Complex or in the Great Valley complex and Coast Range ophiolite. The folds are antiformal or synformal warps in these fault blocks. Other folding in the Great Valley complex and younger deposits is largely subsidiary to the more fundamental warps in the major fault blocks. We therefore focus our discussion of folding around the regional distribution of the antiformal and synformal structures. Structural relations associated with most of these structures have been discussed, in part, in the descriptions of the major faults bounding the structural blocks that incorporate the antiforms and synforms, so the following descriptions are sometimes shortened to avoid repetition.

Bartlett Springs Synform

The original extent of the Bartlett Springs Synform, as discussed in previous sections, is largely dismembered along the Northern Bartlett Springs Fault Zone as an integral part of the Wilbur Springs Dextral Hook structure (figs. 6, 7, 8, sheet 2), but a part of the synform remains essentially intact northeast of the fault zone southwest of Wilbur Springs (map, sheet 1; fig. 5, sheet 2). A large slab of ophiolitic mélange, remnants of lower Great Valley complex strata, overlying Paleogene strata and Miocene marine and estuarine strata distributed along the Northern Bartlett Springs Fault Zone between Wilbur Springs, Rice Valley, and Covelo are interpreted as parts of the former Bartlett Springs Synform that were dismembered along the Northern Bartlett Springs Fault Zone. Reconstruction of these dismembered deposits as a former northwestward extension of the Bartlett Springs Synform suggests ~38–47 km of cumulative dextral displacement and perhaps ~3 mm/yr of long-term slip since the Miocene (~15–12 Ma) along the Northern Bartlett Springs Fault Zone (figs. 6, 7, 8). The timing of initiation of this dismemberment is poorly constrained and, therefore, this estimate of slip rate is considered highly speculative.

Wilbur Springs Antiform

The Wilbur Springs Antiform is a major southeast-plunging antiformal structure adjacent to and northeast of the Bartlett Springs Synform that folds the lower Great Valley complex and Coast Range ophiolite over underlying Yolla Bolly terrane rocks of the Franciscan Complex. The northeast flank and crest of the antiform where the Coast Range ophiolite overlies the Franciscan Complex is clearly seen in down-plunge views to the southeast from Little Indian Valley. The axial trend of the antiform apparently is truncated obliquely with dismembered parts of the Bartlett Springs Synform along the Northern Bartlett Springs Fault Zone northwest of Little Indian Valley (figs. 5, 6, 7, sheet 2). The axial area of the Wilbur Springs Antiform northwest and southeast of Little Indian Valley corresponds with dominant high, dissected topography northeast of the Northern Bartlett Springs Fault Zone. Together with the Pacific Ridge Antiform to the northeast of the Wilbur Springs Antiform, these transpressional structures appear to exert some degree of control on the modern topography. This relation may be significant to our understanding of active deformation along the Northern Bartlett Springs Fault Zone that is shown from microseismicity to dip steeply northeast, beneath the transpressional axes of the Wilbur Springs and Pacific Ridge Antiforms in this area (fig. 11; fig. 12, sheet 2).

Pacific Ridge Antiform

The Pacific Ridge Antiform is a narrow, elongate northwest-striking, topographic high northeast of the Northern Bartlett Springs Fault Zone that is subparallel to, but stepped northeast from, the Wilbur Springs Antiform (figs. 5, 6, 7, sheet 2; map, sheet 1). The Pacific Ridge Antiform is flanked to the northeast by a complex synformal structure between Pacific Ridge and Snow Mountain, but the southwest flank of the fold appears to root into the steep-dipping Pacific Ridge Fault along the contact between Yolla Bolly terrane mélange in the core of the antiform and overlying metasandstone and argillite to the southwest (see structure section *D*–*D′*, sheet 2). The faulting in this southwest limb of the antiform aligns with a narrow band of serpentinite along the fault, which extends southeastward into the main Coast Range ophiolite along the northeast limb of the Wilbur Springs Antiform. Merging of the narrow serpentinite band along the Pacific Ridge Fault with ultramafic rocks of the main Coast Range ophiolite to the southeast mimics the geometry of the larger scale Wilbur Springs Dextral Hook discussed above.

Bartlett Mountain Antiform

The Bartlett Mountain Antiform is inferred within the Sanhedrin Mountain block of Yolla Bolly terrane that overlies the Central Belt southwest of the Northern Bartlett Springs Fault Zone, northeast of the Middle Mountain Synform and Clear Lake. The basis for inferring an antiformal structure in the Sanhedrin Mountain block is partly from the mapped distribution of the metachert (unit cy) plus metavolcanic (unit vy) lithofacies of the Yolla Bolly terrane, particularly where these complexly folded rocks are seen to wrap around the southeastern side of the Sanhedrin Mountain block on the northeast side of Clear Lake. A broad northwest-trending antiformal warp beneath the central Sanhedrin Mountain block is further suggested from the structurally low distribution of mélange mapped in the central part of the Sanhedrin Mountain block (see structure sections, sheet 2). Presence of a broad antiformal warp is consistent with expectations of such a transpressional structure intervening between synformal structures northeast of the Northern Bartlett Springs Fault Zone and the Middle Mountain Synform southwest of the Sanhedrin Mountain block. We acknowledge, however, that the depicted Bartlett Mountain antiformal axis is likely oversimplified, as the structure of the Yolla Bolly terrane rocks of the Sanhedrin Mountain block is clearly more complex in detail than can be depicted.

Middle Mountain Synform

Mapping of the Middle Mountain structural block in some detail in the 1960s and 1970s (CDWR, 1966, 1968, 1969; Berkland, 1969, 1972, 1978) shows it to be composed of a complexly attenuated section of Coast Range ophiolite, Great Valley complex, and Paleogene strata that, in turn, are warped into the southeast-plunging Middle Mountain Synform. The Middle Mountain synformal block does not appear to continue to the thick section of Great Valley complex and Coast Range ophiolite that underlies the Clear Lake Volcanic Field, as rocks of the Franciscan Central Belt intervene. However, similarities in the character of the Mesozoic units in these areas and alignment of the Middle Mountain block with the Clear Lake Mesozoic–Tertiary section across several major northwest-trending faults (fig. 4, map, sheet 1; fig. 5, sheet 2; McLaughlin and others, 1990) suggest that the Middle Mountain block and Clear Lake Mesozoic sections may be linked across some of the seismically active faults of the two areas and have an as-yet-unconstrained strike-slip history.

DESCRIPTION OF MAP UNITS

UNCONSOLIDATED DEPOSITS

af **Artificial fill (Holocene)**—Clay, silt, sand, rock fragments, organic matter, and man-made debris used in road and land fills, in dam construction, and for other anthropogenic purposes

Qls **Landslide deposits (Holocene and Pleistocene)**—Unconsolidated to weakly consolidated rock and soil debris, which has moved downslope by various landslide processes, including rotational slumping, surface creep, flowage, or combinations thereof

ALLUVIAL DEPOSITS

Qal **Alluvial deposits (Holocene and Pleistocene)**—Poorly sorted, unconsolidated sand, silt, gravel, and boulders deposited in modern stream and river channels and on adjacent low-lying flood plains. Include lake deposits of clay and silt and basin deposits (unit bcl of Hearn and others, 1995) along the margins of Clear Lake. Mapped locally, where age relations based on superposition with younger and older Quaternary deposits is unknown

Qoa **Older alluvial deposits (Holocene and Pleistocene)**—Weakly sorted to unsorted, weakly consolidated silt, clay, sand, and gravel deposits that may locally display clast imbrication and crossbedding, but the original depositional environment is unknown; moderately to extremely dissected; preserved along major drainages and valley margins

TERRACE DEPOSITS

Qt **Alluvial terrace deposits (Holocene and Pleistocene)**—Poorly to moderately well sorted, weakly to moderately consolidated sand, silt, gravel, and boulder deposits; deposited along or adjacent to major streams. Locally divided into the following units:

Qty **Younger alluvial terrace deposits and surfaces (Holocene?)**—Stream terraces elevated above the active stream channel with minimal dissection; delineated by flat geomorphic surfaces and in places includes erosional bedrock platforms (strath terraces) that may not be overlain by alluvial deposits

Qto **Older alluvial terrace deposits and surfaces (Pleistocene)**—Alluvial terrace deposits that are elevated above, and more dissected than, young alluvial terrace deposits. Associated with flat-lying surfaces eroded into older deposits and bedrock. Commonly composed of a thin (<5 m thick) layer of gravel and cobbles

Qtvo **Very old alluvial terrace deposits and surfaces (Pleistocene)**—Alluvial stream-terrace remnants associated with flat but highly dissected surfaces typically preserved well above active stream channels. Commonly composed of highly weathered mixture of silt with scattered gravel to cobbles

FAN DEPOSITS

Qf **Alluvial fan deposits (Holocene and Pleistocene)**—Poorly sorted, weakly consolidated sand, silt, gravel, and boulder deposits; deposited where streams disgorge onto flat plains at the mouths of canyons. Locally divided into the following units:

Qfy **Younger alluvial fan deposits and surfaces (Holocene?)**—Poorly sorted, weakly consolidated sand, silt, gravel, and boulder deposits of alluvial fan systems at different elevations, locally overlying or inset into older deposits

Qfo **Older alluvial fan deposits and surfaces (Pleistocene)**—Alluvial fan deposits that are elevated, dissected, and incised by younger fans and alluvial terrace deposits

Qfvo **Very old alluvial fan deposits and surfaces (Pleistocene)**—Topographically high, dissected, and uplifted alluvial fan deposits. Silt and clay with poorly cemented gravel lenses and moderately consolidated sand layers; mapped as continental deposits by Cardwell (1965) in the Potter Valley area

GLACIAL DEPOSITS

Qgd **Glacial deposits, present locally (Pleistocene)**—Unsorted gravel and boulder deposits and silt; at high elevations, in places accompanied by striae on bedrock, small cirques, and moraines. Distinctive flat but irregular surfaces viewed on aerial photographs, seen as far south as Snow Mountain along high divide east of Lake Pillsbury. Described by Holway (1914) and in several other early investigations summarized in Irwin (1960)

SPRING DEPOSITS

Qsn **Hydrothermal deposits (Pleistocene and younger)**—Local sinter-like spring deposits along faults and silica carbonate rock, a product of hydrothermal fluid reaction with serpentinite. Rocks are composed of a mix of Ca-Fe-Mg carbonate plus quartz. Hydrothermal spring sinter is mapped only along the Logan Fault at Lake Pillsbury, associated with serpentinite. Elsewhere, silica carbonate rock alteration of serpentinized ultramafic or other mafic rocks accompanies epithermal precious or base-metal mineralization (especially Hg, Au, Ag, Pb, and Zn). The hydrothermal fluids associated with the silica carbonate and related hydrothermal spring sinter is considered to have been heated by magmas associated with Pleistocene volcanism

Qtrv **Travertine (Pleistocene and younger)**—Layered $CaCO_3$ associated with mineral springs and seeps, commonly forming mineralized terrace deposits along faults or stratigraphic contacts, deposited from $CaCO_3$-saturated low-temperature fluids. Some travertine deposits may exhibit evidence of a mixed fluid history that included hot fluid circulation, evidenced by local occurrences of siliceous sinter

VOLCANIC ROCKS

Qv **Clear Lake Volcanic rocks (Pleistocene)**—Siliceous to andesitic volcanics of the Clear Lake region; includes rhyolites to basaltic andesites that are vitric to porphyritic and erupted as flows and flow breccias, with only minor explosive eruptive activity. These rocks have been described and mapped in great detail by other workers (Hearn and others, 1988, 1995; Donnelly-Nolan and others, 1981; Hammersley and DePaolo, D.J., 2006). Age of volcanism is ~2.1 Ma to 300 ka

FLUVIAL AND LACUSTRINE FILL

QTc **Cache Formation (Pleistocene and upper Pliocene)**—Nonmarine fluvial and lacustrine deposits of gravel, sandstone, siltstone, and mudstone in the greater Clear Lake region, representing paleo-rivers and streams, lakes, and ponds. Gravels and silts locally contain vertebrate and plant fossils. Lacustrine sediments contain plants, freshwater fish, pollen, and ostracodes and locally include tephra layers (Rymer, 1981; Sims and others, 1981). Gravels of the Cache Formation southeast of Clear Lake are overlain by 1.45 Ma basalt and contain pebbles of obsidian derived from eroded 4.5 Ma Pliocene Sonoma Volcanics sources near Santa Rosa, suggesting fluvial transport from the south-southwest and lack of a well-developed divide between Clear Lake basin and the Napa-Santa Rosa areas in early Pleistocene

MARINE OVERLAP DEPOSITS

Tm **Sandstone and lignitic shale of the Covelo area (middle Miocene)**—Largely estuarine to shallow marine and locally coal bearing; correlated with the marine Temblor Formation in the southern Diablo Range of central California (Clark, 1940)

Te **Marine sandstone and shale (Eocene)—**Sandstone locally massive and spheroidally weathering. Deposited in nearshore to shelf or inner bathyal marine setting

Tep **Sandstone, shale, and conglomerate (Eocene and upper Paleocene)**—Deposited in nearshore to shelf marine setting. In most places unit is depositional on older rocks, locally with angular discordance, but in places, contacts with older rocks are sheared along low-angle normal faults. Locally contains the following units:

Tcg **Conglomerate (Eocene and upper Paleocene)**—Near base of unit. Varies in clast content. At Rice Valley, a local unit of conglomerate contains clasts of metasandstone derived from Eastern Belt Franciscan Complex metaclastic rocks that were exhumed from >20 km depth (based on presence of lawsonite in the clasts) before their incorporation in the conglomerate

GREAT VALLEY COMPLEX

Ku **Sandstone, siltstone, and mudstone (Upper Cretaceous, Cenomanian and younger)**—Marine turbidites, locally channelized and conglomeratic with submarine slumps or mass wasting deposits; deposited in shelf to bathyal settings of Great Valley fore-arc basin

Kuls **Limestone (Upper Cretaceous)**—Locally bioclastic; forms concretions in mudstone sections or lenses several meters in length, mapped in the Middle Mountain area. Correlates with similar fossiliferous limestone lenses in the Whispering Pines quadrangle and on the Guenoc Ranch southwest of Clear Lake that formed in submarine cold-seep settings (K. Campbell, oral commun., 2004; Hepper, 2004; Richmond, 2005) and are associated with mudstones having Campanian radiolarian and planktonic foraminifer faunas (E.A. Pessagno, written commun., 1976; W.V. Sliter, written commun., 1976)

Kul **Sandstone, siltstone, and mudstone with concretionary limestone and conglomerate (Upper and Lower Cretaceous, Cenomanian to Hauterivian)**—Limestone interbedded with sandstone, siltstone, mudstone, and conglomeratic turbidites; deposited in outer shelf to bathyal settings; mapped in the Rice Valley area

ELDER CREEK TERRANE

Kl **Siltstone, mudstone, minor sandstone, conglomerate, and sedimentary serpentinite (Lower Cretaceous, Albian to Hauterivian)**—Marine strata deposited in submarine fan, slope, and basin plain settings, locally with submarine-seep and diapir-related mass-wasting deposits. Mudstone locally contains unmapped carbonate lenses in the Middle Mountain

area, described by Berkland (1969) as containing Early Cretaceous dinoflagellates. Included in this unit are exposures of Great Valley-affinity mudstone and siltstone containing both Early Cretaceous (Berriasian) invertebrate and middle Cretaceous radiolarian (Aptian–Albian) faunas, exposed in a small structural window through the Pickett Peak terrane of the Franciscan Complex Eastern Belt in Estell Creek (fossil locality nos. 26, 27; table 1). Based on fossils and well-bedded unmetamorphosed character (Lehman, 1974), we interpret the Estell Creek unit as part of the Elder Creek terrane. See Surpless and others (2006) and McLaughlin and others (2016) for additional age constraints from U-Pb dating of detrital zircons in other sandstones of the Elder Creek terrane. Elsewhere in the map area, Lower Cretaceous strata of the Elder Creek terrane includes the following units:

Klcg **Conglomerate (Lower Cretaceous, Albian to Hauterivian)**—Mapped in Clear Lake Highlands quadrangle as lenses and channels

Klls **Bioclastic limestone (Lower Cretaceous, Hauterivian)**—Containing fossil cold-seep-related macrofauna, locally intercalated in sedimentary serpentinite

Kssp **Sedimentary serpentinite (Lower Cretaceous)**—Coarse submarine debris-flow deposits and fine-grained serpentinitic sandstone and mudstone turbidites, locally with intercalated bioclastic limestone; occurs at several horizons; locally includes rare boulder-size blocks of high-grade blueschist metamorphosed from garnet-amphibolite. Hornblende from amphibolite blocks in ophiolitic mélange and sedimentary serpentinite in the Wilbur Springs area has $^{40}Ar/^{39}Ar$ plateau ages of 165.6–167.5 Ma, similar to published ages of high-grade blocks within the Franciscan Complex and to crystallization ages in the Coast Range ophiolite (Shervais and others, 2011)

KJs **Argillite, siltstone, and sandstone (Lower Cretaceous, upper Valanginian, to Upper Jurassic, Tithonian)**—Thin bedded, locally with concretionary carbonate lenses, commonly containing Early Cretaceous and Late Jurassic *Buchias* and other macrofauna. Includes the Knoxville Formation of Lawton (1956). Considered equivalent to lithologically identical but highly disrupted and sheared rocks incorporated in ophiolitic mélange (unit KJom). About 35 km south of the map area, along Pope Creek, a siliceous tuff ~10 cm thick is interbedded with argillite overlying basal megabreccia of the Great Valley complex. Sparse zircons in the tuff, believed to represent remnants from tephra air fall, were U-Pb dated at the Stanford-USGS SHRIMP lab at 151.1±2.5 Ma (McLaughlin and others, 2016), consistent with ages assigned to *Buchia*s collected nearby in the lower part of the Elder Creek terrane

Jgb **Megabreccia (Upper Jurassic, Tithonian to Kimmeridgian)**—Sedimentary megabreccia, composed of gabbroic and basaltic clasts, with minor interbedded turbiditic basaltic sandstone. Present only locally at base of Elder Creek terrane sedimentary section. Angular blocky to sandy mafic igneous debris is considered to be derived from depositionally underlying Coast Range ophiolite. Gabbroic and basaltic breccia clasts are derived largely from mafic dikes, basaltic flows, and gabbroic rocks of the underlying Coast Range ophiolite. Megabreccia resembles breccias described from submarine fault scarps and along active strike-slip faults. Similar Upper Jurassic breccia occurs along the southwest side of Sacramento Valley at the base of the Elder Creek terrane in the Elder Creek and Paskenta areas (Blake and others, 1992, 1987; Robertson, 1990; Hopson and others, 2008).

KJom **Ophiolitic mélange (Lower Cretaceous)**—Fault bounded; present in structurally lower part of Elder Creek terrane; comprised of lower Great Valley strata, tectonically mixed with underlying rocks of the Coast Range ophiolite (see, for example, photos of "Grizzly Creek mélange terrane" in McLaughlin and Ohlin, 1984). Unit age is based on inferred time of tectonic mixing and penetrative shearing; ages of rocks in the unit indicate mixing was no earlier than the Valanginian (~134 Ma) and probably coeval with Albian to Hauterivian (~113–134 Ma) deposition of youngest Elder Creek terrane strata and sedimentary serpentinites (Hauterivian, ~131–134 Ma). Unit forms a thick zone of mélange, showing evidence of extensional (for example, boudinage with phacoid-shaped intact masses of serpentinized peridotite enclosed in a penetratively sheared serpentinitic matrix) and contractional deformation (for example, complex folding locally at outcrop scale within blocks and slabs of clastic strata); contraction thus appears to predate latest extension. Matrix areas of mélange may be either sheared serpentinite or argillite. Individually mapped blocks and slabs in mélange include the following units:

omv **Mafic volcanic rocks, including pillow basalt, diabase, and noncumulate gabbroic intrusive rocks**—Locally abundant in Morgan Valley area; locally includes minor blocks of mafic breccia that may correlate with megabreccia (unit Jgb)

oms **Undivided marine clastic rocks, commonly argillitic (Lower Cretaceous and Upper Jurassic)**—Sheared and isoclinally folded at outcrop scale; locally contains concretionary carbonate lenses containing Late Jurassic and Early Cretaceous *Buchias* and rarely conglomerate

omd **Diabase, mapped locally**—Sheared and coarse to fine grained with ophitic texture; may display chill zones; probably represents dike screens, but an in-situ origin is not evident

omg **Gabbro, mapped locally**—Sheared and medium- to fine-grained, largely noncumulate rocks with granular textures, with clinopyroxene and secondary amphibole, probably derived from deep-seated intrusives; evidence of an in-place origin is lacking

omc **Radiolarian chert, mapped locally (Upper Jurassic, Kimmeridgian)**—Locally tuffaceous; contains Late Kimmeridgian radiolarian fauna in Little Indian Valley area (McLaughlin and others, 1990)

omb **Blueschist, mapped locally**

omun **Blocks of unknown lithology**—Mapped aerially but not examined in the field

COAST RANGE OPHIOLITE

Joc **Pelagic chert (Upper to Middle Jurassic, Tithonian to Bajocian)**—Locally tuffaceous; depositional on basalt flows and may correlate with radiolarian chert in blocks of mafic volcanic rocks in ophiolitic mélange unit. Radiolarians from tuffaceous chert in the Stonyford section of the Coast Range ophiolite (Shervais and others, 2005a) are Middle to Late Jurassic (Kimmeridgian to Bajocian); in the nearby Geysers-Clear Lake region, correlative pelagic tuffaceous radiolarian chert in the Coast Range ophiolite is Late Jurassic (Kimmeridgian to Tithonian) (McLaughlin and others, 1988)

Jov **Basaltic pillowed flows and flow breccias (Middle Jurassic)**—Includes shallow-level diabase feeder dikes and sills that intrude pillow flows and breccias locally. Probably equivalent to some extrusive basaltic rocks in ophiolitic mélange unit

Jod **Diabase dikes and sills (Middle Jurassic)**—Mafic dikes and sills, with ophitic and microgranular textures. Structurally underlie or locally intrude the lower part of basaltic flows and flow breccias and, in part, the same age or younger; may correlate with some blocks of diabase in ophiolitic mélange unit

Jog **Gabbro and ultramafic rocks (Middle Jurassic)**—Gabbro, coarsely crystalline to medium grained locally with layered (cumulate) texture. Structurally underlies intrusive and extrusive parts of the Coast Range ophiolite; in places, includes plagiogranite and intrusive hornblende gabbro dikes or sills. Locally, unit grades downward into layered (cumulate) ultramafic rocks; pods and lenses of chromitite locally occur in cumulate layering transitional from dunite to gabbro. U-Pb ages on zircon (Hopson and others, 1981; McLaughlin and others, 1988), $^{40}Ar/^{39}Ar$ ages on glass (Shervais and others, 2005b), and K-Ar ages from hornblende (Lanphere and others, 1971) in cumulate and noncumulate gabbroic rocks of the Coast Range ophiolite in the northern Sacramento Valley (Paskenta and Elder Creek), and its structural outliers in the nearby Clear Lake area (Harbin Springs) range from 155 Ma (K-Ar, hornblende) to 169–163 Ma (U-Pb, zircon)

Josp **Serpentinized ultramafic rocks (Middle Jurassic)**—Layered ultramafic cumulate rocks that are transitional upward, or that alternate laterally, with tectonized harzburgite, dunite, peridotite, and rare screens of cumulate gabbro. The serpentinized ultramafic rocks are generally penetratively sheared and commonly form folded sheet-like zones of serpentinite-matrix mélange. A penetrative shear fabric and widespread boudinage have extensively overprinted any primary layering in these serpentinized rocks. In least sheared parts of the serpentinized ultramafic unit, primary compositional layering in dunite and peridotite may be locally preserved. Rare screens of noncumulate microgabbro or diabase, which weather into pinnacle-like topographically resistant exposures above an enclosing softer serpentinite matrix, may have been intrusive into the ultramafic rocks prior to their shearing into the enclosing mélange (for example, Macpherson and Phipps, 1988). The serpentinized ultramafic rocks mapped here as parts of the Coast Range ophiolite are incorporated in places into ophiolitic mélange (unit KJom) as intact kilometer-scale or smaller mélange slabs and sheared mélange matrix. (See Correlation of Map Units, sheet 2)

FRANCISCAN COMPLEX

CENTRAL BELT

Central Belt Mélange terrane (lower Tertiary and Upper Cretaceous)

fcm **Undivided mélange (lower Tertiary and Upper Cretaceous)**—Unit contains both large broken slabs of intact to semi-intact rock up to several kilometers in length and much smaller mappable blocks ("knockers") from 1 m to hundreds of meters in length, all enclosed by a mélange matrix of crushed, penetratively sheared and boudinaged argillite and sandstone. The large, intact slab-like bodies consist largely of sandstone and basalt, or a composite of interlayered basalt, chert, and sandstone. Areas underlain by extensive mélange matrix commonly exhibit numerous earth flows. The blocks are identified where known, but many blocks visible aerially were not accessed on the ground and are labeled only as blocks of unknown composition. Undivided mélange includes blocks too small to show at map scale, but locally, the lithologies of small blocks are delineated by symbols where accessed. Some chert in large slabs of interlayered basalt, chert, and sandstone contains radiolarians that correlate in age with parts of the Marin Headlands-Geysers terrane (McLaughlin, 1978; McLaughlin and Pessagno, 1978; Murchey and Jones, 1984). Other smaller mélange blocks of sandstone, basalt, and chert may also correlate with the Marin Headlands-Geysers terrane and probably represent dismembered fragments of that terrane. Interlayered basalt, chert, sandstone, and rare conglomerate in the large coherent slabs, some of which may have radiolarian or other fossil control, are assigned to the Marin Headlands-Geysers terrane. Smaller, individual mélange blocks of basalt, chert, and sandstone without any biostratigraphic age control are delineated only as generic blocks of their respective lithologies (ss, c, or v). Some of these mélange blocks are of higher metamorphic grade than the Marin Headlands-Geysers terrane and possibly are derived from metachert, metabasalt, and metasandstone in the Eastern Belt. We have included two additional tectonostratigraphic terranes in the Central Belt (the Pomo terrane and Snow Mountain volcanic terrane) that occur only in the map area and are distinguished by their distinctive tectonostratigraphy and igneous characteristics. Individually mapped undivided mélange slabs and blocks on the geologic map include the following units:

ss **Sandstone and argillite (in part, Upper Cretaceous, Cenomanian or younger; middle Cretaceous, Aptian or younger; and possibly, Upper Jurassic, Tithonian or younger)**

c **Radiolarian chert (Upper Cretaceous to Middle Jurassic)**

v **Basaltic volcanic rocks (Jurassic)**

cgl **Conglomerate (Lower Cretaceous and (or) Upper Jurassic or younger)**—Rare, occurs as block in mélange northeast of Willis Ridge in northwestern part of map

db **Diabase (Cretaceous or Jurassic?)**

ms **Metasedimentary rocks (Lower Cretaceous? or younger)**

b **Blueschist blocks (Jurassic)**

un **Blocks of unknown lithology**—Viewed aerially but not accessed on ground

Pomo terrane (Upper Cretaceous to Upper Jurassic)

spo **Basaltic breccia, sandstone, and shale (Upper Cretaceous, Maastrichtean)**

vpo **Alkalic pillow basalt, pillow-breccias, and minor diabase and chert (Jurassic)**

Marin Headlands-Geysers terrane (Upper Cretaceous to Lower Jurassic)

smg **Sandstone and argillite (Upper Cretaceous, Cenomanian? or younger)**

cgmg **Conglomerate (Upper Cretaceous, Cenomanian? or younger)**—Large, thick, coarse, cobbly to bouldery lenses interbedded with unit smg southwest of Camelback Ridge and serpentinite sheet (unit Josp) in southwest corner of the map

cmg **Radiolarian chert (Upper Cretaceous, lower Cenomanian to Lower Jurassic, Pliensbachian)**

vmg **Basaltic volcanic rocks (Lower Jurassic)**

Snow Mountain volcanic terrane (Lower Cretaceous, Valanginian or younger?)

vsm **Basaltic to rhyolitic volcanics and intrusive rocks**

dsm **Diabasic intrusive rocks, largely sill-like**—Locally mapped as intruding basaltic to rhyolitic rocks

psm **Porphyritic basaltic rocks**—Possibly includes intrusive sills and non-pillowed flows

ssm **Metasandstone and argillite**—Locally intercalated with volcanic rocks; lawsonite-bearing, with minor chert

EASTERN BELT

Yolla Bolly terrane (Upper and Lower Cretaceous to Upper Jurassic, Tithonian)

fym **Mélange of the Yolla Bolly terrane (Upper Cretaceous)**—Includes the following blocks:

by **Blueschist**

cgy **Conglomerate**

cy **Metachert (Early Cretaceous, Albian or Aptian, to Middle Jurassic, Aelenian)**—Also structurally interlayered with unit vy in unit fys; inferred correlation of cy blocks to cy interlayered in fys is speculative

gy **Gabbro**

lsy **Limey mudstone**—Mapped in one area of Mendocino National Forest

vy **Metavolcanic rocks (Middle Jurassic, Aelenian or older)**—Also structurally interlayered with unit cy in unit fys; inferred correlation of vy blocks to vy interlayered in fys is speculative

mspy **Metaserpentinite blocks or lenses**

uny **Unidentified blocks**

fys **Metasandstone and argillite, locally conglomeratic (Upper and Lower Cretaceous, Cenomanian to Aptian, to Late Jurassic, Tithonian)**—Rhythmically interbedded, thick- to thin-bedded, turbiditic, slaty metasandstone and argillite, reconstituted to high textural zone 1 to textural zone 2 (Blake and others, 1967), commonly displaying graded bedding. Metasandstone locally with interbedded, thin lenses of dark chert-pebble-rich metaconglomerate. Rocks generally are highly folded isoclinally, with a prominent axial planar cleavage at high to low angle to bedding. Petrographically, metasedimentary rocks that are reconstituted to textural zone 2 commonly contain neoblastic lawsonite and phengitic white mica growing parallel to platy partings and in places deformed along the parting. Very rarely, jadeitic pyroxene and (or) sodic amphibole is present in some lithic metasandstone with significant mafic igneous detritus. Structurally low, fine-grained metasedimentary rocks, reconstituted only to textural zone 1 in the Little Indian Valley area, do not contain lawsonite or other identifiable blueschist minerals; nevertheless, they still display a prominent slaty parting and have yielded numerous Lower Cretaceous and Late Jurassic (Tithonian–Valanginian) fossils (largely *Buchia sp.*)

cy **Metachert (Lower Cretaceous, Albian to Aptian, to Middle Jurassic, Aalenian)**—Red to green, tuffaceous radiolarian metachert with a prominent axial planar slaty parting, locally folded isoclinally. Overlies a thin unit of metabasaltic flows and breccias that is, in turn, faulted at the base. Analysis of radiolarians from the metachert have yielded somewhat different age relations. West of Covelo, along Hwy 162, a section of metachert studied by Isozaki and Blake (1994) was found to contain a Middle Jurassic (Aalenian) to Late Jurassic (Tithonian) fauna. Elsewhere, in the Sanhedrin Mountain area (Ohlin and others, 2010), along Hwy 20 north of Clear Lake, near Clear Lake Highlands, and near Borax Lake to the south (sheet 1), radiolarians range from Late Jurassic to Middle Cretaceous (Aptian or Albian) in Yolla Bolly terrane metacherts (this report and Ohlin and others, 2010). Although this unit is assigned the same unit symbol as metachert blocks in Mélange of the Yolla Bolly terrane (fym), direct correlation with cy blocks in unit fym is largely speculative

vy **Metavolcanic rocks (Middle Jurassic, Aalenian or older)**—As described in Ohlin and others (2010), mafic metavolcanic rocks of the Yolla Bolly terrane collectively mapped as greenstone include tuff, basaltic pillow flows, breccias, and diabase. In the Sanhedrin Mountain block, sparse lenses of metavolcanic rocks are locally interleaved structurally with thick lenses of metachert and metasandstone and argillite. We interpret these contacts of interleaved metasandstone, metachert, and metavolcanics rocks as probable faults. In the structurally lower part of the Sanhedrin Mountain block, adjacent to the Bartlett Springs Fault Zone, sheared lenses of tuffaceous greenstone are intersheared with lenses of conglomerate and feldspathic metasandstone. In the Hull Mountain block east of the Bartlett Springs Fault Zone, porphyritic pillow basalt and tuff are also locally present and well exposed in lower Mendenhall Creek, interlayered with metasandstone and folded at outcrop scale. Along Forest Service Road M1 north of Hull Mountain and south of Monkey Rock, a zone of metatuff is interlayered in metasandstone. The fine-grained metatuff locally contains blue sodic amphibole, light-green hornblende (edenite?), pumpellyite, and stilpnomelane, compatible with the metamorphic

grade of the enclosing metasandstone and argillite. Although this unit is assigned the same map symbol as blocks of metavolcanic rocks that occur in mélange of the Yolla Bolly terrane (unit fym), the implied correlation of the metavolcanic blocks to the metavolcanic rocks interleaved with unit cy in unit fys is highly speculative

miy **Mafic intrusive rocks (Early Cretaceous)**—Ohlin and others (2010) described gabbroic dikes and sills that intrude Cenomanian(?) and older metasandstone and argillite in the Hull Mountain block, near Monkey Rock, and at a locality along the Hull Mountain road 1 km to the southeast. The intrusive rocks were earlier shown to have well-preserved chilled contacts (Layman, 1977; Echeverria, 1980) and they trend northwest discontinuously for 1 km. The largest intrusive body is 20 m thick (Layman, 1977). The intrusives exhibit chilled margins and the adjacent metasandstone shows evidence of baking along contacts with metasedimentary rocks. Metamorphic minerals present in the metagabbro include lawsonite, pumpellyite, albite, sodic amphibole, carbonate minerals, stilpnomelane, chlorite, quartz, and white mica (Layman, 1977), indicating that intrusion predated blueschist-grade metamorphism

Pickett Peak terrane (Lower Cretaceous, Aptian to Barremian)

fpp **Undivided metasedimentary and metavolcanic rocks and metachert**

cpp **Metachert**

vpp **Basaltic metavolcanic rocks**

Mendocino Pass terrane (Lower Cretaceous, Valanginian)

fmp **Foliated metasandstone, argillite, and minor undivided metachert and greenstone**

cmp **Metachert and greenstone blocks**

References Cited

Bailey, E.H., Blake, M.C., Jr., and Jones, D.L., 1970, On-land Mesozoic ocean crust in California Coast Ranges: U.S. Geological Survey Professional Paper 700–C, p. C70–C81.

Bailey, E.H., Irwin, W.P., and Jones, D.L., 1964, Franciscan and related rocks and their significance in the geology of western California: California Division of Mines and Geology Bulletin 183, 177 p.

Berkland, J.O., 1969, Late Mesozoic and Tertiary sequence near the proposed Garrett Tunnel, Mendocino and Lake Counties, California: Sacramento, Calif., U.S. Bureau of Reclamation, Region 2, unpublished file report and field sheets, 13 p.

Berkland, J.O., 1972, Paleogene "frozen" subduction zone in the Coast Ranges of northern California: International Geologic Congress, v. 24, sec. 3, p. 99–105.

Berkland, J.O., 1973, Rice Valley outlier—New sequence of Cretaceous–Paleocene strata in northern Coast Ranges, California: Geological Society of America Bulletin, v. 84, p. 2389–2406.

Berkland, J.O., 1978, Franciscan Complex-Great Valley Sequence relationships north of Clear Lake, California: American Association of Petroleum Geologists Pacific Section field trip guidebook, Castle Steam Field, p. 9–25.

Bishop, D.G., 1977, South Fork Mountain Schist at Black Butte and Cottonwood Creek, northern California: Geology, v. 55, p. 595–599.

Blake, M.C., Jr., Harwood, D.S., Helley, E.J., Irwin, W.P., Jayko, A.S., and Jones, D.L., 2000, Geologic map of the Red Bluff 30′ × 60′ quadrangle, California: U.S. Geological Survey Miscellaneous Investigations Series Map, I–2542, scale 1:100,000.

Blake, M.C., Jr., Helley, E.J., Jayko, A.S., Jones, D.L., and Ohlin, H.N., 1992, Geologic map of the Willows 1:100,000 quadrangle, California: U.S. Geological Survey Open-File Report 92–271, scale 1:100,000.

Blake, M.C., Jr., Howell, D.G., and Jones, D.L., 1982, Preliminary tectonostratigraphic terrane map of California: U.S. Geological Survey Open-File Report 82–593, 9 p., 3 sheets.

Blake, M.C., Jr., Irwin, W.P., and Coleman, R.G., 1967, Upside-down metamorphic zonation, blueschist facies, along a regional thrust in California and Oregon, *in* Geological Survey Research, 1967: U.S. Geological Survey Professional Paper 575–C, p. C1–C9.

Blake, M.C., Jr., and Jayko, A.S., 1983, Geologic map of the Yolla Bolly Middle Eel Wilderness and adjacent roadless areas: U.S. Geological Survey Miscellaneous Field Studies Map 1595–A, scale 1:62,500.

Blake, M.C., Jr., Jayko, A.S., Jones, D.L., and Rogers, B.W., 1987, Unconformity between Coast Range ophiolite and part of the lower Great Valley sequence, South Fork of Elder Creek, Tehama County, California, *in* Hill, M.L., ed., Centennial Field Guide Volume 1: Geological Society of America, Cordilleran Section, p. 279–282.

Blake, M.C., Jr., Jayko, A.S., and McLaughlin, R.J., 1985, Tectonostratigraphic terranes of northern California, *in* Howell, D.G., ed., Tectonostratigraphic terranes of the circum-Pacific region: Houston, Tex., Circum-Pacific Council for Energy and Mineral Resources, Earth Science Series, v. 1, p. 159–171.

Blake, M.C., Jr., Jayko, A.S., McLaughlin, R.J., and Underwood, M.B., 1988, Metamorphic and tectonic evolution of the Franciscan Complex, northern California, chap. 38 *of* Ernst, W.G. ed., Metamorphism and crustal evolution of the western United States (Rubey Volume VII): Englewood Cliffs, N.J., Prentice Hall, p. 1035–1060.

Blake, M.C., Jr., and Jones, D.L., 1974, Origin of Franciscan mélanges in northern California: Society of Economic Paleontologists and Mineralogists Special Publication 19, p. 345–357.
Bolt, B.A., and Oakeshott, G.B., 1982, Seismic and tectonic evaluation for Scott Dam and vicinity: San Francisco, Calif., unpublished report for Pacific Gas and Electric Company.
Brown, E.H., and Ghent, E.D., 1983, Mineralogy and phase relations in the blueschist facies of the Black Butte and Ball Rock areas, northern California Coast Ranges: American Mineralogist, v. 68, p. 365–372.
Brown, R.D., Jr., 1964, Geologic map of the Stonyford quadrangle, Glenn, Colusa and Lake Counties, California: U.S. Geological Survey Mineral Investigations Field Studies Map MF–279, scale 1:48,000, 3 pp.
Brown, R.D., Jr., Grimes, D.J., Leinz, R., Federspiel, F.E., Leszcykowsky, A.M., and Griscom, A., 1981, Mineral Resources of the Snow Mountain Wilderness Study Area, California: U.S. Geological Survey Bulletin 1495, 48 p., 2 map plates.
Bufe, C.G., Marks, S.M., Lester, F.W., Ludwin, R.S. and Stickney, M.C., 1981, Seismicity of The Geysers-Clear Lake region, *in* McLaughlin, R.J., and Donnelly-Nolan, J.M., eds, Research in the The Geysers-Clear Lake Geothermal area, northern California: U.S. Geological Survey Professional Paper 1141, p. 129–138.
Campbell, K.A., and Bottjer, D.J., 1995, *Peregrinella*; an Early Cretaceous cold-seep-restricted brachiopod: Paleobiology, v. 24, p. 461–478.
Campbell, K.A., Carlson, C., and Bottjer, D.J., 1993, Fossil cold seep limestones and associated chemosymbiotic macroinvertebrate faunas, Jurassic–Cretaceous Great Valley Group, California, *in* Graham, S.A., and Lowe, D.R., eds., Advances in the sedimentary geology of the Great Valley Group, Sacramento Valley, California: Los Angeles, Pacific Section of the Society of Economic Paleontologists and Mineralogists, p. 37–50.
Campbell, K.A., Farmer, J.D., and Des Marais, D., 2002, Ancient hydrocarbon seeps from the Mesozoic convergent margin of California; carbonate geochemistry, fluids and palaeoenvironments: Geofluids, v. 2, p. 63–94.
Campbell, K.A., Peterson, D., and Alfaro, A.C., 2008, Two new species of Retiskenea? (Gastropoda: Neomphalidae) from Lower Cretaceous hydrocarbon seep—carbonates of northern California: Journal of Paleontology, v. 82, p. 140–153.
Cardwell, 1965, Geology and ground water in Russian River valley areas: U.S. Geological Survey Water-Supply Paper 1548.
Carver, G.A., 1987, Late Cenozoic tectonics of the Eel River basin region, coastal northern California, *in* Schymiczek, H., and Suchland, R., eds, Tectonics, sedimentation, and evolution of the Eel River and coastal basins of northern California: San Joaquin Geological Society Miscellaneous Publication 37, p. 61–72.
CDWR, 1966, Engineering geology of Dos Rios-Grindstone Tunnel: California Department of Water Resources, unpublished office report.
CDWR, 1968, Areal geology Hayshed-Grindstone and Elk-Grindstone tunnels: California Department of Water Resources, unpublished map.
CDWR, 1969, Areal geology, Elk Creek tunnel: California Department of Water Resources, unpublished office report.
Chapman, A.D., Kidder, S., Saleeby, J.B., and Ducea, M.N., 2010, Extrusion of the Rand and Sierra de Salinas schists in Late Cretaceous extension and rotation of the southern Sierra Nevada and vicinity: Tectonics, v. 29, TC5006, https://doi.org/10.1929/2009TC002597.
Chapman, A.D., Saleeby, J.B., Wood, D.J., Piasecki, A., Kidder, S., Ducea, M.N., and Farley, K.A., 2012, Late Cretaceous gravitational collapse of the southern Sierra Nevada batholith, California: Geosphere, v. 8, p. 314–341, https://doi.org/10.1130/GES00740.1.
Clark, S.G., 1940, Geology of the Covelo District, Mendocino County, California: University of California Department of Geology Bulletin, v. 82, p. 119–142.
Clarke, S.H., Jr., 1990, Map showing geologic structures of the northern California continental margin: U.S. Geological Survey Miscellaneous Field Studies Map MF–2130, scale 1:250,000.
Clarke, S.H., Jr., and Carver, G.A., 1992, Late Holocene tectonics and paleoseismicity, southern Cascadia subduction zone: Science, v. 255, p. 188–192.
Coleman, R.G., and Lanphere, M.A., 1971, Distribution and age of the high-grade blueschists, associated eclogites, and amphibolites from Oregon and California: Geological Society of America Bulletin, v. 82, p. 2397–2412.
Colgan, J.P., McPhee, D.K., McDougall, Kristin, and Hourigan, J.K., 2012, Superimposed extension and shortening in the southern Salinas Basin and La Panza Range, California; A guide to Neogene deformation in the Salinian block of the central California Coast Ranges: Lithosphere, v. 4, no. 5, p. 411–429; GSA Data Repository Item 2012244; https://doi.org/10.1130/L208.1.
DePolo, C.M., and Ohlin, H.N., 1984, The Bartlett Springs Fault Zone—An eastern member of the California plate boundary system: Geological Society of America, Abstracts with Programs, v. 16, no. 6, p. 486.
Dickinson, W.R., Ingersoll, R.V., and Graham, S.A., 1979, Paleogene sediment dispersal and paleotectonics in northern California: Geological Society of America Bulletin, v. 90, p. 1458–1528, https://doi.org/10.1130/GSAB-P2-90-1458.
Donnelly-Nolan, J.M., Hearn, B.C., Jr., Curtis, G.H., and Drake, R.E., 1981, Geochronology and evolution of the Clear Lake volcanics: U.S. Geological Survey Professional Paper 1141, p. 47–60.
Dumitru, T.A., Ernst, W.G., Hourigan, J.K., and McLaughlin, R.J., 2015, Detrital zircon U-Pb reconnaissance of the Franciscan subduction complex in northwestern California: International Geology Review, v. 57, no. 5–8, p. 767–800, https://doi.org/10.1080/00206814.2015.1008060.
Dumitru, T.A., Wakabayashi, J., and Wright, J.E., 2009, Time-varying accretion, nonaccretion, and high-pressure metamorphism in the Franciscan subduction complex, from the initiation of subduction until ca. 80 Ma: Geological Society of America Abstracts with Programs, v. 41, no.7, p. 404.
Dumitru, T.A., Wright, J.E., Wakabayashi, J., and Wooden, J.L., 2010, Early Cretaceous transition from nonaccretionary behavior to strongly accretionary behavior within the Franciscan subduction complex: Tectonics, v. 29, TC5001, https://doi.org/10.1029/2009TC002542.
Eberhart-Phillips, D., 1988, Seismicity in the Clear Lake area, California, 1975–1983, *in* Sims, J.D., ed., Late Quaternary climate tectonism and sedimentation in Clear Lake, northern California Coast Ranges: Geological Society of America Special Paper 214, p. 195–206.
Echeverria, L.M., 1980, Oceanic basaltic magmas in accretionary prisms—The Franciscan intrusive gabbros: American Journal of Science, v. 280, p. 697–724.

Ernst, W.G., 1971, Petrologic reconnaissance of Franciscan metagraywackes from the Diablo Range, central California Coast Ranges: Journal of Petrology, v. 12, p. 413–437, https://doi.org/10.1093/petrology/12.2.413.
Ernst, W.G., and McLaughlin, R.J., 2012, Mineral parageneses, regional architecture, and tectonic evolution of Franciscan metagraywackes, Cape Mendocino-Garberville-Covelo 30° × 60° quadrangles, northwest California: Tectonics, v. 31, TC1001, https://doi.org/10.1029/2011TC002987V.E.
Ernst, W.G., Seki, Y., Onuki, H., and Gilbert, M.C., 1970, Comparative study of low-grade metamorphism in the California Coast Ranges and Outer Metamorphic Belt of Japan: Geological Society of America Memoir 124, 276 p.
Etter, S.D., 1979, Geology of the Lake Pillsbury area, northern Coast Ranges: Austin, University of Texas, Ph.D. dissertation, 275 p.
Gabb, W.M., 1869, Cretaceous and Tertiary fossils: Palaeontology, v. II., Geological Survey of California, p. 1–299.
Gaines, J.M., 2008, Fluvial strath terrace formation and soil development with tectonic implications along Cache Creek, California: Arcata, Calif., Humboldt State University, M.S. thesis, 113 p.
Geomatrix Consultants, 1986, Final report, geological assessment of the seismic potential of the Bartlett Springs shear zone for Scott Dam, Lake County, California: San Francisco, unpublished report for Pacific Gas and Electric Company.
Ghent, E.D., 1965, Glaucophane-schist facies metamorphism in the Black Butte area, northern Coast Ranges, California: American Journal of Science, v. 263, no. 5, p. 385–400.
Godfrey, N.J., 1997, Ophiolitic basement to the Great Valley forearc basin, California, from seismic and gravity data; Implications for crustal growth at the North American continental margin: Geological Society of America Bulletin, v. 108, no. 12, p. 1536–1562.
Graymer, R.W., Jones, D.L., and Brabb, E.E., 2002a, Geologic map and database of northeastern San Francisco Bay Region, California: U.S. Geological Survey Miscellaneous Field Studies Map MF–2403, scale 1:100,000, 28 p.
Graymer, R.W., Sarna-Wojcicki, A.M., Walker, J.P., McLaughlin, R.J., Fleck, R.J., 2002b, Controls on timing and amount of right-lateral offset on the East Bay fault system, San Francisco Bay region, California: Geological Society of America Bulletin, v. 114, no. 12, p. 1471–1479.
Hagstrum, J.T., and Murchey, B.L., 1993, Deposition of Franciscan Complex cherts along the paleoequator and accretion to the American margin at tropical paleolatitudes: Geological Society of America Bulletin v. 105, p. 766–778.
Hammersley, L., and DePaolo, D.J., 2006, Isotopic and geophysical constraints on the structure and evolution of the Clear Lake volcanic system: Journal of Volcanology and Geothermal Research, v. 153, p. 331–356.
Hayes, G.P., Johnson, C.B., and Furlong, K.P., 2006, Evidence for melt injection in the crust of northern California?: Earth and Planetary Science Letters, v. 248, p. 638–649, https://doi.org/10.1016/j.epsl.2006.05.008.
Hearn, B.C., Jr., Donnelly-Nolan, J.M., and Goff, F.E., 1995, Geologic map and structure sections of the Clear Lake volcanics, northern California: U.S. Geological Survey Miscellaneous Investigation Series I–2362, scale 1:24,000.
Hearn, B.C., Jr., McLaughlin, R.J., and Donnelly-Nolan, J.M., 1988, Tectonic framework of the Clear Lake basin, California, *in* Sims, J.D., ed., Late Quaternary climate, tectonism, and sedimentation in Clear Lake, northern California Coast Ranges: Geological Society of America Special Paper 214, p. 9–20.
Hepper, Kristin, 2004, A new hydrocarbon seep locality in the Mesozoic Great Valley Group, Guenoc Ranch, northern California: San Francisco State University, unpublished M.S. thesis, 154 p.
Herd, D.G., 1978, Intracontinental plate boundary east of Cape Mendocino, California: Geology, v. 6, p. 721–725.
Holway, R.S., 1914, Apparent limits of former glaciation in the northern coast ranges of California: Geological Society of America Abstracts with Programs, v. 25, p. 120–121.
Hopson, C.A., Mattinson, J.M., and Pessagno, E.A., Jr., 1981, Coast Range ophiolite, western California, *in* Ernst, W.G., ed., The geotectonic development of California, Rubey Volume I: Englewood Cliffs, N.J., Prentice-Hall, p. 418–510.
Hopson, C.A., Mattinson, J.M., Pessagno, E.A., Jr., and Luyendyk, B.P., 2008, California Coast Range ophiolite; Composite Middle and Late Jurassic oceanic lithosphere, *in* Wright, J.E., and Shervais, J.W., eds, Ophiolites, arcs, and batholiths—A tribute to Cliff Hopson: Geological Society of America Special Paper 438, p. 1–101, https://doi.org/10.1130/2008.2438(01).
Irwin, W.P., 1960, Geologic Reconnaissance of the northern Coast Ranges and Klamath Mountains, California: California Division of Mines Bulletin 179, 80 p., map plate, scale 1: 500,000.
Irwin, W.P., Wolfe, E.W., Blake, M.C., Jr., and Cunningham, C.G., Jr., 1974, Geologic map of the Pickett Peak quadrangle, Trinity County, California: U.S. Geological Survey Geologic Quadrangle Map GQ–1111, scale 1:62,500.
Isozaki, Y., and Blake, M.C., Jr., 1994, Biostratigraphic constraints on formation and timing of accretion in a subduction complex—An example from the Franciscan Complex of northern California: Journal of Geology, v. 102, p. 283–296.
Jachens, R.C., Griscom, Andrew, and Roberts, C.W., 1995, Regional extent of Great Valley basement west of the Great Valley, California; Implications for extensive tectonic wedging in the California Coast Ranges: Journal of Geophysical Research, v. 100, no. B7, p. 12769–12790.
Jayko, A.S., 1984, Structure and deformation of the eastern Franciscan belt, northern California: Santa Cruz, University of California, Ph.D. dissertation, 206 p.
Jayko, A.S., Blake, M.C., Jr., and Harms, Tekla, 1987, Attenuation of the Coast Range ophiolite by extensional faulting and nature of the Coast Range "thrust," California: Tectonics, v. 6, p. 475–488.
Jayko, A.S., Blake, M.C., Jr., McLaughlin, R.J., Ohlin, H.N., Ellen, S.D., and Kelsey, H., 1989, Reconnaissance geologic map of the Covelo 30- by 60-minute quadrangle, northern California: U.S. Geological Survey Miscellaneous Field Studies Map MF–2001, scale 1:100,000, http://ngmdb.usgs.gov/Prodesc/proddesc_327.htm.
Jennings, C.W., 1977, Geologic map of California, updated version, 2010, Guttierrez, C., Bryant, W., Saucedo, G. and Wills, C., compilers: California Geological Survey, scale 1:750,000.
Jennings, C.W., and Strand, R.G., 1960, Geologic map of Ukiah quadrangle, California: California Division of Mines and Geology Regional Geologic Map Series, scale, 1:250,000.

Jones, D.E., Bailey, E.H., and Imlay, R.W., 1969, Structural and stratigraphic significance of the Buchia zones in the Colyear Springs-Paskenta area, California: U.S. Geological Survey Professional Paper 647–A, p. 1–24.

Kiel, S., and Campbell, K.A., 2005, Lithomphalus enderlini gen. et sp. nov. from cold-seep carbonates in California—A Cretaceous neomphalid gastropod?: Palaeogeography, Palaeoclimatology, Palaeoecology, v. 227, p. 232–241.

Kiel, S., Campbell, K.A., Elder, W.P., and Little, C.T.S., 2008, Jurassic and Cretaceous gastropods from hydrocarbon seeps in forearc basin and accretionary prism settings, California: Acta Palaeontologica Polonica, v. 53, no. 4, p. 679–703.

Kiel, S., Glodny, J., Birgel, D., Bulot, L.G., Campbell, K,A,, Gaillard, C., Graziano, R., Kaim, A., Lazar, I., Sandy, M.Rl, and Peckmann, J., 2014, The paleoecology, habitats, and stratigraphic range of the enigmatic Cretaceous brachiopod Peregrinella: PLos ONE, v. 9, no.10:e109260. https://doi.org/10.1371/journal.pone0109260.

Koski, R.A., Lamons, R.C., Dumoulin, J.A., and Bouse, R.M., 1993, Massive sulfide metallogenesis at a late Mesozoic sediment-covered spreading axis—Evidence from the Franciscan Complex and contemporary analogues: Geology, v. 21, p. 137–140, https://doi.org/10.1130/0091-7613(1993)021<0137:MSMAAL>2.3.CO;2.

Langenheim, V.E., Jachens, R.C., Morin, R.L. and McCabe, C.A., 2007, Preliminary gravity and magnetic data of the Lake Pillsbury region, northern Coast Ranges, California: U.S. Geological Survey Open-File Report 2007–1368, 22 p.

Langenheim, V.E., Jachens, R.C., Wentworth, C.M., and McLaughlin, R.J., 2011, Aeromagnetic and aeromagnetic-based geologic maps of the Coastal Belt, Franciscan Complex, northern California: U.S. Geological Survey Scientific Investigations Map 3188, pamphlet 20 p., 3 sheets, scales 1:100,000 and 1:250,000, and database, available at http://pubs.usgs.gov/sim/3188/.

Lanphere, M.A., 1971, Age of the Mesozoic oceanic crust in the California Coast Ranges: Geological Society of America Bulletin, v. 82, p. 3209–3211.

Lanphere, M.A., Blake, M.C., Jr., and Irwin, W.P., 1978, Early Cretaceous metamorphic age of the South Fork Mountain Schist in the northern Coast Ranges of California: America Journal of Science, v. 278, p. 798–815.

Lawton, J.E., 1956, Geology of the north half of the Morgan Valley quadrangle and the south half of the Wilbur Springs quadrangle, California: Stanford, Calif., Stanford University, Ph.D. dissertation, 223 p.

Layman, E.B., 1977, Intrusive rocks in the near-trench environment—Two localities in the northern California Franciscan complex: Stanford, Calif., Stanford University, M.S. thesis, 55 p.

Lehman, D.H., 1974, Structure and petrology of the Hull Mountain area, northern California Coast Ranges: Austin, University of Texas, Ph.D. dissertation, 126 p.

Lienkaemper, J.J., 2010, Recently active traces of the Bartlett Springs Fault, California; A Digital Database: U.S. Geological Survey Data Series 541, version 1.0, http://pubs.usgs.gov/ds/541/.

Lienkaemper, J.J., DeLong, S., McPherson, R.C., Mielke, J., Avdievitch, N., Pickering, A., and Lloyd, C., 2014, Characterizing recent slip on the Kuikui Fault, a link between the Green Valley and Bartlett Springs Fault Zones, Wilson Valley, northern California: American Geophysical Union, Fall Meeting, abstract T41C-4665.

Lozos, J.C., Harris, R.A., Murray, J.R., and Lienkaemper, J.J., 2015, Dynamic rupture models of earthquakes on the Bartlett Springs Fault, northern California: Geophysical Research Letters, v. 42, p. 4343–4349, https://doi.org/10.1002/2015GL063802.

Macpherson, G.J., 1983, The Snow Mountain Volcanic Complex—On-land seamount in the Franciscan terrain, California: Journal of Geology, v. 91, p. 73–92.

Macpherson, G.J., and Phipps, S.P., 1988, Geochemistry and petrology of mafic volcanic rocks from olistostromes in the basal Great Valley Group, northern California Coast Ranges: Geological Society of America Bulletin, v. 100, no. 11, p. 1770–1779, https://doi.org/10.1130/0016-7606(1988)100<1770:GAPOMV>2.3.CO;2.

Mattinson, J.M., and Echeverria, L.M., 1980, Ortigalita Peak gabbro, Franciscan complex—U-Pb dates of intrusion and high-pressure low-temperature metamorphism: Geology, v. 8, p. 589–593.

McFarland, F.S., Lienkaemper, J.J., and Caskey, S.J., 2016, Data from theodolite measurements of creep rates on San Francisco Bay Region faults, California: U.S. Geological Survey Open-File Report 2009–1119, ver. 1.8, 21 p. and data files, accessed September 24, 2018, at https://pubs.usgs.gov/of/2009/1119.

McLaren, M.K., Wooddell, K.E., Page W.D., van der Elst, N., Stanton, M.A., and Walter, S.R., 2007, The McCreary Glade earthquake sequence—Possible reactivation of ancient structures near Lake Pillsbury, northern Coast Ranges, Mendocino County, California: Eos, Transactions of the American Geophysical Union, v. 88, no. 52, Fall Meeting Supplement, abstract S21A-0245.

McLaughlin, R.J., 1978, Preliminary geologic map and structural sections of the central Mayacmas Mountains and The Geysers steam field, Sonoma, Lake, and Mendocino Counties, California: U.S. Geological Survey Open-File Map 78-389, scale 1:24,000, with structure sections and explanation, 2 sheets.

McLaughlin, R.J., Blake, M.C., Jr., Griscom, A., Blome, C.D., and Murchey, B., 1988, Tectonics of formation, translation, and dispersal of the Coast Range ophiolite of California: Tectonics, v. 7, no. 5, p. 1033–1056.

McLaughlin, R.J., Campbell, K.A. Lienkaemper, J.J., Graymer, R.W., Moring, B.C, Ohlin, H.N., and Enderlin, D.A., 2010, Long term displacement across the Bartlett Springs Fault Zone—Implications for evolution of the east San Francisco Bay Fault System and structural hooks in the northern Coast Ranges, California: Geological Society of America Abstracts with Programs, v. 42, no. 5, p. 478, https://gsa.confex.com/gsa/2010AM/finalprogram/abstract_177965.htm.

McLaughlin, R.J., Colgan, J.P., Elder, W.P., Enderlin, D.A., Dumitru, T.A., and Holm-Denoma, C., 2016, Maximum depositional ages and provenance from detrital zircons compared to paleontologic ages and implications for deformation timing, Lower Great Valley Sequence, Knoxville to Lake Berryessa, west of Sacramento Valley, CA: Geological Society of America Abstracts with Programs, v. 48, no. 4, https://doi.org/10.1130/abs/2016CD-27421.

McLaughlin, R.J., Ellen, S.D., Blake, M.C., Jr., Jayko, A.S., Irwin, W.P., Aalto, K.R., Carver, G.A., and Clarke, S.H., Jr., 2000, Geology of the Cape Mendocino, Eureka, Garberville, and southwestern part of the Hayfork 30- × 60-minute quadrangles and adjacent offshore area, northern California: U.S. Geological Survey Miscellaneous Field Studies Map MF–2336, scale 1:100,000, 6 sheets including maps, explanation, cross sections, pamphlet, http://geopubs.wr.usgs.gov/map-mf/mf2336/.

McLaughlin, R.J., and Moring, B.A., 2013, The Bartlett Springs Fault Zone—Long term multi-episodic deformation of an early Tertiary synformal down-warp in the northern California Coast Ranges: Geological Society of America Abstracts with Programs, v. 45, no. 7, p. 167.

McLaughlin, R.J., and Ohlin, H.N., 1984, Tectonostratigraphic framework of the Geysers-Clear Lake region, California, *in* Blake, M.C., Jr., ed., Franciscan geology of northern California: Pacific section, Society of Economic Paleontologists and Mineralogists, v. 43, p. 221–254.

McLaughlin, R.J., Ohlin, H.N., and Thormahlen, D.J., 1990, Geologic map and structure sections of the Little Indian Valley-Wilbur Springs geothermal area, northern Coast Ranges, California: U.S. Geological Survey Miscellaneous Investigations Map I–1706, scale 1:24,000, structure sections, explanation and interpretive text (2 sheets).

McLaughlin, R.J., and Pessagno, E.A., Jr., 1978, Significance of age relations above and below Upper Jurassic ophiolite in the Geysers-Clear Lake region, California: U.S. Geological Survey Journal of Research, v. 6, p. 715–726.

McLaughlin, R.J., Sliter, W.V., Sorg, D.H., and Russell, P.C., 1996, Large-scale right-slip displacement on the East San Francisco Bay Region fault system, California—Implications for location of late Miocene to Pliocene Pacific plate boundary: Tectonics, v. 15, no. 1, p. 1–18.

McPeak, A.J., Cloos, M., and Stockli, D.F., 2015, Seamount arrival into the Franciscan subduction complex at 100 Ma, Marin Headlands, San Francisco Bay, California: Geological Society of America Abstracts with Programs, v. 47, no. 4, p. 45.

Mertz, D.F., Weinrich, A.J., Sharp, W.D., and Renne, P.R., 2001, Alkaline intrusions in a near-trench setting, Franciscan Complex, California—Constraints from geochemistry, petrology and $^{40}Ar/^{39}Ar$ chronology: American Journal of Science, v. 301, p. 877–911, https://doi.org/10.2475/ajs.301.10.877.

Metro Engineering, 2011, California ARRA lidar: Open Topography, https://doi.org/10.5069/G9H70CRD.

Moore, D.E., McLaughlin, R.J., and Lienkaemper, J.J., 2015, Serpentinite in a creeping trace of the Bartlett Springs Fault, northern California: Geological Society of America Abstracts with Programs, v. 47, p. 774.

Moore, D.E., Rymer, M.J., McLaughlin, R.J., and Lienkaemper, J.J., 2011, Mineralogy of faults in the San Andreas System that are characterized by creep: American Geophysical Union, 2011 Fall Meeting, San Francisco, Calif., abstract V11A-2504 poster.

Murchey, B.L., 1984, Biostratigraphy and lithostratigraphy of chert in the Franciscan Complex, Marin Headlands, California, *in* Blake, M.C., Jr., ed., Franciscan geology of northern California: Society of Economic and Paleontologists and Mineralogists, Pacific Section, v. 43, p. 51–70.

Murchey, B.L., and Jones, D.L., 1984, Age and significance of chert in the Franciscan Complex, in the San Francisco region, *in* Blake, M.C., Jr., ed., Franciscan geology of northern California: Pacific Section Society of Economic Paleontologists and Mineralogists, Book 43, p. 23–30

Murray, J.R., Minson, S.E., and Svarc, J.L., 2014, Slip rates and spatially variable creep on faults of the northern San Andreas system inferred through Bayesian inversion of Global Positioning System data: Journal of Geophysical Research, Solid Earth, v. 119, p. 6023–6047, https://doi.org/10.1002/2014JB010966.

Nilsen, T.H., and Clarke, S.H., Jr., 1989, Late Cenozoic basins of northern California: Tectonics, v. 8, no. 6, p. 1137–1158.

Ohlin, H.N., McLaughlin, R.J., Moring, B.C., and Sawyer, T.L., 2010, Geologic map of the Bartlett Springs Fault Zone in the vicinity of Lake Pillsbury and adjacent areas of Mendocino, Lake, and Glenn Counties, California: U.S. Geological Survey Open-File Report 2010–1301, scale 1:30,000, 32 p., http://pubs.usgs.gov/of/2010/1301/.

Pessagno, E.A., Jr., 1977, Upper Jurassic radiolaria and radiolarian biostratigraphy of the California Coast Ranges: Micropaleontology, v. 23, p. 56–113.

Pitt, A.M., Hill, D.P., Walter, S.W., and Johnson, M.J.S., 2002, Midcrustal, long-period earthquakes beneath northern California volcanic areas: Seismological Research Letters, v. 73, no. 2, p. 144–152.

Platt, J.P., 1986, Dynamics of orogenic wedges and the uplift of high-pressure metamorphic rocks: Geological Society of America Bulletin, v. 97, p. 1037–1053.

Raymond, L.A., 2014, Designating tectonostratigraphic terranes versus mapping rock units in subduction complexes; perspectives from the Franciscan Complex of California, USA: International Geology Review, v. 57, p. 801–823, https://doi.org/10.1080/00206814.2014.911124.

Richmond, J.A., 2005, New paleontological data for Great Valley Group sediments in the Guenoc Ranch area, Lake County, California: Geological Society of America, Abstracts with Programs, v. 37, no. 4, p. 42.

Robertson, A.H.F., 1990, Sedimentology and tectonic implications of ophiolite-derived clastics overlying the Jurassic Coast Range ophiolite, northern California: American Journal of Science, v. 290, no. 2, p. 109–163.

Rymer, M.J., 1981, Stratigraphic revision of the Cache Formation (Pliocene and Pleistocene), Lake County, California: U.S. Geological Survey Bulletin 1502–C, 35 p.

Saleeby, J., 2003, Segmentation of the Laramide slab—Evidence from the southern Sierra Nevada region: Geological Society of America Bulletin, v. 115, p. 655–668, https://doi.org/10.1130/0016-7606(2003)115<0655:SOTLSF>2.0.CO;2.

Shervais, J.W., Choi, S.H., Sharp, W.D., Ross, J., Zoglman-Schuman, M., and Mukasa, S.B., 2011, Serpentinite matrix mélange—Implications of mixed provenance for mélange formation, *in* Wakabayashi, J., and Dilek, Y., eds., Mélanges—Processes of Formation and Societal Significance: Geological Society of America Special Paper 480, p. 1–30, https://doi.org/10.1130/2011.2480(01).

Shervais, J.W., Murchey, B.L., Kimbrough, D.L., Renne, P.R., and Hanan, B.B., 2005a, Radioisotopic and biostratigraphic age relations in the Coast Range ophiolite of northern California—Implications for the tectonic evolution of the Western Cordillera: Geological Society of America Bulletin, v. 117, no. 5–6, p. 633–653.

Shervais, J.W., Zoglman Schuman, M.M., and Hanan, B.B., 2005b, The Stonyford Volcanic Complex; a forearc seamount in the northern California Coast Ranges: Journal of Petrology, v. 46, no. 10, p. 2091–2128, https://doi.org/10.1093/petrology/egi048.

Sibson, R.H., 1985, Stopping of earthquake ruptures at dilatational fault jogs: Nature, v. 316 no. 6025, p. 248–251.

Sims, J.D., Adam, D.P., and Rymer, M.J., 1981, Stratigraphy and palynology of Clear Lake, California, *in* McLaughlin, R.J., and Donnelly-Nolan, J., eds., Research in the Geysers-Clear Lake geothermal area, northern California: U.S. Geological Survey Professional Paper 1141, p. 219–230.

Sims, J.D., and Rymer, M.J., 1976, Map of gaseous springs and associated faults in Clear Lake, California: U.S. Geological Survey Miscellaneous Field Investigations Map MF–721, scale 1:48,000.

Slowey, A.J., and Rytuba, J.J., 2008, Mercury release from the Rathburn Mine, Petray Mine, and Bear Valley saline springs, Colusa County, California 2004–2006: U.S. Geological Survey Open-File Report 2008–1179, 49 p.

Stanford, J.E., 1991, Geology of the Franciscan Complex Central Belt between Redwood Valley and Potter Valley, Mendocino County, California: Hayward, California State University, M.S. thesis, 149 p., 2 map plates.

Stanton, T.W., 1895, Contributions to the Cretaceous paleontology of the Pacific coast; the fauna of the Knoxville beds: U.S. Geological Survey Bulletin 133, p. 1–132.

Stinson, M.C., 1957, Geology of the Island Mountain Copper Mine, Trinity County, California: California Journal of Mines and Geology, v. 53, p. 9–33.

Suppe, John, 1973, Geology of the Leech Lake Mountain-Ball Mountain region, California: University of California Publications in Geological Sciences, v. 107, p. 1–81.

Suppe, John, 1979, Cross section of the southern part of the northern Coast Ranges and Sacramento Valley, California: Geological Society of America Map and Chart Series, MC–28B.

Suppe, John, and Armstrong, R.L., 1972, K-Ar dating of Franciscan metamorphic rocks: American Journal of Science, v. 272, p. 217–233.

Suppe, John, and Foland, K.A., 1978, The Goat Mountain Schists and Pacific Ridge Complex—A redeformed but still-intact late Mesozoic Franciscan schuppen complex, *in* Howell, D.G., and McDougall, Kristen, eds., Mesozoic paleogeography of the western United States: Society of Economic Paleontologists and Mineralogists, Pacific Section, Pacific Coast Paleogeography Symposium 2, p. 431–451.

Surpless, K.D., Graham, S.A., Covault, J.A., and Wooden, J.L., 2006, "Does the Great Valley Group contain Jurassic strata?" Reevaluation of the age and early evolution of a classic forearc basin: Geology, v. 34, p. 21–24, https://doi.org/10.1130/G21940.1.

Swe, Win, 1968, Stratigraphy and structure of late Mesozoic rocks south and southeast of Clear Lake, California: Stanford, Calif., Stanford University, unpublished Ph.D. dissertation, 75 p., 4 tables, 12 figures, 3 plates.

Swe, Win, and Dickinson, W.R., 1970, Sedimentation and thrusting of late Mesozoic rocks in the Coast Ranges near Clear Lake, California: Geological Society of America Bulletin, v. 81, no. 12, p. 3513–3536.

Thomas, A.M., Bergmann, R., and Dreger, D.S., 2013, Incipient faulting near Lake Pillsbury, California, and the role of accessory faults in plate boundary evolution: Geology, v. 41, no. 10, p. 1123–1126, https://doi.org/10.1130/G34588.1.

U.S. Geological Survey Geologic Names Committee, 2010, Divisions of geologic time—major chronostratigraphic and geochronologic units: U.S. Geological Survey Fact Sheet 2010–3059, 2 p.

Wagner, D.L., and Bortugno, E.B., 1982, Geologic map of the Santa Rosa quadrangle: California Division of Mines and Geology Regional Geologic Map Series Map 2A, scale 1:250,000.

Waldhauser, Felix, and Engebreth, Ben, 2017, Real-time double-difference earthquake locations for northern California [database]: U.S. Geological Survey National Earthquake Reduction Program (NEHRP) and Lamont-Doherty Earth Observatory (LDEO), accessed August 2016 and downloaded February 2017 from http://ddrt.ldeo.columbia.edu.

Waldhauser, F., and Schaff, D.P., 2008, Large-scale relocation of two decades of northern California seismicity using cross-correlation and double-difference methods: Journal of Geophysical Research, v. 113, no. B08311, https://doi.org/10.1029/2007JB005479.

Wentworth, C.M., Blake, M.C., Jr., Jones, D.L., Walter, A.W., and Zoback, M.D., 1984, Tectonic wedging associated with emplacement of the Franciscan assemblage, California Coast Ranges, *in* Blake, M.C., Jr., ed., Franciscan geology of northern California: Pacific Section, Society of Economic Paleontologists and Mineralogists Book 43, p. 163–173.

Wentworth, C.M., Blake, M.C., Jr., McLaughlin, R.J., and Graymer, R.W., 1999, Preliminary geologic map of the San Jose 30- × 60-minute quadrangle, California—A digital database: U.S. Geological Survey Open-File Report 98–795, scale 1:100,000, 2 plates, interpretive geologic map pamphlet 52 p., database pamphlet 13 p., map database, text files.

Wentworth, C.M., and Zoback, M.D., 1990, Structure of the Coalinga region and thrust origin of the earthquake, *in* Rymer, M.J., and Ellsworth, W.L., eds, The Coalinga earthquake of May 2, 1983: U.S. Geological Survey Professional Paper 1487, p. 41–68.

Worrall, D.M., 1981, Imbricate low-angle faulting in uppermost Franciscan rocks, south Yolla Bolly area, northern California: Geological Society of America Bulletin, v. 92, p. 703–729, https://doi.org/10.1130/0016-7606(1981)92<703:ILFIUF>2.0.CO;2.

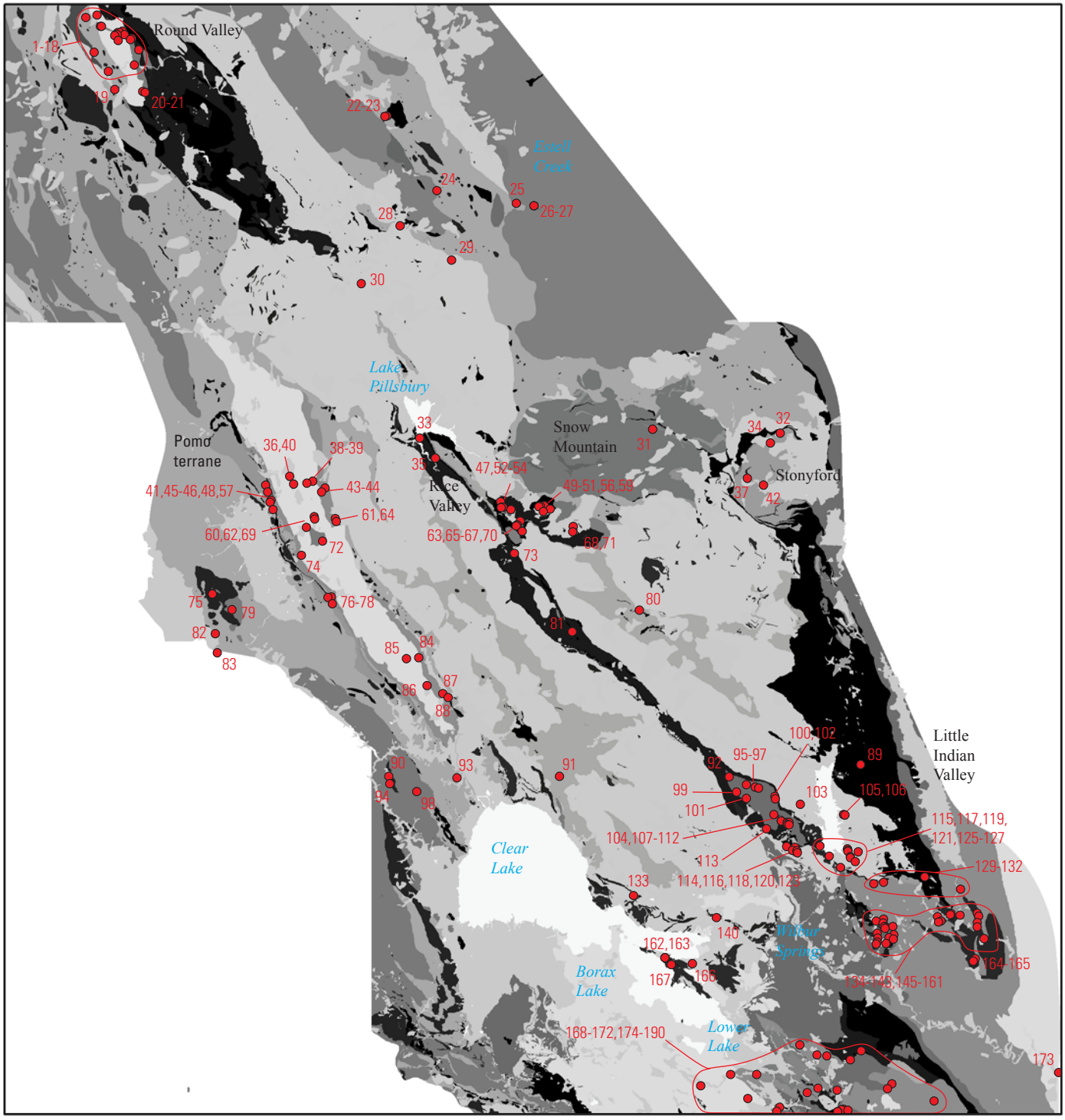

Figure 14. Map showing locations and locality numbers of fossils listed in table 1 (https://doi.org/10.3133/sim3395) and plotted on the geologic map (sheet 1). The geology is shown in grayscale to provide a context for locating the fossil occurrences on the geologic map. Where fossil localities are numerous and closely spaced, locality numbers may be grouped. Some specific fossil localities or groups of localities cited in the text discussion are also labeled on the map.

Table 1. Paleontological data from Tertiary and Mesozoic rocks of the map area from Round Valley to Wilbur Springs, northern Coast Ranges, California. Figure 14 shows the fossil localities on a page-size figure in grayscale, to help the user find fossil localities on the map (sheet 1). Some localities of Mesozoic fossils that plot on the geologic map within or surrounded by Quaternary deposits are in isolated areas of bedrock underlying alluvium that are too limited to show at the scale of the geologic map (for example, small bedrock windows in stream bottoms, or bedrock interspersed in flights of grouped fluvial terraces of varying age). Some localities might also be associated with Quaternary erosional surfaces on bedrock that do not include actual deposits and instead are only geomorphic surfaces. We include the coordinates for some fossil localities in the Franciscan Complex and Great Valley Complex that are outside of the area of this map (designated as map no. 999) but are in adjacent or nearby areas of the northern Coast Ranges. Refer to the cited sources of the fossil data for more information on the geology of these areas.

[Map_No, location number shown on the geologic map (sheet 1) and fig. 14, as well as included in the database. ID, field or laboratory identification number from sample collector. Lat and Long, latitude (N.) and longitude (W.). Fossil and age, identified fossils and ages. Source, source of fossil data. Lith, lithology of enclosing rock. Unit, lithologic or geologic formational source of fossil, where known]

Map_No.	ID	Latitude	Longitude	Fossil and age	Source	Lithology	Unit
1	143	39.7420	-123.2809	Ammonite: *Pachydiscus*; Ammonoid: *Nostoceras*; Mollusks: *Inoceramus;* Upper Cretaceous	Clark, 1940	Sandstone, shale, and conglomerate	
2	144	39.7400	-123.2924	Ammonite: *Pachydiscus*; Ammonoid: *Nostoceras*; Mollusks: *Inoceramus;* Upper Cretaceous	Clark, 1940	Sandstone, shale, and conglomerate	
3	161A	39.7332	-123.2775	Ammonite: *Pachydiscus*; Ammonoid: *Nostoceras*; Mollusks: *Inoceramus;* Upper Cretaceous	Clark, 1940	Sandstone, shale, and conglomerate	
4	161	39.7330	-123.2763	Ammonite: *Pachydiscus*; Ammonoid: *Nostoceras*; Mollusks: *Inoceramus*; Upper Cretaceous	Clark, 1940	Sandstone, shale, and conglomerate	
5	~(149,148,153)	39.7293	-123.2546	Ammonite: *Pachydiscus*; Ammonoid: *Nostoceras*; Mollusks: *Inoceramus*; Upper Cretaceous	Clark, 1940	Sandstone, shale, and conglomerate	
6	~(149,150)	39.7283	-123.2597	Ammonite: *Pachydiscus*; Ammonoid: *Nostoceras*; Mollusks: *Inoceramus*; Upper Cretaceous	Clark, 1940	Sandstone, shale, and conglomerate	
7	146	39.7281	-123.2572	Macrofossils: *Brachysphingus liratus* Gabb; *Turritella infragranulata* Gabb; *Tellina undulifera* Gabb; Eocene	Clark, 1940	Sandstone and shale	
8	~105	39.7268	-123.2619	Macrofossils: *Brachysphingus liratus* Gabb; *Turritella infragranulat*a Gabb; *Tellina undulifera* Gabb; Eocene	Clark, 1940	Sandstone and shale	
9	156	39.7266	-123.2530	Macrofossils: *Brachysphingus liratus* Gabb; *Turritella infragranulata* Gabb; *Tellina undulifera* Gabb; Eocene	Clark, 1940	Sandstone and shale	
10	89	39.7265	-123.2602	Macrofossils: *Brachysphingus liratus* Gabb; *Turritella infragranulata* Gabb; *Tellina undulifera* Gabb; Eocene	Clark, 1940	Sandstone and shale	
11	85,85A	39.7257	-123.2629	Ammonite: *Pachydiscus*; Ammonoid: *Nostoceras*; Mollusks: *Inoceramus*; Upper Cretaceous	Clark, 1940	Sandstone, shale, and conglomerate	
12	158	39.7234	-123.2451	Ammonite: *Pachydiscus*; Ammonoid: *Nostoceras*; Mollusks: *Inoceramus*; Upper Cretaceous	Clark, 1940	Sandstone, shale, and conglomerate	
13	92,92-1	39.7230	-123.2468	Macrofossils: Brachysphingus liratus Gabb; Turritella infragranulata Gabb; Tellina undulifera Gabb; Eocene	Clark, 1940	Sandstone and shale	

Table 1.—Continued

Map_No.	ID	Latitude	Longitude	Fossil and age	Source	Lithology	Unit
14	49	39.7221	-123.2595	Ammonite: *Pachydiscus*; Ammonoid: *Nostoceras*; Mollusks: *Inoceramus;* Upper Cretaceous	Clark, 1940	Sandstone, shale, and conglomerate	
15	168	39.7146	-123.2384	Macrofossils: *Desmostylus* tooth; *Ostrea appressa*; *Ostrea*; *Natrica sp.*; *Corbicula (?); Pecten*; Middle (to Early?) Miocene	Clark, 1940	Shallow marine to estuarine conglomerate, sandstone, shale, and coal	
16	169-c	39.7126	-123.2837	Macrofossils: *Desmostylus* tooth; *Ostrea appressa*; *Ostrea; Natrica sp.*; *Corbicula (?)*; *Pecten*; Middle (to Early?) Miocene	Clark, 1940	Shallow marine to estuarine conglomerate, sandstone, shale, and coal	
17	50[~50-1,50-3]	39.7028	-123.2426	Macrofossils: *Brachysphingus liratus* Gabb; *Turritella infragranulata* Gabb; *Tellina undulifera* Gabb; Eocene	Clark, 1940	Sandstone and shale	
18	56	39.6975	-123.2691	Macrofossils: *Desmostylus* tooth; *Ostrea appressa*; *Ostrea*; *Natrica sp.*; *Corbicula (?)*; *Pecten*; Middle (to Early?) Miocene	Clark, 1940	Shallow marine to estuarine conglomerate, sandstone, shale, and coal	
19	164	39.6833	-123.2626	Macrofossils: *Desmostylus* tooth; *Ostrea appressa*; *Ostrea; Natrica sp.; Corbicula (?); Pecten*; Middle (to Early?) Miocene	Clark, 1940	Shallow marine to estuarine conglomerate, sandstone, shale, and coal	
20	120	39.6818	-123.2344	Macrofossils: *Brachysphingus liratus* Gabb; *Turritella infragranulata* Gabb; *Tellina undulifera* Gabb; Eocene	Clark, 1940	Sandstone and shale	
21	123	39.6811	-123.2317	Macrofossils: *Brachysphingus liratus* Gabb; *Turritella infragranulata* Gabb; *Tellina undulifera* Gabb; Eocene	Clark, 1940	Sandstone and shale	
22	M6600	39.6628	-122.9853	Pelecypods: *Buchia pacifica* (Jeletzky); Early Cretaceous (middle Valanginian)	Collected by J.C. Maxwell, Univ. of Texas, Austin, 1976; identified by D.L. Jones, 1977	Sheared argillite	Franciscan Complex, Central Belt, "Poison Rock" mélange at Hayden Rock

Table 1.—Continued

Map_No.	ID	Latitude	Longitude	Fossil and age	Source	Lithology	Unit
23	BBH-15	39.6623	-122.9871	Radiolaria: Late Jurassic (Tithonian)	Collected by H.N. Ohlin; identified by C.D. Blome	Radiolarian chert block in mélange	Franciscan Complex, Central Belt (Poison Rock mélange); near Hayden Rock
24	1	39.6042	-122.9343	Mollusks: *Buchia*, Lower Cretaceous, Valanginian	D.L. Jones, in Ohlin and others, 2010	Metasandstone	Franciscan Eastern Belt, Yolla Bolly terrane
25	M6090	39.5942	-122.8536	Pelecypod: *Buchia*; Late Jurassic (Tithonian)	Collected by Calif. Dept. of Water Resources geologists, as listed in Blake and Jones, 1974	Mélange	Franciscan Complex, Central Belt mélange
26	M6601	39.5919	-122.8356	Pelecypods: *Buchia cf. B. uncitoides?* (Pavlow), bivalve fragments; Early Cretaceous (Berriasian?), Radiolaria: sparse, appears to correlate with Early Cretaceous (upper Aptian or lower Albian or younger) section of Dry Creek	Macrofossils collected by J.C. Maxwell, 1976; identified by D.L. Jones, 1977. Radiolaria reported in D.H. Lehman, 1974 (table 7); identified by E.A. Pessagno from same locality	Macrofossils and radiolaria, of mixed age, present in thin carbonate beds and concretions in thin bedded shaley turbidites in structural window through Pickett Peak terrane	Probable Great Valley sequence, imbricated between underlying rocks of Franciscan Central Belt mélange (and possibly, Eastern Belt Yolla Bolly terrane) and overthrust rocks of Franciscan Eastern Belt, Pickett Peak terrane
27	M6603	39.5919	-122.8356	Same loc. as M6601—Pelecypod: *Buchia uncitoides* (Pavlow); Early Cretaceous (Berriasian), but see M6601	Collected by J.C. Maxwell, 1976; identified by D.L. Jones, 1977	Thin carbonate beds and concretions in well-bedded shaley turbidites of Estell Creek	Probable Great Valley sequence
28	2	39.5764	-122.9721	Radiolaria: *Parvicingula(?) procera*, Pessagno; *Parvicingula sp., ?Podubursa sp., Pseudodictyomitra sp.*; Late Jurassic, Tithonian	C.D. Blome in Ohlin and others, 2010	Chert in mélange	Franciscan Complex, Central Belt
29	3	39.5491	-122.9193	Mollusks: *Inoceramus*; Lower Cretaceous, Cenomanian (?)	Blake and Jones, 1974; cited in Ohlin and others, 2010	Metasandstone	Franciscan Eastern Belt, Yolla Bolly terrane
30	4	39.5308	-123.0112	Radiolaria: *Archeodictyomitra sp., aff. A.simplex Pessagno; pseudodictyomitra sp.; Thanarla sp.*; Lower Cretaceous, probably Aptian-Albian	C.D. Blome in Ohlin and others, 2010	Metasandstone	Franciscan Eastern Belt, Yolla Bolly terrane

Table 1.—Continued

Map_No.	ID	Latitude	Longitude	Fossil and age	Source	Lithology	Unit
31	MR0171	39.4158	-122.7153	Radiolaria: cones, very large squashed spheres with stubby spines; no reliable age assignment	Collected by R.D. Brown; described in Brown and others, 1981. Radiolaria examined by E.A. Pessagno	Radiolarian chert at base of volcanic-rich 300- to 500-ft-thick sedimentary unit	Snow Mountain/St. John Mountain volcanic complex of Central Belt of Franciscan Complex
32	ChertB	39.4122	-122.5859	Radiolaria: Zones 3-8 to 7-10 Tethyan UAZ of Baumgartner and others 1995; Middle and Upper Jurassic (lower Bajocian to upper Kimmeridgean)	Collected and identified by B.L. Murchey as reported in Shervais and others, 2005	Radiolarian chert sequence in Stonyford volcanic complex	Stonyford volcanic complex of Coast Range ophiolite
33	5	39.4092	-122.9520	Mollusks: *Buchia piochii*, Late Jurassic, Tithonian	R.W. Imlay in W.P. Irwin, 1960; cited by Ohlin and others, 2010	Shale and sandstone slab	Ophiolitic mélange
34	ChertC	39.4047	-122.5963	Radiolaria: Zones 8-10, Tethyan UAZ of Baumgartner and others 1995; Middle to Upper Jurassic (middle Callovian-upper Kimmeridgean)	Collected and identified by B.L. Murchey as reported in Shervais and others, 2005	Radiolarian chert sequence in Stonyford volcanic complex	Stonyford volcanic complex of Coast Range ophiolite
35	6	39.3933	-122.9361	Mollusks: *Buchia sp*., Probably Late Jurassic, Tithonian based on proximity to *B. piochi*i loc.	Etter, 1979; cited in Ohlin and others, 2010	Shale and sandstone slab	Ophiolitic mélange
36	33	39.3791	-123.0838	Mollusks: Pelecypods; Dinoflagellates; U. Cretaceous, Campanian	J.O. Berkland, Calif. Dept. of Water Resources	Shale and thick bedded sandstone	
37	ChertA	39.3766	-122.6198	Radiolaria: Zones 3-6 to 6-6, Tethyan UAZ of Baumgartner and others 1995; Middle Jurassic (lower Bajocian-upper Bathonian)	Collected and identified by B.L. Murchey as reported in Shervais and others, 2005	Radiolarian chert sequence in Stonyford volcanic complex	Stonyford volcanic complex of Coast Range ophiolite
38	18	39.3750	-123.0607	Microfossils: Lower Cretaceous	J.O. Berkland	Sandstone and shale, thin bedded	
39	29	39.3736	-123.0667	Microfossils: Lower Cretaceous	Shell Oil Co.	Gray sandstone and shale	
40	30	39.3726	-123.0797	Arenaceous foraminifera, nondiagnostic	Shell Oil Co.	Shale and thick bedded sandstone	
41	25	39.3720	-123.1082	Mollusks: oysters, pectens, U. Cretaceous	J.O. Berkland	Volcanic sandstone, conglomerate	
42	ChertD	39.3713	-122.6032	Radiolaria: Zones 9-10, Tethyan UAZ of Baumgartner and others 1995; Upper Jurassic (middle Oxfordian to upper Kimmeridgean)	Originally collected and described by E.A. Pessagno, 1977; revised by B.L. Murchey in Shervais and others, 2005	Radiolarian chert sequence in Stonyford volcanic complex	Stonyford volcanic complex of Coast Range ophiolite
43	19	39.3696	-123.0479	Dinoflagellates: *Ascodinium,* Lower Cretaceous, Albian	J.O. Berkland	Massive sandstone and shale	

Table 1.—Continued

Map_No.	ID	Latitude	Longitude	Fossil and age	Source	Lithology	Unit
44	20	39.3665	-123.0516	Dinoflagellates: *Ascodinium*, Lower Cretaceous, Albian	J.O. Berkland	Massive sandstone and shale	
45	22	39.3664	-123.1062	Ammonite: *Guadryceras*, Microfossils, , U. Cretaceous, Maestrichtean	J.O. Berkland	Volcanic sandstone, conglomerate	
46	28	39.3599	-123.1027	Mollusks: *Meekia*, U. Cretaceous	J.O. Berkland, Calif. Dept. of Water Resources	Volcanic sandstone, conglomerate	
47	M4350	39.3588	-122.8697	Pelecypods: *Nuculana sp., Tellina?*, undet. Fragments; Age indeterminate	Collected by J.O. Berkland, 1970; idenified by W.O. Addicot, 1970	Sandstone in bed of McLeod Creek, Rice Valley	Unnamed formation of presumed early Tertiary age
48	23	39.3585	-123.1036	Mollusks: oysters, pectens, U. Cretaceous	J.O. Berkland	Volcanic sandstone, conglomerate	
49	M6765	39.3558	-122.8256	Pelecypods: *Entolium (?) sp*; Jurassic or Cretaceous	Collected by J. Suppe, 1977; identified by D.L. Jones, 1977	No lithologic data provided	No information
50	M6766	39.3553	-122.8297	Pelecypods: *Buchia sp*., striate form, same as *Buchia sp.* in M6564; Late Jurassic or Early Cretaceous	Collected by J. Suppe, 1977; identified by D.L. Jones, 1977	No lithologic data provided	No information
51	M6767	39.3550	-122.8311	Pelecypods: *Buchia cf. B. fischeriana* (D'Orbigny); Late Jurassic (Tithonian)	Collected by J. Suppe, 1977; identified by D.L. Jones, 1977	No lithologic data provided	No information
52	M4304	39.3547	-122.8688	Gastropods: *Brachysphingus mammilatus* (Clark and Woodford), *Calyptraea sp., Molopophorus?, Neverita cf. N. globosa* (Gabb), *Turbonilla sp., Turrid-Crassispira*-like, *Turritella sp.,* undet. internal molds-several taxa; Pelecypods: *Acila decisa* (Conrad), *Arcid?* fragment, *Cardiid*-fragment, *Diplodonta cf. D. cretacea* (Gabb), *Mytilus sp.*, *Nuculana gabbi* (Gabb)?, *Ostrea sp.*-fragment, *Pitar?, Solen cf. S. stantoni* (Weaver), *Spisula sp., Spisula meganosensis* (Clark and Woodford), *Tellina longa* (Gabb); late Paleocene, "Meganos stage"	Collected by J.O. Berkland, 1970; identified by W.O. Addicot, 1970	Tertiary marine strata, 4-ft-thick red-weathering silty limestone	Unnamed formation of presumed early Tertiary age
53	M4351	39.3544	-122.8669	Gastropods: *Scaphander costatus* (Gabb); Crustaceans: broken appendages and fragment of crab carapace	Collected by J.O. Berkland, 1970; identified by W.O. Addicot, 1970	Tertiary marine sandstone stratigraphically above (E. of) M4303, M4304	Unnamed formation of presumed early Tertiary age
54	M4352	39.3544	-122.8675	Gastropods: *Scaphander?*, *Trochid-Bathybembix*-like, Undet. Internal molds-2 taxa; Pelecypods: undet. Molds; Age indet.	Collected by J.O. Berkland, 1970; identified by W.O. Addicot, 1970	Tertiary marine sandstone stratigraphically above (E. of) M4303, M4304	Unnamed formation of presumed early Tertiary age

Table 1.—Continued

Map_No.	ID	Latitude	Longitude	Fossil and age	Source	Lithology	Unit
55	M4303	39.3542	-122.8693	Gastropods: *Brachysphingus mammilatus* (Clark and Woodford), *Calyptraea cf. C. diegoana, Cryptoconus injucundus* (Hanna)?, *Ficopsis sp., Neverita cf. N. globosa* (Gabb), *Scaphander costatus* (Gabb), *Turbonilla sp., Turritella maganosensis* (Clark and Woodford), *T. cf. T. merriami brevitabulata* (Merriam and Turner), *Whitneyella meganosensis* (Turner); Pelecypods: *Acila sp.*-fragment, *Diplodonta cretacea* (Gabb), *Nuculana gabbi* (Gabb), *Pitar sp., Schedocardia hartleyensis* (Clark and Woodford), *Solen cf. S. stantoni* (Weaver), *Sphenia meganosensis* (Clark and Woodford)?, *Spisula sp., Tellina longa* (Gabb), *Vericardia sp.*-fragment; late Paleocene, "Meganos Stage" of Clark and Vokes, 1936.	Collected by J.O. Berkland, 1970; identified by W.O. Addicot, 1970	Tertiary marine strata, 4-ft-thick red-weathering silty limestone	Unnamed formation of presumed early Tertiary age
56	M6769,M6769A	39.3528	-122.8197	Pelecypods: *Buchia cf. B. fischeriana* (D'Orbigny), *Buchia piochii* (Gabb); Late Jurassic (Tithonian)	Collected by J. Suppe, 1977; identified by D.L. Jones, 1977	No lithologic data provided	No information
57	24	39.3526	-123.1009	Mollusks: oysters, pectens, U. Cretaceous	J.O. Berkland	Volcanic sandstone, conglomerate	
58	M6771	39.3525	-122.8594	Cephalopod: *Phylloceras sp.*, Pelecypod: *Buchia sp.* Juv. cf. *B. piochii* (Gabb); Late Jurassic (Tithonian)	Collected by J. Suppe, 1977; identified by D.L. Jones, 1977	No lithologic data provided	No information
59	M6768	39.3511	-122.8267	Pelecypods: *Buchia pacifica* (Jeletzky); Early Cretaceous (early to middle Valanginian)	Collected by J. Suppe, 1977; identified by D.L. Jones, 1977	No lithologic data provided	No information
60	7,27	39.3471	-123.0587	Mollusks: *Inoceramus schmidti, Canadoceras, Baculites*, U. Cretaceous, Campanian	J.O. Berkland, Calif. Dept. of Water Resources	Limestone lens	
61	26	39.3456	-123.0374	Microfossils Lower Cretaceous	Shell Oil Co.	Shale in Bucknell Creek bed	
62	27	39.3455	-123.0586	Mollusks: *Inoceramus*, U. Cretaceous	J.O. Berkland, Calif. Dept. of Water Resources	Limestone lens	
63	M6770	39.3436	-122.8503	Cephalopod: *Ammonite*-indet. heteromorph, *Belemnite-Acroteuthis sp.*; Pelecypods: *Entolium operculiformis*, clams; Early Cretaceous (Hauterivian or Barremian)	Collected by J. Suppe, 1977; identified by D.L. Jones, 1977	No lithologic data provided	No information
64	8	39.3434	-123.0365	Microfossils, Lower Cretaceous	J.O. Berkland? Shell Oil Co.	Shale	

Table 1.—Continued

Map_No.	ID	Latitude	Longitude	Fossil and age	Source	Lithology	Unit
65	kiel-rice.vly	39.3406	-122.8538	Brachiopods: *Peregrinella whitneyi*; Bivalves: *Pecten complexicosta, "Modiola" major*; Gastropods: *Paskentana paskentaensis*, *Retiskenea? Tuberculata*; Early Cretaceous (probably late Berriasian-early Hauterivian)	Collected by J.O. Berkland, 1973; Campbell and others, 2008; identified by Campbell and others, 2008; Kiel and others, 2008	Small, isolated carbonate lenses in sandstone and shale, along margin of Rice Valley basin; interpreted as fossil cold-seep deposits	Lower Great Valley sequence
66	M6395	39.3406	-122.8531	Brachiopods: *Peregrinella whitneyi* (Gabb); Early Cretaceous (Berriasian-Hauterivian)	Collected by J. Suppe, 1975; identified by D.L. Jones and J.W. Miller, 1975	No lithologic data provided	See also Kiel and others, 2008
67	M6396	39.3397	-122.8542	Brachiopods: *Peregrinella whitneyi* (Gabb); Early Cretaceous (Berriasian-Hauterivian)	Collected by J. Suppe, 1975; identified by D.L. Jones and J.W. Miller, 1975	No lithologic data provided	See also Kiel and others, 2008
68	M6763	39.3394	-122.7964	Pelecypods: *Buchia cf. B. fischeriana* (D'Orbigny); Cephalopod: *Belemnite- Cylindroteuthis sp.*; Late Jurassic (Tithonian)	Collected by J. Suppe, 1977; identified by D.L. Jones, 1977	No lithologic data provided	No information
69	9	39.3387	-123.0667	Pollen, U. Cretaceous, Maastrichtian?	J.O. Berkland	Thick-bedded sandstone and shale	
70	M6394	39.3356	-122.8483	Pelecypods: *Buchia uncitoides* (Pavlow); Early Cretaceous (Berriasian)	Collected by J. Suppe, 1975; identified by D.L. Jones and J.W. Miller, 1975	No lithologic data provided	
71	M6764	39.3350	-122.7969	Pelecypods: *Buchia piochii* (Gabb); Late Jurassic (Tithonian)	Collected by J. Suppe, 1977; identified by D.L. Jones, 1977	No lithologic data provided	No information
72	10	39.3279	-123.0503	Mollusks: *Turitella*, Paleocene	J.O. Berkland, Calif. Dept. of Water Resources	Sandstone	
73	M6987	39.3181	-122.8561	Pelecypods: *Buchia sp.*; Late Jurassic or Early Cretaceous	Collected by S. Etter, Univ. Texas, Austin, 1978; identified by D.L. Jones	Conglomeratic sandstone in ophiolitic mélange	Lower Great Valley sequence; Etter's blue slides formation (Etter's unit Jbs); ophiolitic mélange of this report
74	11	39.3167	-123.0718	Microfossils Late Cretaceous, post Cenomanian	J.O. Berkland	Thick-bedded Sandstone and shale	
75	247	39.2861	-123.1625	Radiolaria: in overturned partial stratigraphic sequence: late Middle or early Late Jurassic (~MH-4B) to Early Cretaceous (probably Albian, ~MH-6 or MH-7B)	Collected by J. Stanford (Stanford, 1991); Identified by Y. Isozaki, Yamaguchi Univ., Japan	28 m of radiolarian chert in mélange terrane of basalt, chert, greywacke	Franciscan Complex, Central Belt

Table 1.—Continued

Map_No.	ID	Latitude	Longitude	Fossil and age	Source	Lithology	Unit
76	12	39.2841	-123.0414	Mollusks: *Buchia elderensis*, Late Jurassic	J.O. Berkland, Calif. Dept. of Water Resources	Mélange	
77	13	39.2835	-123.0448	Mollusks: Inoceramus sp., U. Cretaceous	J.O. Berkland	Sandstone and shale	
78	14	39.2786	-123.0404	Mollusks: *Meekia sella*, U. Cretaceous	J.O. Berkland	Sandstone, volcanic conglomerate	
79	225	39.2737	-123.1422	Radiolaria: Latest Jurassic to early Early Cretaceous (~MH-4 to MH-5B)	Collected by J. Stanford (Stanford, 1991); identified by Y. Isozaki, Yamaguchi Univ., Japan	38 m of radiolarian chert in mélange terrane of basalt, chert, greywacke	Franciscan Complex, Central Belt
80	M6564	39.2731	-122.7297	Pelecypods: *Buchia pacifica* (Jeletzky); striated *Buchia* (new?) *sp.*, *B. elderensis* (Anderson); this is a mixed collection- Early Cretaceous (Valanginian) and Late Jurassic (Tithonian); depositional age is thus Early Cretaceous (Valanginian) or younger	Collected by J. Suppe, 1975; identified by D.L. Jones and J.W. Miller, 1977	*B. pacifica* is from matrix of metasandstone; other Buchias are from a silicified concretion	Franciscan Complex, Eastern Belt, mélange of Yolla Bolly terrane, Goat Mountain area
81	M6397	39.2564	-122.7975	Pelecypods: *Buchia pacifica Jeletzky*; Early Cretaceous (Valanginian)	Collected by J. Suppe, 1975; identified by D.L. Jones and J.W. Miller, 1975	No lithologic data provided	
82	675	39.2548	-123.1590	Radiolaria: Latest Jurassic to early Early Cretaceous (~MH-4 to MH-5B)	Collected by J. Stanford (Stanford, 1991); Identified by Y. Isozaki, Yamaguchi Univ., Japan	4.5 m of radiolarian chert in mélange terrane of basalt, chert, greywacke	Franciscan Complex, Central Belt
83	676	39.2400	-123.1573	Radiolaria: in partial stratigraphic sequence: Early Jurassic (Pliensbachian-Bajocian,~MH-1 to MH-2B) to Middle Jurassic (Bathonian, ~ MH-3 or MH-4B)	Collected by J. Stanford (Stanford, 1991); Identified by Y. Isozaki, Yamaguchi Univ., Japan	36.4 m of radiolarian chert overlying basalt in mélange terrane of basalt, chert, greywacke	Franciscan Complex, Central Belt
84	15	39.2361	-122.9533	Spores: Lower Cretaceous	J.O. Berkland	Sandstone and shale, thin bedded	
85	16	39.2354	-122.9654	Mollusks: *Inoceramus*, L. Cretaceous	J.O. Berkland	Shale	
86	17	39.2141	-122.9446	Dinoflagellates: *Lituosphaeridium*, Lower Cretaceous	J.O. Berkland, Calif. Dept. of Water Resources	Sandstone and shale, thin bedded	
87	31	39.2078	-122.9288	Microfossils Middle Eocene, probably Domengine or Capay	Shell Oil Co.	Sandstone and shale, thin bedded	
88	32	39.2046	-122.9232	Mollusks: *Buchia piochii*, Upper Jurassic	J.O. Berkland, Calif. Dept. of Water Resources	Mélange	
89	M6407	39.1508	-122.5064	Pelecypods: *Buchia piochii* (Gabb)?; Late Jurassic (Tithonian?), based on *B. piochii*	Collected by J. Suppe, 1975; identified by D.L. Jones and J.W. Miller, 1975	No lithologic data provided	No information

Table 1.—Continued

Map_No.	ID	Latitude	Longitude	Fossil and age	Source	Lithology	Unit
90	OG81-57	39.1427	-122.9832	Radiolaria: Late Jurassic (Tithonian)	Collected by H.N. Ohlin; identified By C.D. Blome	Radiolarian chert in basaltic volcanic rocks	Franciscan Complex, Central Belt (probably Marin Headlands-Geysers terrane)
91	MG81-171	39.1424	-122.8110	Radiolaria: Late Jurassic (Tithonian) to Early Cretaceous (early Valanginian)	Collected by R.J. McLaughlin; identified By C.D. Blome	Radiolarian chert in mélange	
92	M6398	39.1417	-122.6394	Pelecypods: *Buchia cf. B. piochii* (Gabb) *sp*. Juvenile; Late Jurassic (Tithonian)	Collected by J. Suppe, 1975; identified by D.L. Jones and J.W. Miller, 1975	No lithologic data provided	
93	HS-309(MR1076)	39.1413	-122.9146	Radiolaria: Late Jurassic (late Kimmeridgean/early Tithonian-*Emiluvia Hopsoni* Zone 2 of Pessagno, 1977)	Collected by H.N. Ohlin; identified By C.D. Blome	Radiolarian chert in mélange	Franciscan Complex, Central Belt
94	OG81-47	39.1368	-122.9827	Radiolaria: Late Jurassic (Tithonian)	Collected by H.N. Ohlin; identified By C.D. Blome	Radiolarian chert in basaltic volcanic rocks	Franciscan Complex, Central Belt (probably Marin Headlands-Geysers terrane)
95	M6399	39.1353	-122.6217	Pelecypods: *Buchia cf. B. piochii* (Gabb), *Inoceramus sp*.; Late Jurassic (Tithonian), based on *B. piochii*	Collected by J. Suppe, 1975; identified by D.L. Jones and J.W. Miller, 1975	No lithologic data provided	
96	M6400	39.1333	-122.6128	Pelecypods: *Buchia cf. B. elderensis* (Anderson); Late Jurassic (Tithonian)	Collected by J. Suppe, 1975; identified by D.L. Jones and J.W. Miller, 1975	No lithologic data provided	
97	M6401	39.1325	-122.6097	Pelecypods: *Buchia piochii* (Gabb) or *Buchia elderensis* (Anderson); Late Jurassic (Tithonian)	Unknown	No lithologic data provided	No information
98	OG81-29	39.1305	-122.9553	Radiolaria: Late Jurassic (Tithonian) to Early Cretaceous (early Valanginian)?	Collected by H.N. Ohlin; identified By C.D. Blome	Radiolarian chert in mélange	Franciscan Complex, Central Belt
99	M6404	39.1297	-122.6319	Pelecypods: *Buchia elderensis* (Anderson) or *B. piochii* (Gabb); Late Jurassic (Tithonian)	Collected by J. Suppe, 1975; identified by D.L. Jones and J.W. Miller, 1975	No lithologic data provided	No information
100	M6402	39.1261	-122.5933	Pelecypods: *Buchia piochii* (Gabb) or *Buchia elderensis* (Anderson); Late Jurassic (Tithonian)	Collected by J. Suppe, 1975; identified by D.L. Jones and J.W. Miller, 1975	No lithologic data provided	No information
101	M6403	39.1244	-122.6219	Pelecypods: *Buchia sp*., indeterminable; Late Jurassic or Early Cretaceous	Collected by J. Suppe, 1975; identified by D.L. Jones and J.W. Miller, 1975	No lithologic data provided	No information

Table 1.—Continued

Map_No.	ID	Latitude	Longitude	Fossil and age	Source	Lithology	Unit
102	LIS7	39.1241	-122.5927	Mollusks: *Buchia sp.*, Late Jurassic or Early Cretaceous	McLaughlin and others, 1990; Identified by D.L Jones, J.W. Miller	Shale and sandstone	
103	LIS23	39.1197	-122.5674	Mollusks: *Buchia pacifica* (Jeletzky), Early Cretaceous (Valanginian)	McLaughlin and others, 1990; identified by D.L Jones, J.W. Miller	Slate and metasandstone, textural zones 1-2, and minor metavolcanic rocks	
104	LIS14	39.1117	-122.5944	Mollusks: *Buchia sp.*, Late Jurassic or Early Cretaceous	McLaughlin and others, 1990; identified by D.L Jones, J.W. Miller	Shale and sandstone	
105	LIS15	39.1115	-122.5240	Mollusk:, *Buchia piochii* (Gabb), Late Jurassic (Tithonian)	McLaughlin and others, 1990; identified by D.L Jones, J.W. Miller	Slate and metasandstone, textural zones 1–3	
106	LIS16	39.1110	-122.5226	Mollusks: *Buchia elderensis* (Anderson), Late Jurassic (Tithonian)	McLaughlin and others, 1990; identified by D.L Jones, J.W. Miller	Slate and metasandstone, textural zones 1–2	
107	M6405	39.1067	-122.5867	Pelecypods: *Buchia elderensis* (Anderson); Late Jurassic (Tithonian)	Collected by J. Suppe, 1975; identified by D.L. Jones and J.W. Miller, 1975	No lithologic data provided	No information
108	M6406	39.1067	-122.5867	Pelecypods: *Buchia elderensis* (Anderson); Late Jurassic (Tithonian)	Collected by J. Suppe, 1975; identified by D.L. Jones and J.W. Miller, 1975	No lithologic data provided	No information
109	LIS13	39.1055	-122.5808	Mollusks: *Buchia cf. B. piochii* (Gabb); Late Jurassic (Tithonian)	McLaughlin and others, 1990; identified by D.L Jones, J.W. Miller	Shale and sandstone	
110	LIS12	39.1054	-122.5791	Mollusks: *Buchia elderensis* (Anderson), Late Jurassic (Tithonian)	McLaughlin and others, 1990; identified by D.L Jones, J.W. Miller	Shale and sandstone	
111	LIS10	39.1041	-122.5802	Mollusks: *Buchia elderensis* (Anderson); *B. piochii* (Gabb), Late Jurassic (Tithonian)	McLaughlin and others, 1990; identified by D.L Jones, J.W. Miller	Shale, sandstone	
112	LIS11	39.1038	-122.5788	Mollusks: *Buchia piochii* (Gabb), Late Jurassic (Tithonian)	McLaughlin and others, 1990; identified by D.L Jones, J.W. Miller	Shale and sandstone	
113	LIS31	39.1008	-122.6019	Mollusks: *Buchia elderensis* (Anderson); *B. piochii* (Gabb), Late Jurassic (Tithonian)	McLaughlin and others, 1990; identified by D.L Jones, J.W. Miller	Sandstone and shale	

Table 1.—Continued

Map_No.	ID	Latitude	Longitude	Fossil and age	Source	Lithology	Unit
114	LIS8	39.0868	-122.5814	Mollusks: *Buchia sp.*, Late Jurassic or Early Cretaceous	McLaughlin and others, 1990; identified by D.L Jones, J.W. Miller	Mélange of sheared shale, sandstone, and ophiolitic rocks	
115	LIS1	39.0867	-122.5480	Radiolaria: *Mirifusis sp.; Parvicingula sp.*, Late Jurassic (late Kimmeridgean)	McLaughlin and others, 1990; identified by C. Blome	Radiolarian chert in basalt	
116	LIS9	39.0856	-122.5732	Mollusks: *Buchia elderensis* (Anderson), Late Jurassic (Tithonian)	McLaughlin and others 1990; identified by D.L Jones, J.W. Miller	Sheared shale in mélange of sheared shale, sandstone, and ophiolitic rocks	
117	LIS21	39.0844	-122.5200	Mollusks: *Buchia sp.*, Late Jurassic or Early Cretaceous	McLaughlin and others, 1990; identified by D.L Jones, J.W. Miller	Slate and metasandstone, textural zones 1–2	
118	LIS24	39.0835	-122.5755	Mollusks: *Buchia sp.*, Late Jurassic or Early Cretaceous	McLaughlin and others, 1990; identified by D.L Jones, J.W. Miller	Slate and metasandstone, textural zones 1–2	
119	LIS20	39.0832	-122.5197	Cephalopod: indeterminate ammonite	McLaughlin and others, 1990; identified by D.L Jones, J.W. Miller	Slate and metasandstone, textural zones 1–2	
120	LIS25	39.0831	-122.5711	Mollusks: *Buchia keyserlingi(?)* (Lahusen), Early Cretaceous (probably Valanginian)	McLaughlin and others, 1990; identified by D.L Jones, J.W. Miller	Slate and metasandstone, textural zones 1–2	
121	LIS19	39.0826	-122.5194	Mollusks: *Buchia keyserlingi* (Lahusen), Early Cretaceous (Valanginian)	McLaughlin and others, 1990; identified by D.L Jones, J.W. Miller	Slate and metasandstone, textural zones 1–2	
122	LIS22	39.0820	-122.5093	Mollusks: *Buchia pacifica* (Jeletzky), Early Cretaceous (Valanginian)	McLaughlin and others, 1990; identified by D.L Jones, J.W. Miller	Slate and metasandstone, textural zones 1–2	
123	LIS26	39.0815	-122.5706	Mollusks: *Turbo sp.; Buchia sp.*, probably *B. Keyserlingi* (Lahusen); Early Cretaceous (probably Valanginian)	McLaughlin and others, 1990; identified by D.L Jones, J.W. Miller	Slate and metasandstone, textural zones 1–2, and minor metavolcanic rocks	
124	LIS32	39.0788	-122.5383	Mollusk: *Inoceramus sp.*, probably Cretaceous (maybe Late Cretaceous?)	McLaughlin and others, 1990; identified by D.L Jones, J.W. Miller	Sheared argillite and serpentinite in fault zone	
125	LIS18	39.0783	-122.5170	Mollusks: *Buchia sp.*, probably *B. pacifica* (Jeletzky), probably Early Cretaceous (Valanginian)	McLaughlin and others, 1990; identified by D.L Jones, J.W. Miller	Slate and metasandstone, textural zones 1–2	

Table 1.—Continued

Map_No.	ID	Latitude	Longitude	Fossil and age	Source	Lithology	Unit
126	LIS17	39.0774	-122.5169	Mollusks: *Buchia pacifica* (Jeletzky), Early Cretaceous (Valanginian)	McLaughlin and others, 1990; identified by D.L Jones, J.W. Miller	Slate and metasandstone, textural zones 1–2	
127	LIS28	39.0743	-122.5121	Mollusks: *Buchia sp.*, possibly *B. uncitoides* (Pavlow), Late Jurassic or Early Cretaceous. If *B. uncitoides*, then Early Cretaceous (Valanginian)	McLaughlin and others, 1990; identified by D.L Jones, J.W. Miller	Float; derived from slate and metasandstone, textural zones 1–2	
128	LIS33	39.0697	-122.5273	Mollusks: *Buchia elderensis* (Anderson), Late Jurassic (Tithonian)	McLaughlin and others, 1990; identified by D.L Jones, J.W. Miller	Sheared shale in mélange of sheared shale, sandstone, and ophiolitic rocks	
129	LIS41	39.0622	-122.4420	Radiolaria: *Parvicingula altissima; P. hsuii sp.; P. turrita; Mirifusus baileyi sp., M.(?) mediodilitata; Pedobursa sp.; Saitoum pagei sp., Eucyrtidium(?) ptyctum; Archaeodictyomitra rigida sp.*; Late Jurassic (Tithonian, subzone 2B of Pessagno, 1977)	Identified by E.A. Pessagno (Pessagno, 1977; loc. NSF997-A,B,C); cited in McLaughlin and others, 1990	Radiolarian chert in basalt	
130	LIS27	39.0581	-122.4835	Mollusks: *Buchia pacifica* (Jeletzky), Early Cretaceous (Valanginian)	McLaughlin and others, 1990; identified by D.L Jones, J.W. Miller	Shale and sandstone	
131	LIS30	39.0570	-122.4937	Mollusks: *Buchia crassicolis* (Lahusen) *sensu lata.*, Late Cretaceous (Valanginian)	McLaughlin and others, 1990; identified by D.L Jones, J.W. Miller	Sandstone and shale	
132	kiel-bear.ck	39.0521	-122.4058	Bivalves: probable *Buchia crassicollis solida*, *"Modiola" major*; Gastropods: *Lithomphalus enderlini, Paskentana paskentaensis, fissurellid* limpet; *Serpulid* worm tubes; *solemyids; arcoids*; Early Cretaceous, probably Valanginian	Univ. of California collections UCMP A-7308 , UCMP D-2725; Location examined by K. Campbell, 1996, as reported in Kiel and others, 2008	Thin-bedded siltstone turbidites with in situ carbonate pods (0.1–1.5 m diam.); interpreted as fossil cold-seep deposits	Lower Great Valley sequence
133	MG81-79	39.0486	-122.7364	Radiolaria: Late Jurassic (Tithonian) to Early Cretaceous (Valanginian)	Collected by R.J. McLaughlin; identified By C.D. Blome	Metachert, associated with slaty metasandstone +metavolcanic rocks	Franciscan Complex, Eastern Belt, (Yolla Bolly terrane)

Table 1.—Continued

Map_No.	ID	Latitude	Longitude	Fossil and age	Source	Lithology	Unit
134	P4	39.0424	-122.4204	Brachiopods: *Peregrinella whitneyi* Gabb; Mollusks: *Modiola major*; *Pecten complexicosta*; *Lucina colusaensis; Turbo wilburensis; Turbo colusaensis; Turbo? Humerosus*, Lower Cretaceous, late Berriassian-early Hauterivian, based on *P. whitneyi*	J.E. Lawton, 1956; age based on Kiel and others, 2014	Detrital serpentinite	
135	P1	39.0331	-122.3893	Brachiopods: *Peregrinella sp.*; Lower Cretaceous, late Berriasian-early Hauterivian	J.E. Lawton, 1956; age based on Kiel and others, 2014	Detrital serpentinite	
136	LIS38	39.0331	-122.4156	Brachiopods: *Peregrinella whitneyi* Gabb; Early Cretaceous, late Berriassian-early Hauterivian	McLaughlin and others, 1990; identified by D.L. Jones, J.W. Miller	Cold-seep-related limestone lens in detrital serpentinite	
137	LIS37	39.0322	-122.4162	Brachiopods: *Peregrinella whitneyi* Gabb; Early Cretaceous, late Berriassian-early Hauterivian	McLaughlin and others, 1990; identified by D.L. Jones, J.W. Miller	Cold-seep-related limestone lens in detrital serpentinite	
138	P3	39.0316	-122.4063	Brachiopods: *Peregrinella sp.*; Lower Cretaceous, late Berriasian-early Hauterivian	J.E. Lawton, 1956; age based on Kiel and others, 2014	Detrital serpentinite	
139	LIS36	39.0307	-122.4292	Brachiopods: *Peregrinella whitneyi* Gabb; Early Cretaceous, late Berriassian-early Hauterivian	McLaughlin and others, 1990; identified by D.L. Jones, J.W. Miller	Detrital serpentinite	
140	P2	39.0307	-122.3875	Brachiopods: *Peregrinella sp.*; Lower Cretaceous, late Berriasian-early Hauterivian	J.E. Lawton, 1956; age based on Kiel and others, 2014	Detrital serpentinite	
141	MG81-96	39.0307	-122.6525	Radiolaria: Late Jurassic (Tithonian)	Collected by R.J. McLaughlin; identified by C.D. Blome	Metachert, associated with slaty metasandstone +metavolcanic rocks	
142	M5929	39.0292	-122.4836	Pelecypods: *Buchia piochii* or *B. uncitoides*; Late Jurassic (Tithonian or Berriasian)	Collected by J.C. Maxwell, 1972; identified by D.L. Jones, 1972	Shale and minor sandstone	Lower Great Valley sequence
143	M5931	39.0275	-122.4911	Pelecypods: *Buchia piochii*; Late Jurassic (Tithonian)	Collected by J.C. Maxwell, 1972; identified by D.L. Jones, 1972	Shale and minor sandstone	Lower Great Valley sequence
144	kiel-wlbr	39.0274	-122.4258	Bivalves: *"Modiola" major, Solemya stantoni, "Lucina" colusaensis, Pecten complexicosta;* Gastropods: *Paskentana paskentaensis, Retiskenea? tuberculata*; Brachiopods: *Peregrinella whitneyi*; Early Cretaceous (Hauterivian).	Collected by K. Campbell. Reported in Campbell and Bottjer, 1995; Campbell and others, 2008; Kiel and others, 2008	Fibrous cemented micritic carbonate, within sedimentary serpentinite; interpreted as fossil cold-seep deposits	Sedimentary serpentinite in lower Great Valley sequence

Table 1.—Continued

Map_No.	ID	Latitude	Longitude	Fossil and age	Source	Lithology	Unit
145	LIS29	39.0265	-122.4285	Brachiopods: *Peregrinella whitneyi* Gabb; Lower Cretaceous, late Berriassian-early Hauterivian	McLaughlin and others, 1990; identified by D.L. Jones, J.W. Miller	Shale, sandstone, and detrital serpentinite	
146	LIS39	39.0261	-122.3891	Brachiopods: *Peregrinella whitneyi* Gabb; Early Cretaceous, late Berriassian-early Hauterivian	McLaughlin and others, 1990; identified by D.L. Jones, J.W. Miller	Cold-seep-related limestone lens in detrital serpentinite	
147	M5928	39.0258	-122.4844	Pelecypods: probably Buchia piochii; Late Jurassic (Tithonian)	Collected by J.C. Maxwell, 1972; identified by D.L. Jones, 1972	Shale and minor sandstone	Lower Great Valley sequence
148	M5932	39.0231	-122.4819	Pelecypod: probably *Buchia piochii*; Late Jurassic (Tithonian)	Collected by J.C. Maxwell, 1972; identified by D.L. Jones, 1972	Shale and minor sandstone	Lower Great Valley sequence
149	LIS4	39.0231	-122.4744	Mollusks: *Buchia cf. pacifica* (Jeletzky); Early Cretaceous (Valanginian)	McLaughlin and others, 1990; identified by D.L. Jones, J.W. Miller	Sandstone and shale with carbonate lenses	
150	LIS6	39.0228	-122.4834	Mollusks: *Buchia elderensis* (Anderson), Late Jurassic (Tithonian)	McLaughlin and others, 1990; identified by D.L. Jones, J.W. Miller	Isoclinally folded shale in ophiolitic mélange	
151	FL5	39.0224	-122.3895	Brachiopods: *Peregrinella sp.*; unidentified macrofossils; unidentified foraminifers; Lower Cretaceous	J.E. Lawton, 1956	Detrital serpentinite	
152	LIS5	39.0218	-122.4823	Mollusks: *Buchia elderensis* (Anderson); *B. piochii* (Gabb), Late Jurassic (Tithonian)	McLaughlin and others, 1990; identified by D.L. Jones, J.W. Miller	Isoclinally folded shale in ophiolitic mélange	
153	M5933	39.0181	-122.4906	Pelecypods: *Buchia piochii*; Late Jurassic (Tithonian)	Collected by J.C. Maxwell, 1972; identified by D.L. Jones, 1972	Shale and minor sandstone	Lower Great Valley sequence
154	M5936	39.0167	-122.4733	Pelecypods: *Buchia fischeriana*; Late Jurassic (Tithonian)	Collected by J.C. Maxwell, 1972; identified by D.L. Jones, 1972	Shale and minor sandstone	Lower Great Valley sequence
155	LIS34	39.0143	-122.4787	Mollusks: *Buchia piochii* (Gabb); Late Jurassic (Tithonian)	McLaughlin and others, 1990; identified by D.L. Jones, J.W. Miller	Shale and sandstone	
156	LIS2	39.0138	-122.4899	Mollusks: Turbo sp.; *Buchia piochii* (Gabb); *B. elderensis* (Anderson), Late Jurassic (Tithonian)	McLaughlin and others, 1990; identified by D.L. Jones, J.W. Miller	Mélange of sheared shale, sandstone, and ophiolitic rocks	

Table 1.—Continued

Map_No.	ID	Latitude	Longitude	Fossil and age	Source	Lithology	Unit
157	LIS35	39.0133	-122.4743	Mollusks: *Buchia piochii* (Gabb)	McLaughlin and others, 1990; identified by D.L. Jones,	Shale and sandstone	
158	LIS40	39.0131	-122.3826	Brachiopods: *Peregrinella whitneyi* Gabb; Early Cretaceous, late Berriassian-early Hauterivian	McLaughlin and others, 1990; identified by D.L. Jones, J.W. Miller	Cold-seep-related limestone lens in detrital serpentinite	
159	M5937	39.0111	-122.4903	Pelecypod: *Buchia piochii*; Late Jurassic (Tithonian)	Collected by J.C. Maxwell, 1972; identified by D.L. Jones, 1972	Shale and minor sandstone	Lower Great Valley sequence
160	M5935	39.0097	-122.4814	Pelecypods: *Buchia fischeriana*; Late Jurassic (Tithonian)	Collected by J.C. Maxwell, 1972; identified by D.L. Jones, 1972	Shale and minor sandstone	Lower Great Valley sequence
161	LIS3	39.0094	-122.4914	Mollusks: *Buchia elderensis* (Anderson); *B. piochii* (Gabb), Late Jurassic (Tithonian)	McLaughlin and others, 1990; identified by D.L. Jones, J.W. Miller	Mélange of sheared shale, sandstone, and ophiolitic rocks	
162	MG81-28	38.9995	-122.7049	Radiolaria: Early Cretaceous (Probably Aptian/Albian)	Collected by R.J. McLaughlin; identified by C.D. Blome	Metachert, associated with slaty metasandstone +metavolcanic rocks	Franciscan Complex, Eastern Belt (Yolla Bolly terrane)
164	P5	38.9973	-122.3917	Brachiopods: *Peregrinella sp.*; Lower Cretaceous, late Berriasian-early Hauterivian	J.E. Lawton, 1956; age based on Kiel and others, 2014	Detrital serpentinite	
165	P6	38.9953	-122.3935	Brachiopods: *Peregrinella sp.*; Lower Cretaceous, late Berriasian-early Hauterivian	J.E. Lawton, 1956; age based on Kiel and others, 2014	Detrital serpentinite	
166	MG81-20	38.9945	-122.6773	Radiolaria: Late Jurassic (Tithonian) to Early Cretaceous (Valanginian)	Collected by R.J. McLaughlin; identified by C.D. Blome	Metachert, associated with slaty metasandstone +metavolcanic rocks	Franciscan Complex, Eastern Belt (Yolla Bolly terrane)
167	MG81-31	38.9937	-122.6983	Radiolaria: Late Jurassic (Tithonian) to Early Cretaceous (Valanginian)	Collected by R.J. McLaughlin; identified by C.D. Blome	Metachert, associated with slaty metasandstone +metavolcanic rocks	

Table 1.—Continued

Map_No.	ID	Latitude	Longitude	Fossil and age	Source	Lithology	Unit
168	JL-11-4	38.9303	-122.5692	Unidentified *ammonite*, Lower Cretaceous	Swe, 1968	Dominantly feldspathic, brownish- to tan-weathering sandstone plus conglomerate	
169	F-23-3	38.9252	-122.5073	*B. piochi*i; Late Jurassic, Tithonian	Swe, 1968; identified by Win Swe	Dominantly mudstone, minor lithic greywacke, thin-bedded chert associated with pillow basalt in lowest beds	
170	S-30-1	38.9224	-122.5517	Dinoflagellates: Late Lower-Early Upper Cretaceous, Albian-Cenomanian?	Swe, 1968; identified by W.R. Evitt	Feldspathic brownish- to tan-weathering sandstone with conglomerate lenses	
171	MG81-230	38.9216	-122.5418	Cephalopods: *Baculites sp.*; a ribbed *Ammonite sp*; Late Cretaceous, possibly as young as Campanian	Collected by R.J. McLaughlin, 1981; identified by D.L. Jones, personal commun., 8/11/81	Lithic quartzose wacke with gray carbonate concrets	Great Valley sequence
172	N-3-F	38.9183	-122.5184	*B. piochii*; Late Jurassic, Tithonian	Swe, 1968; identified by D.L. Jones	Dominantly mudstone, minor lithic greywacke	
173	FL3	38.9074	-122.3084	Foraminifers: *Globotruncana* (Rotudina) *stephani* (Gandolfi); *Globigerina infracretacea* Glaessner; *Globigerina sp.; Dentalina sp.; Cibicides sp.; Marsonella oxygona* (Reuss); *Bathysiphon sp.*; Upper Cretaceous (middle-upper Cenomanian);	J.E. Lawton, 1956; identified by K. Kupper	Mudstone and clay shale	
174	MG81-113	38.9073	-122.6389	Radiolaria: Late Cretaceous (Coniacian/Santonian)	Collected by R.J. McLaughlin; identified by C.D. Blome	Sheared silty mudstone with carbonate concretions in fault zone	
175	A-24-16	38.9073	-122.6127	Spores, dinoflagellates; Lower Cretaceous (may include Upper Jurassic?)	Swe, 1968; identified by W.R. Evitt	Conglomerate, sandstone, interbedded mudstone	

Table 1.—Continued

Map_No.	ID	Latitude	Longitude	Fossil and age	Source	Lithology	Unit
176	kiel-rcky.ck	38.8991	-122.4765	Bivalves: *Pecten complexicosta, Astarte trapezoidealis, Buchia sp.*, possibly *B. pacifica or B. crassicollis;* Gastropods: *Atresius liratus, Amberleya morganensis, Lithomphalus enderlini*; Early Cretaceous (Valanginian).	Described in Kiel and Campbell, 2005; earlier by Gabb, 1869, and Stanton, 1895	Isolated white carbonate lenses; interpreted as fossil cold-seep deposits	Lower Great Valley sequence, Blue Ridge Member of lower Crack Canyon Formation
177	F-3-3	38.8985	-122.6691	Dinoflagellates; uppermost Lower to lowermost Upper Cretaceous, Albian-Cenomanian	Swe, 1968; identified by W.R. Evitt	Dominantly mudstone	
178	MG80-150	38.8961	-122.5512	Mollusk: *Nucula sp.*; indet. Gastropod; tube, unknown origin; age indet.	Collected by J. Donnelly-Nolan and F. Goff; identified by D.L. Jones and J.W. Miller	Carbonate concretion in arkosic wacke, float near spring. In situ wacke sandstone nearby	Great Valley sequence
179	FL7	38.8954	-122.4806	Mollusks: *Pecten complexicosta* Gabb; *Turbo morganensis* Stanton; *Astarte(?) trapezoidalis* Stanton; *Atresius liratus* Gabb(?); *Buchia sp.* (inflated, unnamed); Lower Cretaceous, Valanginian, based on "Turbo" morganensis	J.E. Lawton, 1956; age based on Kiel and others, 2008	Limestone lens near base of Crack Canyon Formation	
180	F-14	38.8944	-122.5317	*B. uncitoides*; Lower Cretaceous, Berriasian	Swe, 1968; identified by D.L. Jones	Dominantly mudstone, minor lithic greywacke	
181	N-26-5	38.8928	-122.5619	Unidentified pelecypods, Upper Cretaceous	Swe, 1968	Conglomerate, sandstone, interbedded mudstone	
182	S-29-10	38.8883	-122.6220	Pollen, dinoflagellates; Upper Cretaceous	Swe, 1968; identified by W.R. Evitt	Massive lithofeldspathic, brownish-weathering sandstone	
183	A-23	38.8856	-122.4342	Mollusks: *Buchia crassicolis*; *Pecten complexicosta* Gabb; Lower Cretaceous, Valanginian;	J.E. Lawton, 1956; age based on Jones and others, 1969	Sandstone, grit, pebble conglomerate, and limestone	
184	F-22-3	38.8812	-122.5895	Spores, dinoflagellates; Lower Cretaceous (lower part?)	Swe, 1968; identified by W.R. Evitt	Dominantly mudstone, minor lithic greywacke	
185	F-6	38.8793	-122.5256	*B. pacifica*; Lower Cretaceous, Valanginian	Swe, 1968; identified by D.L. Jones	Dominantly mudstone, minor lithic greywacke	

Table 1.—Continued

Map_No.	ID	Latitude	Longitude	Fossil and age	Source	Lithology	Unit
186	F-5b	38.8792	-122.5276	*B. uncitoides*; Lower Cretaceous, Berriasian	Swe, 1968; identified by Win Swe	Dominantly mudstone, minor lithic greywacke	
187	F-11	38.8785	-122.5208	*B. uncitoides*; Lower Cretaceous, Berriasian	Swe, 1968; identified by D.L. Jones	Dominantly mudstone, minor lithic greywacke	
188	D-11-4	38.8781	-122.5928	Unidentified pelecypods and echinoderm	Swe, 1968	Massive lithofeldspathic, brownish-weathering sandstone	
189	F-10(a,b)	38.8773	-122.5316	*B. piochii*; Late Jurassic, Tithonian	Swe, 1968; identified by D.L. Jones	Dominantly mudstone, minor lithic greywacke, thin-bedded chert associated with pillow basalt in lowest beds	
190	F-10a	38.8773	-122.5316	Dinoflagellates; Upper Jurassic	Swe, 1968; identified by W.R. Evitt	Dominantly mudstone, minor lithic greywacke, thin-bedded chert associated with pillow basalt in lowest beds	
999	M5171	39.9544	-123.0306	Cephalopod: *Belemnite* fragment; Pelecypods: scraps of large, coarse-ribbed *Buchia*, possibly *B. pacifica;* probably Cretaceous	Collected by J. Suppe, 1969; identified by D.L. Jones, 1969	No lithologic data provided	No information
999	M5169	39.9442	-123.0417	Pelecypod: *Buchia piochi*i; Late Jurassic (Tithonian)	Collected by J. Suppe, 1969; identified by D.L. Jones, 1969	No lithologic data provided	No information
999	M5168	39.8842	-123.0731	Pelecypod: *Arca tehamaensis?* Stanton, *Amberleya dilleri* Stanton; Early Cretaceous (upper Valanginian)	Collected by J. Suppe, 1969; identified by D.L. Jones, 1969	No lithologic data provided	No information
999	M5173	39.8081	-122.9878	Pelecypod: probably *Buchia cf. B. piochii*; probably Late Jurassic (Tithonian), but preservation poor	Collected by J. Suppe, 1969; identified by D.L. Jones, 1969	No lithologic data provided	No information
999	M5172	39.8022	-123.0389	Pelecypod: *Buchia cf. B. pacifica*; Early Cretaceous (Valanginian?)	Collected by J. Suppe, 1969; identified by D.L. Jones, 1969	No lithologic data provided	No information
999	M5170	39.8006	-123.0344	Pelecypod: *Buchia piochii?*; Late Jurassic (Tithonian)?	Collected by J. Suppe, 1969; identified by D.L. Jones, 1969	No lithologic data provided	No information

Table 1.—Continued

Map_No.	ID	Latitude	Longitude	Fossil and age	Source	Lithology	Unit
999	M6563	39.7736	-122.7278	Pelecypods: *Buchia pacifica* (Jeletzky); Early Cretaceous (early middle Valanginian)	Collected by J. Suppe, 1977; identified by D.L. Jones, 1977	Meta argillite and metasandstone	Franciscan Complex, Eastern Belt, mélange of Yolla Bolly terrane, Goat Mountain area
999	M6598	39.7628	-123.0686	Pelecypods: possibly *Buchia sp., cf. B. keyserlingi* (Lahusen); possibly Early Cretaceous (latest Valanginian)?	Collected by J.C. Maxwell, Univ. of Texas, Austin, 1976; identified by D.L. Jones, 1977	Sheared argillite	Franciscan Complex, Central Belt, "Poison Rock" mélange
999	M6599	39.7625	-123.0683	Pelecypod: too poorly preserved for definitive ident, but may be *B. keyserlingi*	Collected by J.C. Maxwell, Univ. of Texas, Austin, 1976; identified by D.L. Jones, 1977	Sheared argillite	Franciscan Complex, Central Belt, "Poison Rock" mélange
999	O-8-2	38.8719	-122.5279	Dinoflagellates; Upper Jurassic	Swe, 1968; identified by W.R. Evitt	Ophiolitic mélange	
999	A-3-8	38.8710	-122.6141	*Turritella pachecoensis*, Paleocene	Swe, 1968; identified by Win Swe	Massive, structureless sandstone, mudstone, and conglomerate	
999	O-25-5a	38.8680	-122.5619	*B. pacifica*; Lower Cretaceous, Valanginian	Swe, 1968; identified by Win Swe	Conglomerate, sandstone, interbedded mudstone	
999	D-10-3	38.8634	-122.5431	*Buchia piochii*, reworked in Lower Cretaceous	Swe, 1968; identified by D.L. Jones	Sandstone, interbedded mudstone	
999	D-10-3(1)	38.8634	-122.5431	Dinoflagellates; Lower Cretaceous	Swe, 1968; identified by W.R. Evitt	Conglomerate, sandstone, interbedded mudstone	
999	D-10-3(2)	38.8634	-122.5431	Dinoflagellates; Upper Jurassic reworked into Lower Cretaceous	Swe, 1968; identified by W.R. Evitt	Conglomerate, sandstone, interbedded mudstone	
999	MG81-162	38.8616	-122.6694	Radiolaria: Late Jurassic (Tithonian)	Collected by R.J. McLaughlin; identified by C.D. Blome	Radiolarian chert in ophiolitic mélange	
999	F-4-3	38.8611	-122.7421	Pollen, dinoflagellates; Upper Cretaceous	Swe, 1968; identified by W.R. Evitt	Siltstone and interbedded massive fine-grained white sandstone	

Table 1.—Continued

Map_No.	ID	Latitude	Longitude	Fossil and age	Source	Lithology	Unit
999	D-17-6	38.8596	-122.6590	*B. pacifica*; Lower Cretaceous, Valanginian	Swe, 1968; identified By Win Swe	Dominantly mudstone, minor lithic greywacke	
999	N-10-2	38.8579	-122.5495	*B. uncitoides*; Lower Cretaceous, Berriasian	Swe, 1968; identified by D.L. Jones	Conglomerate, sandstone, interbedded mudstone	
999	F05	38.8570	-122.3703	Cephalopod: *Belemnite, Cylindroteuthis tehamaensis*, Late Jurassic (Tithonian?)	Collected by D. Enderlin, 1986	Mudstone	Lower Great Valley sequence
999	D-17-3	38.8555	-122.6483	Pollen, dinoflagellates; Upper Cretaceous	Swe, 1968; identified by W.R. Evitt	Dominantly sandstone	
999	F016	38.8551	-122.3674	Cephalopods: *Ammonite, Phylloceras knoxvillense; Belemnite, Cylindroteuthis tehamaensis*; Mollusks: *Buchiids*; Late Jurassic (Tithonian)?—Reworked?	Collected by D. Enderlin, 1987	Chert-volcanic-rich conglomerate and greywacke, fossils in conglomerate	Lower Great Valley sequence (Knoxville Formation?)
999	F017	38.8538	-122.3632	Mollusks: *Buchia piochii*; Late Jurassic (Tithonian); disarticulated valves	Collected by D. Enderlin	Chert-volcanic-rich pebble conglomerate and greywacke, casts and molds	Lower Great Valley sequence (Knoxville Formation?)
999	F018	38.8528	-122.3637	Cephalopods: *Ammonite*, rostrum fragment, possibly Spiticeras sp.?; no age assigned	Collected by D. Enderlin	Chert-volcanic-rich conglomerate	Lower Great Valley sequence (Knoxville Formation?)
999	A-24-2	38.8501	-122.6042	Pollen, dinoflagellates; Upper Cretaceous (possibly lower Maestrichtean)	Swe, 1968; identified by W.R. Evitt	Alternating sandstone, mudstone	
999	F02	38.8499	-122.3573	Mollusks: *Buchia piochii*; Late Jurassic (Tithonian)	Enderlin	Fragments in greywacke	Lower Great Valley sequence
999	O-9-8	38.8499	-122.7276	Dinoflagellates, preservation poor; probably Lower Cretaceous or Upper Jurassic	Swe, 1968; identified By W.R. Evitt	Dominantly mudstone, minor lithic greywacke, thin-bedded chert associated with pillow basalt in lowest beds	
999	M-7-4	38.8498	-122.6858	*B. piochii*; Late Jurassic, Tithonian	Swe, 1968; identified by D.L. Jones	Dominantly mudstone, minor lithic greywacke, thin-bedded chert associated with pillow basalt in lowest beds	

Table 1.—Continued

Map_No.	ID	Latitude	Longitude	Fossil and age	Source	Lithology	Unit
999	M-7-4	38.8498	-122.6858	Dinoflagellates; Upper Jurassic	Swe, 1968; identified By W.R. Evitt	Dominantly mudstone, minor lithic greywacke, thin-bedded chert associated with pillow basalt in lowest beds	
999	N-10-3	38.8489	-122.5247	*B. fischeriana?*; Late Jurassic, Tithonian	Swe, 1968; identified by D.L. Jones	Dominantly mudstone, minor lithic greywacke, thin-bedded chert assoiated with pillow basalt in lowest beds	
999	F01	38.8489	-122.3565	Mollusks: *Buchia piochii*; Late Jurassic (Tithonian)	Enderlin	Fragments in greywacke	Lower Great Valley sequence
999	F025	38.8476	-122.3446	*Buchiids* (inflated forms, disarticulated valves) cobble in creek; no outcrop; Early Cretaceous?	Collected by D. Enderlin	Calcareous sandstone	Lower Great Valley sequence (Crack Canyon Formation)
999	N-10-4	38.8476	-122.5216	*B. piochii;* Late Jurassic, Tithonian	Swe, 1968; identified by D.L. Jones	Dominantly mudstone, minor lithic greywacke	
999	F06	38.8472	-122.3487	Mollusks: *Buchia pacifica?*; Early Cretaceous (Valanginian?)	Enderlin	"Marly cobble" in creek; no outcrop	Lower Great Valley sequence (Crack Canyon Formation)
999	F07	38.8472	-122.3467	Mollusks: *Buchia pacifica?*; Early Cretaceous (Valanginian?)	Enderlin	Calcareous fine-grained sandstone and siltstone	Lower Great Valley sequence (Crack Canyon Formation)
999	F019	38.8460	-122.3607	Mollusks: disarticulated small valves, *Buchia piochii*; Cephalopods: *Ammonite* rostrum fragment, *Phylloceras knoxvillense*; Late Jurassic (Tithonian)	Collected by D. Enderlin	Hydrothermally bleached, locally pyritized argillic alteration	Lower Great Valley sequence
999	F026	38.8454	-122.3538	Mollusks: *Buchia piochii*, valves and fragments; Late Jurassic? (Tithonian)?	Collected by D. Enderlin	Massive sandstone	Lower Great Valley sequence (Knoxville Formation?)
999	F-18-16	38.8447	-122.5894	*Desmophyllites diphylloides;* Upper Cretaceous, Campanian and possibly Late Maastrichtian	Swe, 1968; identified By Win Swe	Alternating sandstone, mudstone	

Table 1.—Continued

Map_No.	ID	Latitude	Longitude	Fossil and age	Source	Lithology	Unit
999	D-19-3	38.8413	-122.6466	Dinoflagellates; probably Upper Jurassic	Swe, 1968; identified by W.R. Evitt	Dominantly mudstone, minor lithic greywacke, thin-bedded chert associated with pillow basalt in lowest beds	
999	F04	38.8411	-122.3491	Mollusks: Buchiid valve; Late Jurassic or Early Cretaceous	Enderlin	Siltstone-dominated turbidites, overturned, disrupted	Lower Great Valley sequence
999	F011	38.8404	-122.3363	Mollusks: *Buchiids,* small valves (to 1 cm), inflated form (juvenile?) ; reworked? No age assigned	Collected by D. Enderlin	Marl and greywacke	Lower Great Valley sequence (Crack Canyon Formation?)
999	F021	38.8381	-122.3435	Mollusks: *Buchiids (B. piochii?)*, Late Jurassic? (Tithonian?)	Observed by Enderlin; left in place	Cobble of marl	Lower Great Valley sequence (Knoxville Formation?)
999	F010	38.8376	-122.3342	Mollusks: *Buchia pacifica?*; Early Cretaceous (Valanginian?)	Collected by D. Enderlin	Conglomerate, boulder on ridgetop trail	Lower Great Valley sequence (Crack Canyon Formation)
999	F015	38.8367	-122.3381	Mollusks: valve fragments, *Buchia pacifica?*; Early Cretaceous (Valanginian?)	Collected by D. Enderlin	Orange, marly greywacke	Lower Great Valley sequence (Crack Canyon Formation)
999	F014	38.8355	-122.3274	Mollusks: *Modiola sp; Turbo sp.(possibly T. paskentana?)*; Early Cretaceous (probably Hauterivian or younger?)	Collected by D. Enderlin, R.J. McLaughlin, and W. Elder, 2007	Boulders and outcrop in Foley Creek; associated with detrital serpentinite and cold-seep setting	Lower Great Valley sequence (transitional, Crack Canyon and Little Valley Formations)
999	F03	38.8355	-122.3471	Mollusks: *Buchiid* fragments; Late Jurassic or Early Cretaceous	Enderlin	Fragments in 5-ft-thick greywacke bed	Lower Great Valley sequence
999	F09	38.8345	-122.3403	Mollusks: *Buchia piochii?*; Cephalopod: possibly Cylindroteuthis tehamaensis?; Late Jurassic (Tithonian?)	Collected by D. Enderlin	Marly mudstone	Lower Great Valley sequence

Table 1.—Continued

Map_No.	ID	Latitude	Longitude	Fossil and age	Source	Lithology	Unit
999	F08	38.8341	-122.3371	Mollusks: *Buchia pacifica?*; Early Cretaceous (Valanginian?)	Enderlin	Greywacke float; not abundant	Lower Great Valley sequence (Crack Canyon Formation)
999	F020	38.8324	-122.3423	Mollusks: *Buchia piochii*, disarticulated valves; Late Jurassic (Tithonian)	Collected by D. Enderlin	Chert-volcanic-rich pebble conglomerate; below basal contact with basaltic andesite intrusive of Clear Lake Volcanics	Lower Great Valley sequence (Knoxville Formation?)
999	F012	38.8321	-122.3233	Brachiopods: *Peregrinella whitneyi* in bioclastic debris; Early Cretaceous (probably late Berriasian-early Hauterivian)	Collected by D. Enderlin	Detrital serpentinite, micritic mudstone, and brown sandstone; cold-seep deposit	Lower Great Valley sequence (transitional, Crack Canyon and Little Valley Formations)
999	kiel-foley.cyn	38.8316	-122.3231	Bivalves: *"Modiola" major*, "inflated" *Buchia sp.;* Gastropods: *Paskentana paskentaensis*, Brachiopods: *Peregrinella whitneyi*; Early Cretaceous (Valanginian-Hauterivian)	Described by D. Enderlin in Kiel and others, 2008	Two fault-bounded parallel lenses of carbonate near or in sedimentary serpentinite body within Crack Canyon Formation sedimentary section; formerly quarried for lime; interpreted as fossil cold-seep deposits	Lower Great Valley sequence, Crack Canyon Formation
999	F013	38.8316	-122.3228	Mollusks: Turbo sp., *Modiola sp.*, *Pecten sp.*; Early Cretaceous (probably late Berriasian-early Hauterivian) based on F012 loc.	Collected by D. Enderlin	Limestone marl and micritic mudstone associated with detrital serpentinite	Lower Great Valley sequence (transitional, Crack Canyon and Little Valley Formations)
999	Ja-16-5	38.8311	-122.6368	Pollen, dinoflagellates; Upper Cretaceous	Swe, 1968; identified by W.R. Evitt	Dominantly sandstone	
999	D-16-5	38.8311	-122.6368	*B. pacifica*; Lower Cretaceous, Valanginian	Swe, 1968; identified by D.L. Jones	Dominantly mudstone, minor lithic greywacke	

Table 1.—Continued

Map_No.	ID	Latitude	Longitude	Fossil and age	Source	Lithology	Unit
999	F024	38.8308	-122.3369	Mollusks: *Buchia piochii*, well preserved exterior casts; Late Jurassic (Tithonian);	Collected by D. Enderlin	Greywacke; associated with black fossilized plant remains	Lower Great Valley sequence (Knoxville Formation?)
999	F023	38.8265	-122.3369	Mollusks: *Buchia piochii*, only one valve; Late Jurassic (Tithonian);	Collected by D. Enderlin	Gray mudstone	Lower Great Valley sequence (Knoxville Formation?)
999	F022	38.8240	-122.3335	Mollusks: *Buchia piochii*, abundant molds; Late Jurassic (Tithonian);	Observed by D. Enderlin	Gray mudstone and siltstone	Lower Great Valley sequence (Knoxville Formation?)
999	F-4	38.8194	-122.5745	*Inoceramus schmidti*; Upper Cretaceous, Middle-Upper Campanian	Swe, 1968; identified by D.L. Jones	Alternating sandstone, mudstone	
999	WS-F-4	38.8194	-122.5745	Pollen, dinoflagellates; Upper Cretaceous	Swe, 1968; identified by W.R. Evitt	Alternating sandstone, mudstone	
999	M-6-1	38.8099	-122.6156	*Nostroceras ? sp.*; Upper Cretaceous, Campanian	Swe, 1968; identified by D.L. Jones	Dominantly sandstone	
999	Ja-14-8	38.8090	-122.6371	Foraminifers; *Bathysiphon perampla(?)*; Upper Cretaceous	Swe, 1968; identified by Win Swe	Siltstone and interbedded massive fine-grained white sandstone	
999	F-17-1	38.8000	-122.6636	Spores, dinoflagellates; probably Lower Cretaceous	Swe, 1968; identified by W.R. Evitt	Mudstone with thin interbedded quartz-rich sandstone	
999	Ja-13-8	38.7968	-122.6774	Dinoflagellates; Upper Jurassic or Lower Cretaceous	Swe, 1968; identified by W.R. Evitt	Dominantly mudstone, minor lithic greywacke, thin-bedded chert associated with pillow basalt in lowest beds	
999	F-7-6	38.7918	-122.6245	Pollen, dinoflagellates; Upper Cretaceous	Swe, 1968; identified by W.R. Evitt	Dominantly sandstone	
999	Ja-10-F	38.7870	-122.6273	Unidentified pelecypods, Upper Cretaceous	Swe, 1968	Siltstone and interbedded massive fine-grained white sandstone	

Table 1.—Continued

Map_No.	ID	Latitude	Longitude	Fossil and age	Source	Lithology	Unit
999	F-17-13	38.7854	-122.6505	Dinoflagellates; Lower Cretaceous (Upper Berriasian-Valanginian	Swe, 1968; identified by W.R. Evitt	Mudstone with thin interbedded quartz-rich sandstone	
999	Ja-9-12	38.7832	-122.6082	Spores, dinoflagellates; Lower Cretaceous (questionable Aptian?)	Swe, 1968; identified by W.R. Evitt	Mudstone with thin interbedded quartz-rich sandstone	
999	F-8-2	38.7817	-122.6243	*Cucullaea sp.* and straight conical thin-shelled cephalopods	Swe, 1968; identified By A. Myra Keen	Siltstone and interbedded massive fine-grained white sandstone	
999	F-8-2	38.7817	-122.6243	Pollen; Upper Cretaceous	Swe, 1968; identified by W.R. Evitt	Siltstone and interbedded massive fine-grained white sandstone	
999	F-18-14	38.7762	-122.6247	Dinoflagellates: probably Lower Cretaceous	Swe, 1968; identified by W.R. Evitt	Mudstone with thin interbedded quartz-rich sandstone	
999	F-18-15	38.7674	-122.5873	Dinoflagellates; Upper Jurassic	Swe, 1968; identified by W.R. Evitt	Dominantly mudstone, minor lithic greywacke, thin-bedded chert associated with pillow basalt in lowest beds	
999	F-24-6	38.7472	-122.5523	Pollen, dinoflagellates; Upper Cretaceous	Swe, 1968; identified by W.R. Evitt	Dominantly sandstone	
999	M6947	38.6972	-122.3689	Cephalopod: *Phylloceras cf. P. contrarium* (Imlay and Jones), Late Jurassic	Collected by S.P. Phipps and submitted to USGS in 1978; identified by D.L. Jones and J.W Miller, 1979	Not given	Lower Great Valley sequence
999	M6945	38.6931	-122.3658	Radiolaria: Late Jurassic (Tithonian)	Collected by R.J. McLaughlin; identified by C.D. Blome	Radiolarian chert in ophiolitc melange	Ophiolitic melange of Lower Great Valley sequence
999	M6948	38.6895	-122.3555	Radiolaria: Late Cretaceous (Coniacian/Santonian)	Collected by R.J. McLaughlin; identified by C.D. Blome	Sheared silty mudstone with carbonate concretions in fault zone	Great Valley sequence

Table 1.—Continued

Map_No.	ID	Latitude	Longitude	Fossil and age	Source	Lithology	Unit
999	M6946	38.6846	-122.3571	Radiolaria: Late Jurassic (Tithonian) to Early Cretaceous (Valanginian)	Collected by R.J. McLaughlin; identified by C.D. Blome	Metachert, associated with slaty metasandstone +metavolcanic rocks	Franciscan Complex, Eastern Belt (Yolla Bolly terrane)
999	M6944	38.6725	-122.3408	Radiolaria: Late Jurassic (Tithonian) to Early Cretaceous (early Valanginian)	Collected by R.J. McLaughlin; identified by C.D. Blome	Radiolarian chert in melange	Franciscan Complex, Eastern Belt (Yolla Bolly terrane)
999	M6954	38.6667	-122.2779	Radiolaria: Late Jurassic (Tithonian) to Early Cretaceous (Valanginian)	Collected by R.J. McLaughlin; identified by C.D. Blome	Metachert, associated with slaty metasandstone +metavolcanic rocks	Franciscan Complex, Eastern Belt (Yolla Bolly terrane)
999	M6935	38.6653	-122.4166	Mollusks: *Mytilus sp*,; Indet. clams; *Turbo paskentaensis* (Stanton); Late Jurassic or Early Cretaceous	Collected by S.P. Phipps and submitted to USGS in 1978; identified by D.L. Jones and J.W Miller, 1979	No lithologic data provided	Lower Great Valley sequence
999	M6937	38.6621	-122.4153	Mollusks: *Buchia pacifica* (Jeletzky); Early Cretaceous (Valanginian)	Collected by S.P. Phipps and submitted to USGS in 1978; identified by D.L. Jones and J.W Miller, 1979	Not given	Lower Great Valley sequence
999	M6938	38.6598	-122.4242	Mollusks: *Buchia pacifica* (Jeletzky); Early Cretaceous (Valanginian)	Collected by S.P. Phipps and submitted to USGS in 1978; identified by D.L. Jones and J.W. Miller, 1979	No lithologic data provided	Lower Great Valley sequence
999	M6934	38.6519	-122.3943	Mollusks: *Mytilus sp*,; Indet. clams; *Turbo paskentaensis* (Stanton); Late Jurassic or Early Cretaceous	Collected by S.P. Phipps and submitted to USGS in 1978; identified by D.L. Jones and J.W. Miller, 1979	Not given	Lower Great Valley sequence
999	M6942	38.6510	-122.3233	Radiolaria: Late Jurassic (Tithonian) to Early Cretaceous (early Valanginian)?	Collected by H.N. Ohlin; identified by C.D. Blome	Radiolarian chert in melange	Franciscan Complex, Central Belt
999	M6939	38.6316	-122.3485	Mollusks: *Buchia piochii* (Gabb); Late Jurassic (Tithonian)	Collected by S.P. Phipps and submitted to USGS in 1978; identified by D.L. Jones and J.W. Miller, 1979	No lithologic data provided	Lower Great Valley sequence

Table 1.—Continued

Map_No.	ID	Latitude	Longitude	Fossil and age	Source	Lithology	Unit
999	M6941	38.6211	-122.2887	Mollusks: *Buchia sp.*, Late Jurassic or Early Cretaceous	Collected by S.P. Phipps and submitted to USGS in 1978; identified by D.L. Jones and J.W. Miller, 1979	No lithologic data provided	Great Valley sequence
999	M6940	38.5919	-122.2590	Mollusks: *Buchia piochii* (Gabb); Late Jurassic (Tithonian)	Collected by S.P. Phipps and submitted to USGS in 1978; identified by D.L. Jones and J.W. Miller, 1979	No lithologic data provided	Lower Great Valley sequence
999	M6953	38.3882	-122.4033	Radiolaria: Late Jurassic (Tithonian) to Early Cretaceous (Valanginian)	Collected by R.J. McLaughlin; identified by C.D. Blome	Metachert, associated with slaty metasandstone +metavolcanic rocks	Franciscan Complex, Eastern Belt (Yolla Bolly terrane)